THE CONTENTS OF THIS SECTION ARE
THE HIGHEST QUALITY AVAILABLE

INITIAL KH DATE 11/8/04

PAGE NUMBERING SEQUENCE IS INCONSISTENT

Idaho National Engineering and Environmental Laboratory

INEEL/EXT-2000-01089

September 2000

Technical Revision of the Radioactive Waste Management Complex Low-Level Waste Radiological Performance Assessment for Calendar Year 2000

Marilyn J. Case
Arthur S. Rood
James M. McCarthy
Swen O. Magnuson
Bruce H. Becker
Thomas K. Honeycutt

BECHTEL BWXT IDAHO, LLC

INEEL/EXT-2000-01089

Technical Revision of the Radioactive Waste Management Complex Low-Level Waste Radiological Performance Assessment for Calendar Year 2000

Marilyn J. Case
Arthur S. Rood
James M. McCarthy
Swen O. Magnuson
Bruce H. Becker
Thomas K. Honeycutt

Published September 2000

Idaho National Engineering and Environmental Laboratory

Idaho Falls, Idaho 83415

Prepared for the
U.S. Department of Energy

Under DOE Idaho Operations Office
Contract DE-AC07-99ID13727

ABSTRACT

This report documents the projected radiological dose impacts associated with the disposal of radioactive low-level waste at the Radioactive Waste Management Complex at the Idaho National Engineering Laboratory. This radiological performance assessment was conducted to evaluate compliance with applicable radiological criteria of the U.S. Department of Energy and the U.S. Environmental Protection Agency for protection of the public and the environment. The calculations involved modeling the transport of radionuclides from buried waste, to surface soil and subsurface media, and eventually to member of the public via air, groundwater, and food chain pathways. Projections of doses were made for both offsite receptors and individuals inadvertently intruding onto the site after closure. In addition, uncertainty and sensitivity analyses were performed. The results of the analyses indicate compliance with established radiological criteria and provide reasonable assurance that public health and safety will be protected.

SUMMARY

This report documents the projected impacts associated with disposal of radioactive low-level radioactive waste (LLW) at the Idaho National Engineering and Environmental Laboratory (INEEL) Radioactive Waste Management Complex (RWMC). The impacts were compared with applicable U.S. Department of Energy (DOE) and U.S. Environmental Protection Agency (EPA) standards.

The LLW radiological performance assessment for the RWMC presents a comprehensive, systematic analysis of the long-term impacts of LLW disposal in an arid, near-surface environment. Occupational radiological doses and impacts of nonradioactive hazardous constituents are beyond the scope of this radiological performance assessment and will be considered in other assessments.

For the purpose of assessing the performance of LLW disposed of at the RWMC, three time periods are of concern:

1. The operational period, 1984 through 2020, during which radioactive waste is actively disposed of at the facility.

2. The institutional control period, 2021 through 2120, which follows site closure and during which periodic maintenance and monitoring activities are conducted. The facility is assumed to be closed, stabilized, and maintained but is still part of the INEEL reservation and is fenced and patrolled.

3. The post-institutional control period, beginning in 2120, during which the facility is no longer maintained by the DOE and may be accessible to the public. Radiological impacts are presented for a period of 1000 years, the maximum time of compliance for DOE LLW performance assessments. Analyses were also carried out to the time of maximum potential impact.

Two receptor types were assessed. The first was a member of the public. During the operational and institutional control periods this individual resided at the INEEL Site boundary. During the post-institutional control period, the member of the public resided 100 m from the RWMC Subsurface Disposal Area (SDA) boundary.

The second type of receptor evaluated was an intruder. This hypothetical receptor was assumed to inadvertently intrude onto the RWMC SDA during the post-institutional control period. Two general kinds of intruder scenarios were evaluated: chronic and acute. The chronic scenarios included a well-drilling scenario, a basement excavation scenario, a biointrusion scenario, and a radon scenario. These scenarios included the doses from ingestion of contaminated food, inhalation of contaminated air, and external exposure. The acute scenarios included a construction scenario and a well-drilling scenario. These scenarios included the doses from inhalation of contaminated air and external exposure. In both the acute and chronic scenarios, the inhalation and ingestion doses were evaluated using the RESRAD computer code and the external doses were evaluated using the MICROSHIELD computer code.

The performance assessment process consists of conceptual models that link radionuclide inventory, release (or source term), environmental transfer, and impact assessment (see Figure ES-1) and culminate in radiological doses to receptors. The waste inventory used in the performance assessment was derived from the Contaminant Inventory Database for Risk Assessment (CIDRA) and consists of the LLW buried from 1984 through 1999 and LLW projected for future disposal through 2020. Transuranic (TRU) waste and LLW intermixed with TRU waste that was buried before 1984 were not included because they are planned for assessment by the Environmental Restoration Program and because DOE

Order 435.1 directs that the PA focuses on recent LLW disposal (from 1988 on). The LLW disposed from 1984-1987 was included in the PA because it is physically located with the waste disposed of from 1988 on and is easily included in the modeling. Where possible, site-specific data and parameters were used in the analyses.

Results of the monitoring, special studies, and modeling efforts to date indicate that the greatest potential for transport of radionuclides from the RWMC to offsite receptors (now and in the future) is via airborne transport of resuspended contaminated near-surface soil particles from biointrusion and from groundwater transport of radionuclides leached from buried waste. For this reason, the performance assessment focuses on these two transport pathways for members of the public.

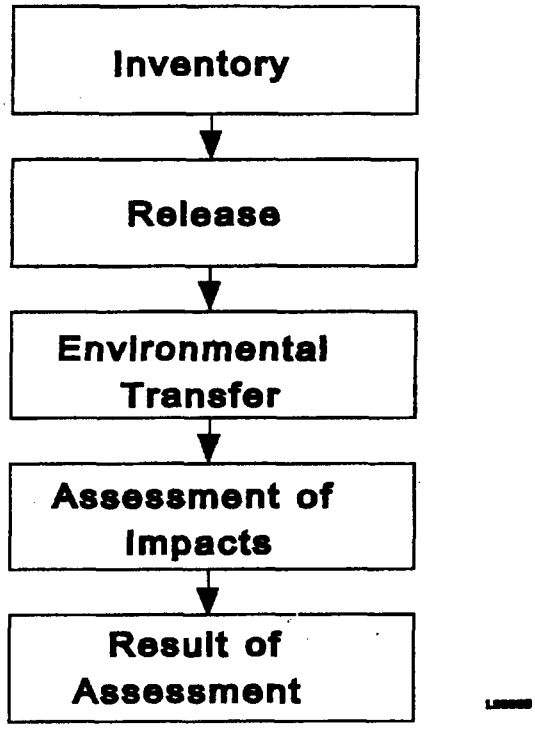

Figure ES-1. Performance assessment process.

The exposure pathways evaluated include ingestion of contaminated food and water, inhalation of contaminated airborne particulates, and external exposure to radionuclides in the air and on the ground (or soil) surface. The agricultural products consumed by members of the public are contaminated via food chain transport of radionuclides deposited from air onto soil or plant surfaces, from radionuclides deposited onto soil or plant surfaces by irrigation water, or from the direct ingestion of contaminated water.

The source of radionuclides for airborne transport during the operational and institutional control periods was diffusion of radioactive gases from the waste to the surface and transport of radioactive particles from the waste to surface soil by plant roots and harvester ants. Carbon-14 and tritium fluxes predicted by the source term model, DUST, were conservatively assumed to diffuse to the surface where they were dispersed to downwind receptors using the ISCST3 computer code and INEEL meteorological data. Radon flux from the waste through the soil surface was evaluated using the RESRAD code. Radioactivity brought to the surface by plant roots and harvester ants was dispersed downwind to a

Table ES-1. (continued).

Performance Objective	Standard	RWMC Performance Assessment Result
		Pits (maximum impact within 10,000 years)
		3.8 mrem/yr (basement excavation and drilling)
		0.01 mrem/yr (biointrusion)
		52.1 mrem/yr (radon)
		55.9 mrem/yr total
Acute inadvertent intrusion	500 mrem	*1000 year time of compliance*
(DOE Order 451.1)		86.7 mrem (soil vaults)
		4.5 mrem (pits)
		Maximum impact within 10,000 years
		86.7 mrem (soil vaults)
		4.5 mrem (pits)
Groundwater protection	4 mrem/yr EDE	3.8e-4 mrem/yr during operational and institutional control periods
		1.4 mrem/yr during post-institutional control period
	20,000 pCi/L H-3	0.29 pCi/L during operational and institutional control periods
		23 pCi/L during post-institutional control period
	8 pCi/L Sr-90	9.1E-8 pCi/L during operational and institutional control periods
		3.2E-6 pCi/L during post-institutional control period
	5 pCi/L Ra-226 and Ra-228	9.2E-5 pCi/L (at 10,000 years)
	15 pCi/L gross alpha	0.31 pCi/L (at 10,000 years)
	20 µg/L uranium	200 µg/L (at 10,000 years)

CONTENTS

FIGURES

TABLES

ACRONYMS

ALARA	as low as reasonably achievable
CEDE	committed effective dose equivalent
CERCLA	Comprehensive Environmental Response, Compensation, and Liability Act
CFA	Central Facilities Area
CR	concentration ratio
DCF	dose conversion factor
DOE	U.S. Department of Energy
EBTF	Engineered Barriers Test Facility
EDE	effective dose equivalent
EPA	U.S. Environmental Protection Agency
FFA/CO	Federal Facility Agreement and Consent Order
ICRP	inhalation rate for reference man
IDHW	Idaho Department of Health and Welfare
INEEL	Idaho National Engineering and Environmental Laboratory
LFRG	Low-Level Waste Disposal Federal Review Group
LLW	low-level radioactive waste
LSIT	large-scale infiltration test
MCL	maximum contaminant level
NESHAP	National Emission Standard for Hazardous Air Pollutants
OU	operable unit
RESL	Radiological and Environmental Sciences Laboratory
RI/FS	Remedial Investigation/Feasibility Study
RWMC	Radioactive Waste Management Complex
RWMIS	Radioactive Waste Management Information System
SDA	Subsurface Disposal Area
TRU	transuranic
TSA	Transuranic Storage Area
USDA	U.S Department of Agriculture
VOC	Volatile organic contaminants
WAG	Waste Area Group

Technical Revision of the Radioactive Waste Management Complex Low-Level Waste Radiological Performance Assessment of Calendar Year 2000

1. INTRODUCTION

1.1 Purpose and Scope

This report documents the projected radiological impacts associated with the disposal of low-level radioactive waste (LLW) at the Radioactive Waste Management Complex (RWMC) at the Idaho National Engineering and Environmental Laboratory (INEEL). The projected impacts are used to demonstrate compliance with applicable radiological dose criteria of the U.S. Department of Energy (DOE) and the U.S. Environmental Protection Agency (EPA) for protection of the public and the environment. The radiological performance assessment is being conducted to fulfill the requirements of DOE Order 435.1, "Radioactive Waste Management" (DOE 1999), which replaces DOE Order 5820.2A (DOE 1988a). A performance assessment is "an analysis of a radioactive waste disposal facility conducted to demonstrate there is a reasonable expectation that performance objectives established for the long-term protection of the public and the environment will not be exceeded following closure of the facility." (DOE 1999). Performance objectives include public and intruder radiological dose limits and drinking water radiological dose limits established by DOE orders and EPA requirements. In the context of this radiological performance assessment, the waste management system consists of the disposed LLW, the LLW disposal facility, and its environs. This radiological performance assessment is a tool used to predict the potential environmental consequences of the LLW disposal facility; its intent is to determine whether waste management activities will accomplish the goal of effectively containing LLW. This goal is accomplished if compliance with performance objectives is demonstrated in the performance assessment.

The LLW radiological performance assessment for the RWMC presents a comprehensive, systematic analysis of the long-term impacts of LLW disposal in an arid near-surface environment. Related assessment activities (e.g., safety assessments, risk assessments, characterizations for siting or construction, engineering evaluations, and cost/design studies) are outside the scope of this document. Potential radiological doses to workers at the RWMC are not assessed in this document. Although occupational doses to workers are an important area of concern for facility operations, they are addressed by regulations and guidance different than those covering performance assessments. Furthermore, compliance with occupational criteria is not necessarily demonstrated by the type of calculations performed for radiological performance assessments. Additionally, this document excludes the potential impacts of chemical toxicity of radiological constituents and nonradiological hazardous constituents that may be in the waste.

A companion document, the Radioactive Waste Management Complex Low-Level Waste Radiological Composite Analysis (McCarthy et al, 2000) assesses the cumulative impacts from active and planned LLW disposal facilities and all other sources of radioacive contamination that could interact with the LLW disposal facility to affect the dose to future members of the publice. It is different from the performance assessment in that it includes inventory disposed at the RWMC since 1952 and it addresses other sources at the INEEL. The performance assessment addresses LLW disposed since 1984.

A performance assessment was initially conducted in 1994 (Maheras et al 1994) to comply with DOE Order 5820.2A. An addendum (Maheras et al 1997) followed. The current revision was conducted primarily to incorporate recommendations made by the Low-Level Waste Disposal Facility Federal

Review Group (LFRG) after a review of the composite analysis. The LFRG stated that the "Performance Assessment is to be revised to be consistent with the conceptual model, inventory, source term model, transport model, and site characteristics presented in the Composite Analysis." The specific issues which this performance assessment addresses are a reanalysis using the updated source inventory, source term model, and subsurface transport models used in the composite analysis. A guide to resolutions of specific LFRG comments on the CA may be found in Appendix A.

Waste has been buried in the Subsurface Disposal Area (SDA) since 1952 in trenches, pits, and soil vault rows. LLW has been buried separately from TRU since 1984 is assessed in this report. Buried transuranic (TRU) waste, stored TRU waste, and buried commingled TRU waste and LLW are not included in the report. Although DOE Order 435.1 requirements for the PA applies only to LLW disposed of after September 26, 1988, LLW disposed of since 1984 was included in this radiological performance assessment because that is when disposal of LLW, separate from TRU waste, began. The waste is physically located with the waste emplaced after 1988 and is easily modeled with the post-1988 waste. The Environmental Restoration Program at the INEEL will assess waste buried in the SDA from 1952 through 1983 in accordance with the National Contingency Plan under the Comprehensive Environmental Response, Compensation, and Liability Act (CERCLA). The year 1983 was selected as the cutoff date for waste to be assessed under CERCLA because waste containing the hazardous materials mercury and cadmium was disposed of in the SDA as late as June 1983. Therefore, the trenches, pits, and soil vault rows that were open before this date could potentially contain mixed waste, which falls under the domain of the Environmental Restoration Program, and will be assessed under CERCLA.

Because it is impractical to remediate only part of a pit or soil vault row, all waste buried in Pit 16 and Soil Vault Row 13 will be assessed under CERCLA even though Pit 16 closed October 25, 1984, and Soil Vault Row 13 closed on December 21, 1984. Soil Vault Row 14 opened on October 16, 1984, and Pit 17 opened on May 5, 1984; they should only contain LLW, not the mixed waste described previously. Therefore, the inventory analyzed in the performance assessment will begin with Soil Vault Row 14 and Pit 17. This provides an effective point of interface with the Environmental Restoration Program. This will ensure that all waste is accounted for either in the radiological performance assessment performed under DOE Order 435.1 or in the baseline risk assessments performed under CERCLA.

The remainder of this section provides background information about the RWMC and regulations, guidelines, and criteria (i.e., performance objectives) applicable to the LLW radiological performance assessment of the RWMC.

1.2 General Description of the RWMC

The INEEL is a DOE facility occupying approximately 2,315 km^2 of land in southeastern Idaho (see Figure 1-1). Activities conducted at the INEEL primarily involve nuclear research and development projects and experiments. The RWMC is one of several waste management facilities at the INEEL; it is the only operating LLW disposal area for solid radioactive wastes at the INEEL.

The RWMC provides a near surface disposal site for solid LLW generated primarily by INEEL activities. The RWMC opened in 1952 near the southwestern corner of the INEEL Site (see Figure 1-1). The initial tract of land used as a burial ground for radioactive waste was 13 acres. This tract became the SDA and was later expanded to 97 acres. In 1970, the 58-acre Transuranic Storage Area (TSA) was added to the RWMC. Over the years, service and operations buildings have been constructed. The SDA and TSA are surrounded by a security fence. A drainage system at the RWMC diverts runoff away from the facility.

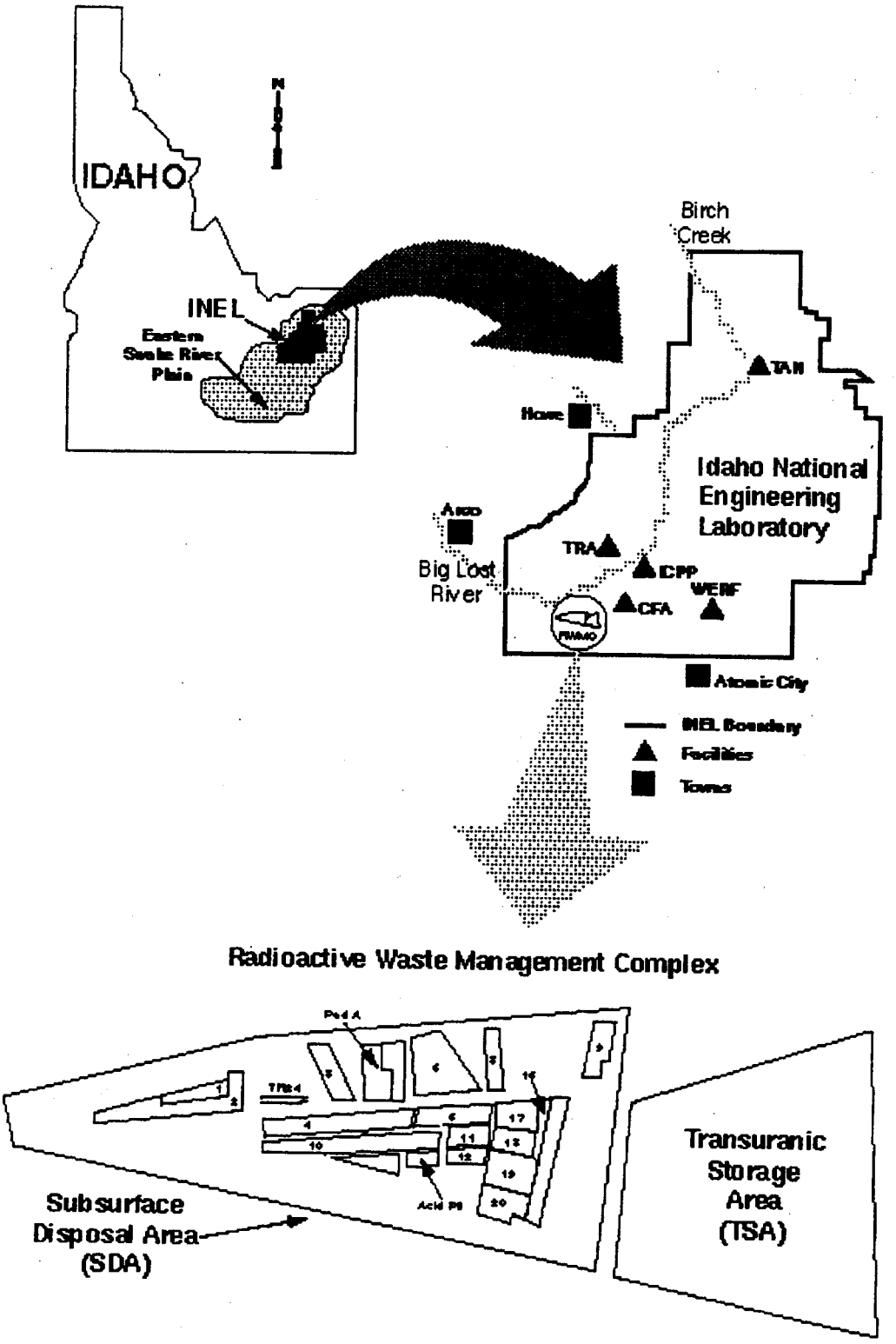

Figure 1-1. Overview of the INEEL, RWMC, and SDA.

Historically, most of the LLW arrived at the RWMC packed in containers such as large wooden boxes with plastic liners. Currently, metal boxes, soft-sided bags, drums, and bulk waste is received at the RWMC. Incineration, compaction, and sizing activities have been conducted on portions of the waste. Waste is buried in large pits that are excavated to a depth of 9 m. After the waste is emplaced, it is covered with 1 to 2 m of soil. Small quantities of LLW with radiation levels greater than 500 mR/hr were historically placed in cylindrical soil vaults drilled into the ground. Currently the vaults are lined with concrete.

LLW generated at the INEEL primarily consists of contaminated or potentially contaminated protective clothing, paper, rags, packing material, glassware, tubing, and other general use items. Also included is contaminated equipment (such as gloveboxes and ventilation ducts) and process waste (such as filter cartridges and sludges). These materials are either surface contaminated with radionuclides or are activated from nuclear reactions. Most of the radioactivity in the LLW at the time of receipt stems from short-lived radionuclides. Most of this LLW has an external exposure rate <500 mR/h at 0.9 m from the container surface.

Environmental surveillance programs are conducted onsite and offsite to monitor for any inadvertent release of radioactivity from the RWMC and the INEEL.

1.3 Performance Objectives

For the purposes of determining which performance objectives are applicable for the LLW analyzed in the RWMC radiological performance assessment, it should be noted that, by definition, the LLW does not contain nonradiological hazardous constituents and is not mixed LLW, TRU waste, high-level waste, or spent nuclear fuel.

The performance objectives for LLW disposal at DOE facilities and requirements for the performance assessment are contained in Chapter IV (Section P) of DOE Order 435.1:

1. **Performance Objectives**. Low-level waste disposal facilities shall be sited, designed, operated, maintained, and closed so that a reasonable expectation exists that the following performance objective will be met for waste disposed of after September 26, 1988:

    a. Dose to representative members of the public shall not exceed 25 mrem (0.25 mSv) in a year total effective dose equivalent from all exposure pathways, excluding the dose from radon and its progeny in air.

    b. Dose to representative members of the public via the air pathway shall not exceed 10 mrem (0.10 mSv) in a year total effective dose equivalent, excluding the dose from radon and its progeny.

    c. Release of radon shall be less that an average flux of 20 pCi/m^2/s (0.74 Bq/m^2/s) at the surface of the disposal facility. Alternatively, a limit of 0.5 pCi/l (0.0185 Bq/l) in air may be applied at the boundary of the facility.

2. **Performance Assessment.** A site-specific radiological performance assessment shall be prepared and maintained for DOE low-level waste disposed of after September 26, 1988. The performance assessment shall include calculations for a 1,000 year period after closure of potential doses to representative future members of the public and potential releases from the facility to provide a reasonable expectation that the performance objectives identified are not exceeded as a result of operation and closure of the facility.

   a. Analyses performed shall be based on reasonable activities in the critical group of exposed individuals. Unless otherwise specified, the assumption of average living habits and exposure conditions in representative critical groups of individuals projected to receive the highest doses is appropriate.

   b. The point of compliance shall correspond to the point of highest projected dose or concentration beyond a 100 meter buffer zone surrounding the disposed waste.

   c. Performance assessment shall address reasonably foreseeable natural processes that might disrupt barriers against release and transport of radioactive materials.

   d. Performance assessments shall use DOE-approved dose coefficients for internal and external exposure of reference adults.

   e. The performance assessment shall include a sensitivity/uncertainty analysis.

   f. Performance assessments shall include a demonstration that projected releases of radionuclides to the environment shal be maintained as low as reasonably achievable (ALARA).

   g. For the purposes of establishing limits on radionuclides that may be disposed of near-surface, the performance assessment shall include an assessment of impacts to water resources.

   h. For purposes of establishing limits on the concentration of radionuclides that may be disposed of near-surface, the performance assessment shall include an assessment of impacts calculated for a hypothetical person assumed to inadvertently intrude for a temporary period into the low-level waste disposal facility. For intruder analyses, institutional controls shall be assumed to be effective in deterring intrusion for at least 100 years following closure. The intruder analyses shall use performance measures for chronic and acute exposure scenarios, respectively, of 100 mrem (1 mSv) in a year and 500 mrem (5 mSv) total effective dose equivalent excluding radon in air.

Based on the Chapter IV requirements, the specific performance objectives for the RWMC performance assessment are shown in Table 1-1.

Table 1-1. Performance objectives for the RWMC.

Performance objective	*Dose or concentration limit*	*Receptor/scenario*
Atmospheric (40 CFR 61Subpart H)	10 mrem/yr EDE	Representative member of the public
Atmospheric (40 CFR 61Subpart Q)	20 pCi/m^2/s radon flux or 0.5 pCi/l radon concentration	Disposal facility surface or Boundary of facility
All pathways (DOE Order 435.1)	25 mrem/yr	Hypothetical future member of the public
Chronic inadvertent intrusion (DOE Order 435.1)	100 mrem/yr	Inadvertant intruder
Acute inadvertent intrusion (DOE Order 435.1)	500 mrem	Inadvertant intruder
Groundwater protection (40 CFR 141) (IDAPA 58.01.11)	4 mrem/yr EDE for β, γ [a] MCL[b] of 15 pCi/L for gross α [c] MCL of 5 pCi/L ^{226}Ra and ^{228}Ra MCL of 8 pCi/L ^{90}Sr MCL of 20,000 pCi/L ^{3}H MCL of 20 µg/L uranium[a]	Dose to a member of the public at INEEL boundary until 2120. Then, it is 100-m downgradient. MCLs are in groundwater at INEEL boundary until 2120. Then 100 m downgradient of RWMC.

a. Proposed rule Vol. 65, No. 78, April 21, 2000 pp. 21576-21628.
b. MCL = maximum concentration level.
c. Includes ^{226}Ra, excludes radon and uranium.

The following sections discuss (a) the performance objective for releases to the atmosphere, (b) the impacts of sole source aquifer designation on the performance objectives, (c) the INEEL Federal Facility Agreement and Consent Order, (d) the performance objective for groundwater protection, and (e) community water systems.

1.3.1 Releases to the Atmosphere

Subpart H of 40 CFR 61, "National Emission Standards for Emissions of Radionuclides Other Than Radon From Department of Energy Facilities," contains radiation dose standards for members of the public resulting from airborne effluents from DOE facilities. The performance objective contained in 40 CFR 61 Subpart H is an EDE of 10 mrem/yr through the atmospheric pathway for radionuclides other than radon. For radon, Subpart Q of 40 CFR 61, "National Emission Standards for Radon Emissions From Department of Energy Facilities," contains a radon flux standard of 20 pCi/m^2-s.

It is not specifically stated whether the performance objective contained in 40 CFR 61 Subpart H, as implemented in DOE Order 435.1, applies just to the LLW disposal facility or to the entire INEEL. However, the EPA, Region 10 approach to 40 CFR 61 Subpart H compliance considers the entire INEEL in the 10 mrem/yr compliance determination. On the other hand, in *Clarification of Requirements of DOE Order 5820.2A*,[a] it is specifically stated that "the performance objectives are intended to apply to each LLW facility on a reservation rather than to the reservation as a whole." Because of these inconsistent positions, it was decided to evaluate atmospheric emissions on both a single facility basis and on an INEEL-wide basis, using the present levels of INEEL emissions as a baseline, and a performance objective of 10 mrem/yr. No attempt was made to derive emission estimates for new facilities that may be built at the INEEL or for projects that may take place in the future.

1.3.2 Sole Source Aquifer Designation

The Eastern Snake River Plain Aquifer has been designated by the EPA as a sole source aquifer (EPA 1991a). After sole source designation, any Federal financial assistance projects are subject to EPA regulation to ensure that these projects do not contaminate the aquifer as to create a significant hazard to public health. However, the INEEL is operated by direct Federal funding and it is not funded through Federal financial assistance projects. Therefore, the designation of the Eastern Snake River Plain Aquifer as a sole source aquifer has no regulatory impact on the performance objectives used in the RWMC performance assessment.

1.3.3 Federal Facility Agreement and Consent Order

In 1989, the INEEL was added to the EPA National Priorities List of Superfund sites. In 1991, a Federal Facility Agreement and Consent Order (FFA/CO) was signed by the DOE Idaho Operations Office (DOE-ID), the EPA, and the Idaho Department of Health and Welfare (IDHW).

The Action Plan for the FFA/CO organized the INEEL into 10 Waste Area Groups (WAGs). The RWMC was designated as WAG-7; the RWMC contains 14 Operable Units (OUs). A comprehensive Remedial Investigation/Feasibility Study (RI/FS) is planned for the waste disposed in the RWMC from 1952 through 1993 (Becker et al. 1996). Forecast waste from 1994 through 2003 will be assessed as a sensitivity case. The work plan for the RI/FS (Becker et al. 1996) initially identified applicable or

---

a. Letter from T. B. Hindman to Distribution, February 28, 1989, and letter from T. B. Hindman to P. Saxman et al., March 28, 1989. These letters are contained in Dodge et al. (1989).

relevant and appropriate requirements (ARARs) for the RWMC. Maximum contaminant levels (MCLs) for radionuclides from 40 CFR 141, "National Primary Drinking Water Regulations," are identified as potential ARARs.

In previous risk assessments conducted at the INEEL as part of the FFA/CO, MCLs for radionuclides have also been used as ARARs for man-made beta particle and photon radioactivity, using a 2 L/d water consumption rate and the dose conversion factors in either DOE (1988b) or Federal Guidance Report No. 11 (Eckerman et al. 1988) (i.e., based on EDE, not total body dose). It should be noted that previous risk assessments have concentrated on OUs contaminated predominately with fission and activation products, not on OUs with significant actinide (i.e., uranium and plutonium) contamination. The ARARs for alpha emitting radionuclides at the RWMC will be determined as part of a phased process as remedial action alternatives appropriate for the site are identified.

1.3.4 Groundwater Protection

The Implementation Guide for use with DOE Manual 435.1 (DOE G 435.1-1) states that the performance assessment shall include an assessment of impacts to water resources. (DOE 1999b). However, DOE M 435.1 does not specify the level of protection for water resources that should be used in a performance assessment for a specific low-level waste disposal facility. Instead, a hierarchical approach, consistent with the Environmental Protection Agency strategy for groundwater protection, is recommended for establishing a site-specific groundwater protection objective.

The hierarchy for establishing water protection is as follows:

- First, the disposal facility must comply with any applicable State or local law, regulation, or other legally applicable requirements for water protection.
- Second, the disposal facility must comply with any formal agreement applicable to water resource protection that is made with appropriate State or local officials.
- Third, if neither of the above conditions apply, the site needs to select assumptions for use in the performance assessment based on criteria established in the site groundwater protection management program and any formal land-use plans.

If none of the above conditions apply, the site may select assumptions for use in the performance assessment for the protection of water resources that are consistent with the use of water as a drinking water source.

For the RWMC performance assessment, current MCLs specified in 40 CFR 141 (EPA 1991) of 5 pCi/L for Ra-226 and Ra-228 (combined) and 15 pCi/L for gross alpha particle activity, including Ra-226, but excluding radon and uranium, will be used. The concentrations that yield 4 mrem/yr total body dose currently specified in 40 CFR 141 of 20,000 pCi/L for H-3 and 8 pCi/L for Sr-90 will also be retained. The 4 mrem/yr effective dose equivalent (EDE) limit for beta particle and photon radioactivity from man-made radionuclides in the proposed revision of 40 CFR 141 (EPA 1991) will be used. In addition, the proposed MCL of 20 µg/L uranium (EPA 1991) will be adopted. This approach is consistent with that used for the previous analysis (Maheras et al 1997) and with guidance from DOE-ID[b].

---

b. Letter from S. P. Cowan to J. T. Case, June 20, 1996, "Groundwater Compliance for the Low-Level Waste Radiological Performance Assessment for the Radioactive Waste Management Complex at the Idaho National Engineering Laboratory."

The use of MCLs as the performance objective for groundwater protection is consistent with the designation of the Eastern Snake River Plain Aquifer as a sole source aquifer. After designation as a sole source aquifer, Federal financial assistance projects are reviewed to ensure that the sole source aquifer is not contaminated as to create a significant hazard to public health. The INEEL is operated by direct Federal funding and is not funded through Federal financial assistance projects, and therefore the Eastern Snake River Plain Aquifer is not subject to EPA regulatory authority. However, using MCLs as the performance objective is consistent with the philosophy of not creating a significant hazard to public health.

1.3.5 Community Water Systems

The closest onsite community water system originates at the RWMC production wells, just to the north but upgradient of the RWMC. The closest offsite community water system is in Atomic City, which is about 21 km southeast of the RWMC, but offgradient. There are no community water system wells in the vicinity of the nearest INEEL Site boundary, 5500 m downgradient.

The "National Primary Drinking Water Regulations" in 40 CFR 141 contain regulations that apply to radioactivity in community water systems (see §141.15 and §141.16). Public water systems provide piped water for human consumption and have at least 15 connections or regularly serve at least 25 people (§141.2); the category public water system is composed of community water systems and noncommunity water systems. Community water systems are public water systems that provide piped water for human consumption and have at least 15 connections used by year-round residents or regularly serve 25 year-round residents (§141.2). The regulations in §141.15 and §141.16 apply at the point of human consumption (i.e., at the tap, not in the groundwater). The IDHW Rules, IDAPA 58.01.08, "Idaho Rules for Public Drinking Water Systems," incorporate 40 CFR 141.15 and 141.16 by reference. Although there are currently no community water systems impacted by the RWMC, it is assumed that community water systems will exist at the point of compliance (100 m downgradient) and beyond after the period of institutional control (see Section 1.4).

In the RWMC performance assessment, the groundwater protection performance objectives (see the discussion in Section 1.3.4) will also be used as the performance objective for radionuclides in community drinking water systems. This approach is consistent with the approach used in risk assessments done at the INEEL as part of the FFA/CO. In addition, the groundwater protection analysis bounds the community water system analysis because (a) the performance objectives for groundwater protection and community water systems are identical, (b) the downgradient receptor locations for groundwater protection are closer to the RWMC than downgradient existing community water systems, and (c) the groundwater performance objectives apply before treatment, not after treatment at the point of use (i.e., at the tap).

1.4 Time Periods of Concern

For the purpose of assessing the performance of the LLW disposed of at the RWMC, three time periods are of concern: the operational period, the institutional control period, and the post-institutional control period. These periods are defined as follows:

- The operational period was assumed to last from 1984 to 2020, at which time the RWMC would be closed. Anticipated disposals of LLW through CY 2020 were included in the RWMC performance assessment to provide consistency with the planned operation of LLW disposal presented in the CA (McCarthy et al 2000). The waste inventory includes the amount accumulated from 1984 through 1999 plus the amount projected to accumulate from 2000 through 2020.

- The period of institutional control was assumed to last for 100 years, from 2021 through 2120, during which time maintenance and surveillance monitoring of the RWMC would continue and no additional waste would be disposed. During this time, the INEEL Site boundary would be maintained, restricting public access to the RWMC. A 100-year period of institutional control is consistent with the INEEL Comprehensive Facility and Land Use Plan (DOE 1996) and risk assessments done at the INEEL as part of the FFA/CO, pending decisions to be made in ongoing CERCLA activities.

- The post-institutional control period, beginning in the year 2120, is the period during which no maintenance or surveillance monitoring would occur. The INEEL Site boundary would cease to exist, and the area near the RWMC would be available for unrestricted access and use by the public. The maximum time of compliance is 1000 years.

1.5 Receptors

Two receptor types were assessed in this radiological performance assessment: (1) members of the public and (2) intruders. During the operational and institutional control periods, the member of the public resided at the INEEL Site boundary at the location of maximum exposure to contaminated air and water. This location is 8000 m SSW from the RWMC for the atmospheric transport calculations and 5,500-m downgradient of the RWMC at the southern INEEL boundary for the subsurface transport calculations. This receptor would be exposed to atmospheric releases from the RWMC and other INEEL facilities, which have a performance objective of 10 mrem/yr. This receptor also would be exposed to radionuclides in contaminated groundwater through all applicable exposure pathways; the appropriate performance objective for this analysis is 25 mrem/yr. The groundwater protection performance objective would also apply at the INEEL Site boundary during this time period. This approach is consistent with risk assessments done at the INEEL as part of the FFA/CO, which evaluate residential scenarios only at the INEEL Site boundary during the operational and institutional control periods.

During the post-institutional control period, the member of the public resided 100 m from the edge of the LLW disposal pits. This receptor would be exposed to atmospheric releases from the RWMC and other INEEL facilities, which have a performance objective of 10 mrem/yr. This receptor also would be exposed to radionuclides in contaminated groundwater through all applicable exposure pathways; the appropriate performance objective for this analysis is 25 mrem/yr. The groundwater protection performance objective (see Section 1.3.4.7) would now apply at 100 m from the edge of the LLW disposal pits during the post-institutional control time period. This approach is consistent with risk assessments done at the INEEL as part of the FFA/CO, which evaluate residential scenarios near the RWMC boundary during the post-institutional control period.[d]

The application of the all-pathways and groundwater protection performance objectives at the INEEL Site boundary during the operational and institutional control periods and at 100 m from the edge of the waste during post-institutional control was based on guidance from DOE-HQ.[e] This guidance states that the performance objective should be based on (a) a legally applicable State or local law,

---

d. FFA/CO risk assessments at the INEEL use the term post 100-year institutional control period instead of post-institutional control period.

e. Letter from S. P. Cowan to J. T. Case, June 20, 1996, "Groundwater Compliance for the Low-Level Waste Radiological Performance Assessment for the Radioactive Waste Management Complex at the Idaho National Engineering Laboratory."

regulation, or other legally applicable requirement for groundwater protection, or (b) a formal agreement with appropriate State or local officials applicable to groundwater protection. As stated previously, risk assessments done as part of the FFA/CO, an agreement between DOE-ID, the EPA, and the Idaho Department of Health and Welfare, evaluate residential scenarios at the INEEL Site boundary during the operational and institutional control periods. The risk assessments do not evaluate onsite residential scenarios and do not apply MCLs as ARARs for onsite residents during the operational and institutional control periods. During post-institutional control, residential scenarios near the RWMC boundary are evaluated in risk assessments done as part of the FFA/CO; therefore, the receptor location was moved to 100 m from the edge of the waste during the post-institutional control period.

Intruder scenarios do not apply during the operational or institutional control periods because access to the INEEL and the RWMC would be restricted. During the post-institutional control period, the intruder was assumed to inadvertently intrude onto the LLW. Two general kinds of intruder scenarios were evaluated: (1) a chronic exposure scenario and (2) an acute exposure scenario. These scenarios were based on a maximum time of compliance of 1000 years. The acute and chronic intruder analyses are based on drilling a well through the waste, an acute construction scenario and a chronic basement excavation scenario. In the acute well drilling scenario, the receptor was exposed to contaminated drill cuttings spread over the ground. In the chronic well drilling scenario, the receptor was exposed to contaminated drill cuttings spread over the ground and also obtained a portion of his food from farming at the RWMC. The intruder also was exposed to radon and its short-lived progeny that diffused through a basement foundation. In the acute construction scenario, the receptor excavates a basement in the waste in pits and is exposed to contaminated dust and waste. The acute construction scenario does not apply to soil vaults, because the soil cover is projected to be deeper than 3 m (the depth of the basement). Finally, in the chronic basement excavation scenario, an intruder excavates a basement and is exposed to contaminated material brought to the surface. The receptor ingests crops grown in the contaminated soil spread on the surface, breaths contaminated dust, and drinks contaminated water via a well drilled into the waste.

2. SITE BACKGROUND AND FACILITY DESCRIPTION

A description of existing conditions at the INEEL Site, RWMC description and waste characteristics, and planned RWMC environmental restoration activities may be found in the original RWMC performance assessment (Maheras et al 1994).

3. ANALYSIS OF PERFORMANCE

This chapter summarizes the conceptual model for the movement of contaminants at the RWMC. It describes potential exposure pathways and provides detailed descriptions of how important pathways were analyzed. The conceptual model for the RWMC is divided into three parts: (1) subsurface release and migration of radionuclides; and (2) atmospheric transport and hypothetical intruder scenarios; and (3) exposure pathways. Sections 3.1 and 3.2 address the subsurface portion of the performance assessment. Sections 3.3 and 3.4 address atmospheric, all-pathways, and intruder scenarios and exposure models.

The assumptions and model summary presented for the subsurface analysis are essentially the same as the description provided in the RWMC Low Level Waste Composite Analysis (McCarthy, et. al. 2000). The conceptual model used to assess atmospheric and intruder scenarios has not been modified from the initial performance assessment (Maheras et al, 1994). However, the methodology used to assess atmospheric and intruder scenarios has been modified from that used in the initial PA and in the addendum (Maheras et al, 1997).

The methodology used to assess the potential subsurface migration of radionuclides from the various sources and the resulting doses to a potential receptor consists of: (1) modeling the source term and release using the DUST-MS code, (2) using the DUST-MS output as input to the TETRAD subsurface transport modeling code, (3) using the output from TETRAD (radionuclide groundwater concentrations) as exposure concentrations in the exposure scenarios, and (4) calculating the predicted radiological dose to the public. Included in Sections 3.1 and 3.2 are a description of the Performance Assessment (low-level waste facility) and SDA closure assumptions, source term release and transport.

3.1 RWMC SDA Closure Assumptions

The final selection of remedial actions for WAG-7 is in progress and a final Record of Decision is expected sometime in the future. For this technical update of the Performance Assessment, it is assumed the RWMC SDA will be closed without any removal of waste and that the entire SDA, including the low-level waste facility will be covered with a surface barrier, and that land-use restrictions are required. Subsequent iterations of the Performance Assessment will incorporate any alternate remedial strategies for the SDA resulting from the CERCLA decision process.

The final design of a surface barrier for use at the SDA has not been selected; therefore, for the Performance Assessment, the RWMC surface barrier is assumed to be constructed of local soil material. It is assumed the surface barrier will reduce infiltration to at least to the ambient background infiltration rate of approximately 1 cm/yr. Maintenance of the surface barrier is assumed to be minimal as the local area including the RWMC is within a sediment depositional zone and the re-establishment of indigenous vegetation on the surface barrier will reduce infiltration to background. Therefore, it is assumed that background infiltration rates will be achieved for at least 10,000 years.

Ongoing investigations at the Engineered Barriers Test Facility (EBTF) are being conducted to test and select engineered surface barriers for adequate closure of the active LLW disposal facility. Barrier performance data resulting from the engineered barrier testing and cover selection will be incorporated into subsequent iterations of Performance Assessment and will be used to develop the final closure cover design and closure plan for the entire SDA.

The Performance Assessment evaluates an infiltration-reducing cap emplaced in the year 2021, after the operational period ends in 2020. An infiltration rate of 1 cm/year is assigned uniformly across the SDA beginning in 2021 and continues in perpetuity. The cover is assumed to consist of additional soil emplaced across the SDA with a vegetated cover. This 1 cm/yr infiltration rate is the same as that

used for the upper boundary condition in the rest of the simulation domain outside the SDA boundary. This 1 cm/yr infiltration rate is believed to be achievable based on Magnuson (1993) simulation study. In this study, a vegetated thick soil barrier is shown to have an estimated net annual infiltration rate of approximately 1 cm/yr. An ongoing study funded by Waste Management and Environmental Restoration at the Engineered Barriers Test Facilities (EBTF) is intended to substantiate this estimate. There has not been any substantiation yet because the EBTF has been monitoring unvegetated conditions. Plans call for switching to vegetated conditions in the fall of CY 2000.

A concern when using a barrier in predictive subsurface pathway simulations is the long-term effectiveness of the barrier. The type of barrier assumed for the subsurface pathway simulations does not involve flexible membrane liners of any type so there is essentially nothing that can fail, with the exception of subsidence. Subsidence events could lead to depressions in the surface that would focus infiltration. It is reasonable to assume that this barrier will be maintained during the 100-yr institutional control period and that any subsidence that occurs in the cover will be rapidly corrected. Another assumption is that subsidence events will cease at some point during the minimum 100-yr institutional control period. After the end of institutional control, it is anticipated that the cover will continue to function since the SDA is in a net depositional sediment area (Forman, 1991).

3.2 Source Term Release and Transport

The modeling performed for the Performance Assessment relies extensively on both the results and the methodology of recent modeling efforts conducted for the RWMC (WAG-7) IRA (Becker et al..1998; Magnuson and Sondrup, 1998). Guidance for the Performance Assessment and Composite Analysis stipulate use of best-estimate waste inventory data, however, the IRA used upper-bound waste inventory estimates. For the lesser or low-risk radionuclides, the results of the IRA (Becker et al., 1998) were scaled to provide CA groundwater concentrations based on the best-estimate waste inventory data and projected waste disposal. Using these results, the contaminants of concern (COPC)for the CA were identified. The COPCs are C-14, Cl-36, I-129, Np-237, U-234, and U-238. Because the PA is a subset of the CA, it was assumed that the PA contaminants of concern are the same as the CA. The groundwater simulations were rerun with updated PA waste disposal inventories for these major radiological risk drivers.

3.2.1 Source Term Model

DUST-MS was used to predict releases from buried waste into the shallow subsurface by modeling container failure and eventual release from the waste (Sullivan 1993). DUST-MS is a one-dimensional model that has three waste form release mechanisms: surface washoff, diffusion, and dissolution. The surface washoff model can be used to estimate the release from general laboratory trash and is equivalent to the first-order leach model used in other codes such as GWSCREEN (Rood 1994). The diffusion model computes the diffusion release from different waste geometry's based on user-supplied diffusion coefficients for each waste form. Diffusion of contaminants from cement-encased waste was estimated with the diffusion release model. The dissolution release model was used to estimate the release caused by general corrosion such as the release of activated metals from the corrosion of the base metal. The simulated mass release is then used as input into the subsurface flow and transport model that was developed with the TETRAD transport modeling code (Vinsome and Shook 1993). Because the release and transport were calculated for a large number of radionuclides, the radionuclides were grouped for fate and transport simulation. Members of a decay chain were in a single group. Other radionuclides with similar retardation values were also grouped. Isotopes in the chain with a half-life of more than one year were included in the simulations. Shorter half-life contaminants were handled by assuming they were in equilibrium with the longer half-life parent and adding the respective toxicity values. This grouping was used in the source term simulations to provide a consistent set of inputs for all of the simulations. Inputs

for the source term model are discussed below and include: (1) waste inventory source term, (2) container failure rates, and (3) waste stream and contaminant-specific release rates.

3.2.1.1 Waste Inventory Source Term. For radionuclides critical to the performance of the active LLW disposal pits at the SDA, the source term used in this PA update is the (1) latest CIDRA (LMITCO 1995a; LMITCO 1995b) inventory with (2) supplemental data for data gaps identified and reconciled in key waste streams from ANL-W, NRF, TRA, and the SMC at TAN, (3) 1994-1999 disposal information obtained from IWTS and (4) projections for 2000-2020 based on the 1994–1999 disposal history.

The waste stream updates will be incorporated into CIDRA in the future. Carboneau (1998) provides a reassessment of neutron activation product radionuclides in EBR-II core non-fuel bearing structural metal hardware disposed from ANL-W. Abbott (1997a,b) and Bradley (1998) provide refined estimates of key environmental radionuclides in NRF core structural waste and expended ion exchange resin waste disposed in the SDA. Schnitzler (1995) calculated refined estimates of the radionuclide inventories in ATR beryllium (Be) reflector blocks and outer shim control cylinders. The data of Schnitzler (1995) were extrapolated by Honeycutt (1998) to estimate the inventory of selected radionuclides in the reported Be block disposals from TRA. Sterbentz (1998) has calculated key environmental radionuclide estimates for all core components removed from the ATR core per the Core Internal Change-out schedules. The ATR core component inventory disposed in the RWMC SDA is not determined therefore, the estimate provides a conservative upper limit. Schnitzler (1995) has calculated an estimate of C-14 production in ATR coolant, providing a basis for the determination of Abbott (1998) for estimated C-14 inventory in TRA resin disposal shipments to the SDA.

Past radiological disposals were decayed to the present, and then release simulations were performed. Yearly waste disposal inventory was used in the Performance Assessment to allow decay and release calculations to begin at the actual year of disposal. This approach prevents underestimation of mobile contaminants with short half-lives. DUST-MS was modified to allow a delay time to be input. Decay and release calculations did not commence until after the input delay time. Inputting the yearly disposal quantity with the appropriate delay time allows direct input of the yearly quantities of contaminants without having to correct for decay until the year of disposal. Validation cases were run to ensure that this change did not affect the release models other than delaying the start of release calculations.

3.2.1.2 Container Failure Rates. Before a contaminant can be released to the environment from the waste form, the containment in which the waste is buried must first degrade. If a contaminant is buried in drums, the contaminant will not be released until the drums are breached. DUST-MS allows the user to specify the time until container failure. If the waste disposal were performed without containment, then the failure time is set at zero and the release mechanisms control the release of the contaminants from the waste. Once the container is breached, the waste is released to the subsurface according to the release mechanisms that are appropriate for that waste stream.

The source term model used the yearly disposal information to assign container type for calculation of the release. In the model, each container had a prescribed time until failure from the time of emplacement. A single contaminant might reside in multiple containers buried in a given year because of the different waste form or different containment to be modeled. For example, if the disposal contents of a particular waste stream were buried in metal containers and in cardboard boxes, two container types would be used to model that year's disposal. One container type would be for the amount of the inventory in the metal containers, and the other container type would be for the amount in cardboard boxes.

Individual waste streams were evaluated for the type of containment used. The disposal contents of many waste streams were buried in wood or other readily degradable boxes. It was assumed that these readily degradable "containers" do not hinder contaminant movement; therefore, no delay of the contaminant release was assumed for the boxes in the model. Polyethylene bags were not accounted for in the release modeling either. This is a conservative assumption for contaminants other than tritium and carbon-14 that may be present in the gas-phase. The 55-gal drums, concrete casks, and metal boxes offer a barrier to contaminant release that is accounted for in the source term model. Waste in the containers is released only after the drums, casks, or metal boxes are assumed to have failed. Waste streams listed as "O" (other) in CIDRA, or as a mix of containment types without a breakdown of the actual amounts in each type, were modeled as having no containment.

The carbon steel corrosion rate (see Table 3-1) was used to determine the failure time of the metal boxes. Release from concrete casks was modeled as a diffusion release from a nominal 15-cm (6-in.) wall thickness cylinder. Using this thickness assumption is conservative for early releases because it assumes that the waste is at the surface of the cask and is readily released. In addition, a conservative diffusion endpoint of 1.0E-06 cm^2/g was used. This is a typical diffusion coefficient for a metal ion in water and is conservative because it does not account for the possible partitioning of the contaminant with the waste form or the porous media that the contaminants must travel through. Any partitioning would slow the contaminant release.

A portion of the containers buried in the SDA are 55-gal drums. A separate study was performed to determine the failure rate of these drums using data gathered during earlier waste retrieval efforts (Becker 1997). The study indicates dumped drums fail more rapidly than stacked drums. Therefore, the two drum disposal methodologies are treated accordingly.

3.2.1.3 Release Mechanisms. DUST-MS has three release models: (1) diffusion, (2) dissolution, and (3) surface washoff. Each contaminant's yearly disposal has been proportioned among the release mechanisms. The percent in a release mechanism is input into DUST-MS. The total disposal inventory has been analyzed to determine the release mechanism and release rate as a function of the waste stream contents put in storage in any given year. Because each contaminant has a unique set of information, each year's disposal for each contaminant is modeled as a separate waste container. The results are summed to provide the total release over the time interval for input into the transport models. Table 3-1 is a summary of the release rate information for the different release models.

Waste streams that have metal listed as the primary waste form can be either a dissolution release (corrosion of the base metal) of activation products or surface washoff (contamination on the metal). Metal waste streams will generally be a surface washoff release for actinides and fission products and dissolution (corrosion) for activation products. Table 3-2 lists the grouping and release mechanism for radionuclides having metal waste streams. Actinides and fission products are surface contaminants on the base metal. The activation products are the result of activation of the base metal and generally are released only as the metal corrodes. Activation products such as Na-22 produced within the coolant and not in the structural components are modeled as surface contamination using the surface washoff model.

Table 3-1. Release rate coefficients.

Contaminant Release	Model Used	Rate	Comment
Release from Be corrosion (diffusion is negligible)	Dissolution	3.0E-04/yr	Nagata (1993)
Release from corrosion of stainless steel	Dissolution	4,500 yr/mm	Nagata (1997)
Release from corrosion of carbon steel	Dissolution	450 to 680 yr/mm	Banaee and Nagata (1996)
Release by leaching	Surface washoff	Soil-to-water partition coefficients	Dicke (1997a)
Release from resin	Surface washoff	Soil-to-water partition coefficients	Dicke (1997a)
Release of metal by corrosion	Surface washoff	Contaminant solubility	Dicke (1997a)

Table 3-2. Metal waste stream release mechanisms.

Group	Release Mechanism	Contaminant
Fission products	Surface washoff	Cs-137, Eu-154, I-129, Sr-90
Activation products	Dissolution	C-14, Co-60, Ni-59, Ni-63, Nb-94, Tc-99
Activation products	Surface washoff	C-14, Cl-36
Actinides	Surface washoff	Am-243, Cm-244, Np-237, Pu, U

For the PA, the corrosion rate of 4,500 yr/mm for stainless steel was taken from Nagata (1997). For metals other than stainless steel such as uranium, the release of the metal into the subsurface is dependent on the chemical properties of the soil water and the solubility of that metal in the INEEL pore water conditions. The soil water has a high pH, causing many contaminants to have a low solubility. To simulate the release of metals like uranium, the surface washoff model has been used with the appropriate solubility limit (Becker et al., 1998; Section 5.2) for the INEEL soil water chemistry.

A surface washoff release mechanism is also used for waste streams that are generic laboratory trash. The surface washoff release mechanism provides the most conservative release rates. Similarly, contaminants identified as surface contamination of a base material, such as radionuclides on anti-contamination clothing, are modeled with the surface washoff model. The surface washoff model uses a partition coefficient to determine the release. As a first approximation, the soil-to-water partition coefficient was used.

Table 3-3 shows the percentage of the disposal of each radionuclide in resins. C-14 in ion exchange resin constitutes a significant potentially mobile fraction. Therefore, it was conservatively assumed that release from ion exchange resin was at the lower end of the K_d range for C-14 in soil, or 0.1 mL/g. The release from resins was then modeled using the more conservative surface washoff release based on the soil-to-water partition coefficients.

Table 3-3. Percentage of contaminant disposal in resins.

Radionuclide	Waste Stream Number	% of Individual Isotope Disposed of in Resins
C-14	TRA-603-1H	9.1
Cm-244	TRA-603-1H	25.7
Co-60	TRA-603-1H	2.5
Cs-137	TRA-603-1H	7.0
Eu-154	TRA-603-1H	39.3
I-129	TRA-603-1H	9.8
Ni-59	TRA-603-1H	6.9
Ni-63	TRA-603-1H	3.7
Pu-238	TRA-603-1H	1.2
Pu-239	RFO-DOW-13H	1.1
Pu-240	RFO-DOW-13H	1.1
Pu-241	RFO-DOW-13H	1.1
Pu-242	RFO-DOW-13H	1.0
Sr-90	TRA-603-1H	9.8
U-234	TRA-603-1H	1.0
U-236	TRA-603-1H	10.9

Beryllium corrosion was studied for the revised SDA scoping risk assessment (Burns et al., 1994) and the RWMC performance assessment (Maheras et al., 1994). Beryllium corrosion primarily controls the release of H-3 and C-14 because beryllium reflector blocks contain most of the H-3 and C-14 that was disposed. The predicted fractional release is within a factor of three for the two studies. The Nagata (1993) study results were used in this performance assessment because they are more conservative.

3.2.1.4 Pit and Trench Grouping. The pits and trenches were grouped for the simulations because DUST-MS is a one-dimensional model that cannot model them individually without numerous separate simulations. Separate simulations were impractical considering the number of contaminants to analyze for in each pit and trench. In addition, the exact disposal location is not always available. An analysis of the contaminant disposal shows a distinct difference in the waste types buried before 1970 and after 1970. Current LLW waste disposal (waste buried during 1984 and after) must meet contemporary SDA waste acceptance criteria. Before 1970, hazardous, mixed, LLW, and TRU waste were accepted for disposal at the SDA. After 1970, TRU waste was no longer accepted. After 1984, hazardous and mixed waste was no longer accepted. Therefore, the waste was divided into three groups based on the time that the pit or trench was open. Pits and trenches opened before 1970 were in one group, pits and trenches opened after 1970 but before 1984 were in a second group, and pits opened after 1984 were in a third group. The simulated source release from the three waste stream groups was input into the subsurface pathway model as shown in Figure 3-1. Figures 3-2 and 3-3 show the simulated DUST source releases for the radionuclides that were re-simulated in the PA.

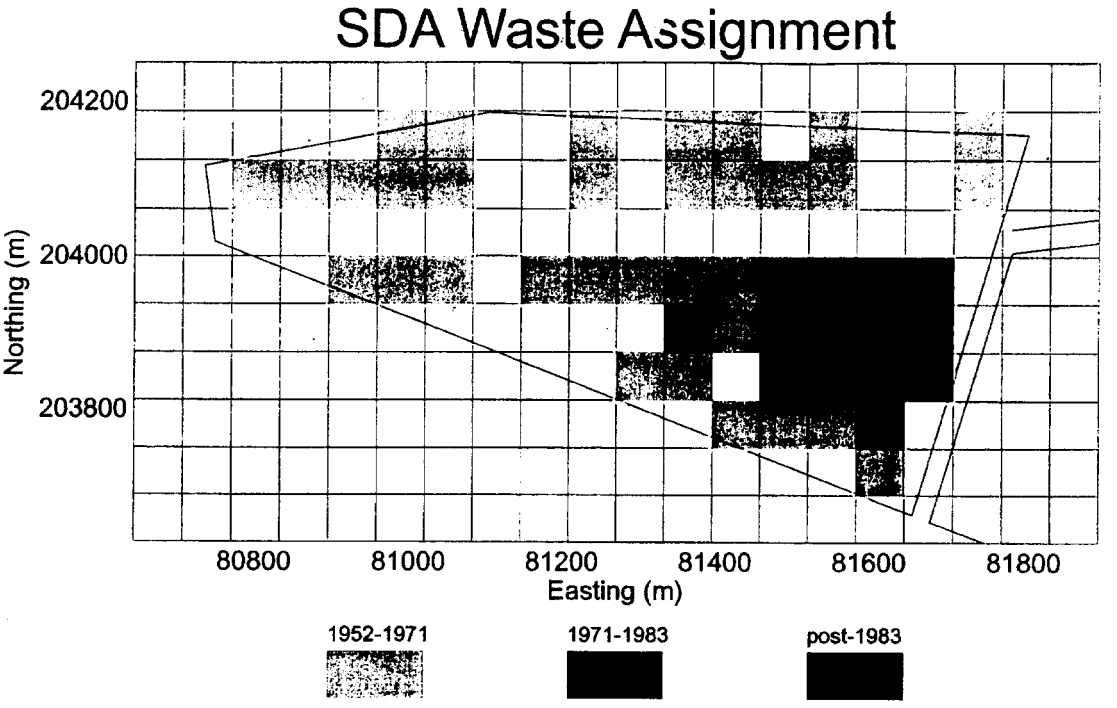

Figure 3-1. Distribution of three waste streams into the third level of grid refinement of the subsurface model. Post 1983 is the PA disposal.

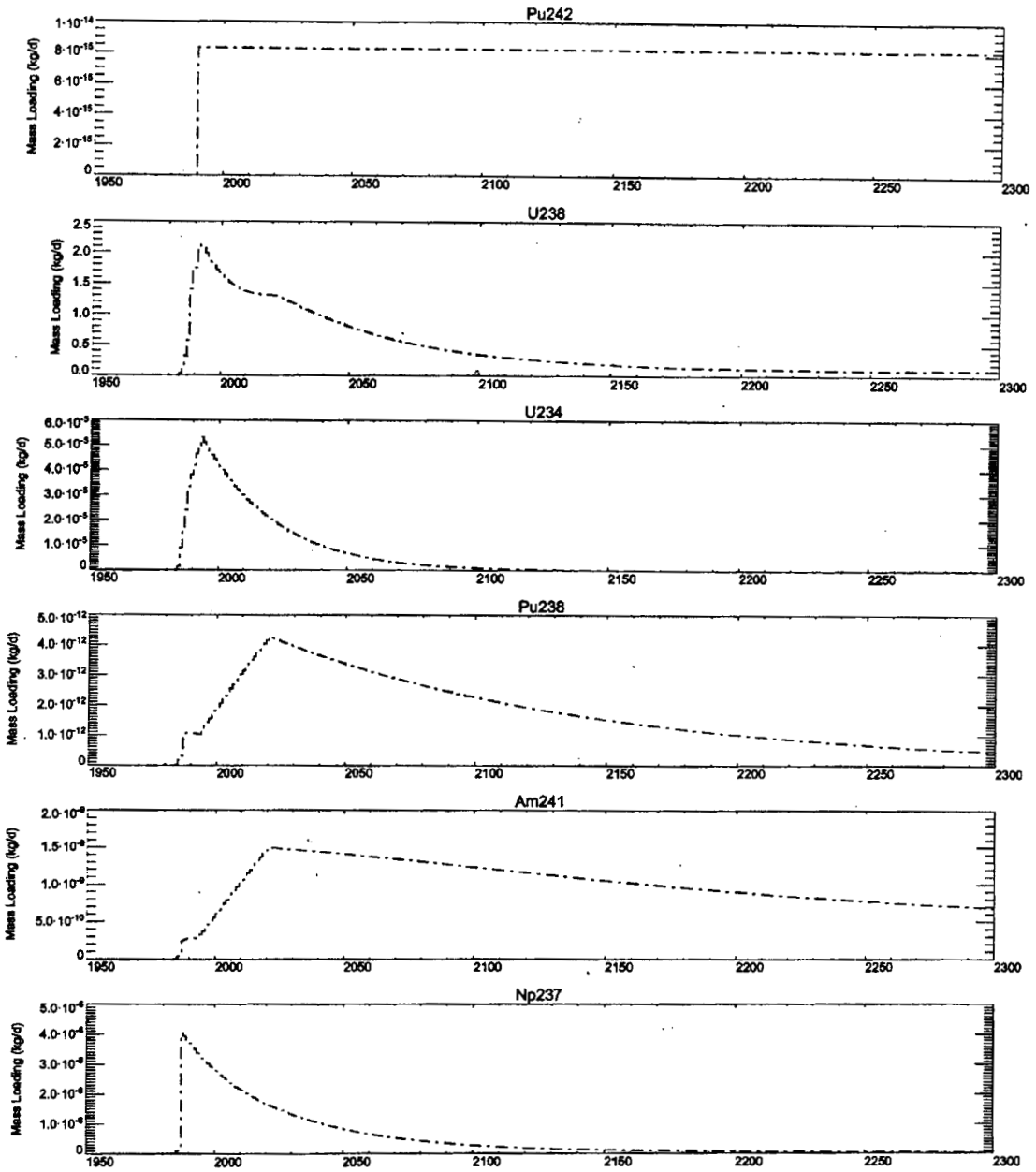

Figure 3-2. Simulated DUST source releases for uranium and other actinides.

receptor using the ISCST3 computer and INEEL specific atmospheric dispersion conditions. The RESRAD computer code was used to calculate doses. Radioactive progeny were included in the calculations.

Impacts from the subsurface migration of radionuclides dissolved in groundwater were estimated using computer models that described release of radionuclides from the RWMC pits and soil vaults and transport in the unsaturated zone and aquifer. A source term model (DUST) that accounted for the time-dependent waste emplacement rate, waste form type, container integrity, and variable infiltration rate, was coupled to the TETRAD code. The TETRAD code was used to calculate transport in the unsaturated zone and aquifer. Concentrations were estimated in the aquifer at a hypothetical receptor well located 100 m downgradient from the edge of the RWMC active pits and at the INEEL Site boundary. Decay and sorption were included throughout the model and reduced or slowed the migration of radionuclides in the subsurface.

This representation of subsurface transport is undoubtedly greatly simplified over the true processes that occur, reflecting the lack of definitive understanding of water movement in the subsurface beneath the RWMC. As a result, the predictive concentrations used in this radiological performance assessment are affected by the uncertainties regarding these processes. An uncertainty analysis was performed on the hydrological transport model to assess the uncertainty of the calculations. Because the extremely long run times associated with TETRAD make uncertainty analysis of this code impractical, a simpler transport model, GWSCREEN, was calibrated to the TETRAD results, was used. The results of the uncertainty analysis indicate that the doses at the 95th percentile are all below the all-pathway performance objective of 25 mrem, within the 1000 year time frame of compliance.

The results of the atmospheric, all-pathways, inadvertent intruder, and groundwater protection analyses are shown in Table ES-1, based on a maximum time of compliance of 1000 years. These results indicate that the atmospheric, all-pathways, chronic intrusion, and acute intrusion performance objectives will be met.

If the time of compliance were extended to 10,000 years, the performance objectives for the atmospheric, all-pathways, inadvertent intruder, and groundwater protection scenarios would still be met, with the exception that the groundwater protection standard of 20 μg/L for uranium would be exceed by ten times (i.e., 200 μg/L). This reflects downgradient subsurface transport of long-lived uranium.

Table ES-1. Comparison of performance objectives and RWMC performance assessment results.

Performance Objective	Standard	RWMC Performance Assessment Result
Atmospheric (40 CFR 61 Subpart H)	10 mrem/yr EDE **(entire INEEL site)**	0.0086 mrem/yr during operational and institutional **control periods (entire INEEL, including RWMC)**
		0.46 mrem/yr during post-institutional control period (entire INEEL, incuding RWMC)
Atmospheric (40 CFR 61 Subpart Q)	20 pCi/m^2-s radon flux	0.37 pCi/m^2-s
All-pathways (DOE Order 5820.2A)	25 mrem/yr	**0.0022 mrem/**yr during operational and institutional control periods
		5.49 mrem/yr during post-institutional control period
		15.9 mrem/yr (at 10,000 years)
Chronic inadvertent intrusion(DOE Order 451.1)	100 mrem/yr	*Soil vaults (1000 year time of compliance)*
		22.0 mrem/yr (drilling)
		0.1 mrem/yr (biointrusion)
		0.001 mrem/yr (radon)
		22.1 mrem/yr total
		Soil vaults (maximum impact within 10,000 years)
		22.0 mrem/yr (drilling)
		0.11 mrem/yr (biointrusion)
		0.09 mrem/yr (radon)
		22.2 mrem/yr total
		Pits (1000 year time of compliance)
		0.35 mrem/yr (basement excavation and drilling)
		0.01 mrem/yr (biointrusion)
		52.1 mrem/yr (radon)
		52.5 mrem/yr total

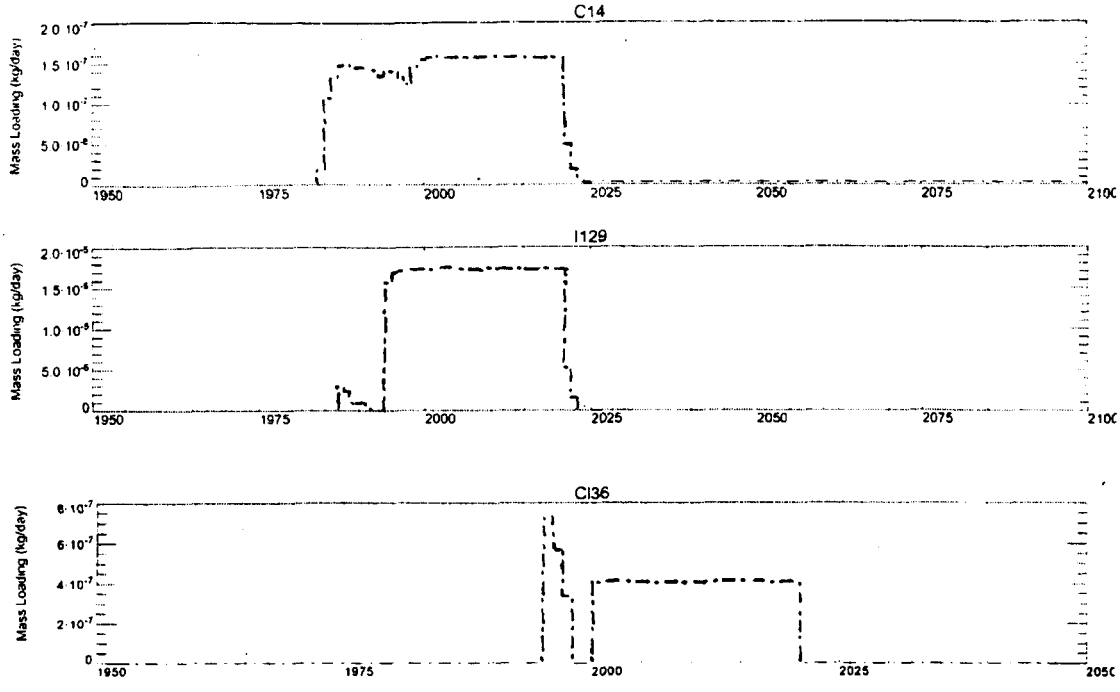

Figure 3-3. Simulated DUST source releases for C-14, I-129, and Cl-36.

3.2.2 Subsurface Model

The subsurface model was developed in stages. First, a flow model was developed that describes the movement of water in the subsurface. This model includes hydraulic descriptions of each lithologic material in the subsurface and boundary conditions related to water sources both from infiltration of water at the surface and from horizontal movement of water within the Snake River Plain Aquifer (SRPA). Calibration of the flow model was obtained by adjusting hydraulic input parameters in the model until simulated water movement agreed with observed water level measurements. Second, a transport model was developed describing the movement of contaminants dissolved in either water or in air. Contaminant release time histories obtained from the source term model were input into the subsurface model and were described in Section 3.2.1. The transport model consists of parameterizing dispersion, diffusion, decay, and sorption and describing additional boundary condition effects that affect pressure and therefore advection within the gaseous phase. Aqueous phase advection was parameterized by the flow model. Calibration data is limited but calibration of the transport model, to the degree possible, was achieved by comparing simulated concentrations of indicator contaminants to observed aquifer concentrations and adjusting transport parameters and boundary conditions to improve the agreement. The flow-and-transport model was used to make predictive simulations. A complete description of the subsurface model developed and used for predictive simulation can be found in Magnuson and Sondrup (1998). A brief overview of the model is presented in the following section.

3.2.2.1 **Conceptual Model for Flow and Transport.** Contaminant fate and transport was simulated for contaminants that exist in a dissolved or aqueous phase and for contaminants such as tritium that could simultaneously exist in both aqueous and gaseous phases. The general conceptual model for flow treats water movement as if the subsurface consisted of a heterogeneous, anisotropic porous medium. Infiltration of meteoric water into the subsurface could be either transient or described by

constant average infiltration rates. The surficial sediments and sedimentary interbeds are simulated with varying thickness and upper surface elevations. Known gaps in the interbeds are included in the model. In the fractured basalt portion of the subsurface, flow is considered to only occur within the fracture network to emulate a medium with a low effective porosity but high permeability. Movement of water within the SRPA is assumed to be steady state given the long time duration of hundreds to thousands of years considered in the subsurface pathway model.

For the dissolved-phase transport conceptual model, the processes that were considered were advective, dispersive, diffusive, radioactive chain decay and ingrowth, and adsorption onto solid surfaces. Because modeled water movement in the basalt was restricted to the fractures, sorption in these same regions was restricted to the surfaces of those fractures. Fracture surfaces were considered lined with either fine-grained sediments or chemical alteration products that resulted from water movement along the fractures over extended periods of time. This treatment of sorption necessitated only K_d values for sorption onto sediments and did not require estimates of sorption onto the basalt matrix itself. Because the sediment lining the basalt fractures makes up a small portion of the basalt region of the model, the basalt K_d values were scaled down from the sediment K_d values. This scaling resulted in basalt K_d values that are small for all contaminants and negligible for all contaminants with sediment K_d values less than 1,000 mL/g. The K_d values used in the model (Table 3-4) were assigned based on best-estimate values from Dicke (1997a), rather than conservative screening values.

Facilitated transport mechanisms, such as colloidal transport, are possible beneath the SDA. However, these transport mechanisms have not been documented as taking place at the SDA, therefore, facilitated transport mechanisms have not been included in the transport conceptual model. Single isolated detections of contaminants have occurred in subsurface contaminant monitoring at the SDA. While these detections may be real, it is not feasible with the current modeling approach to try to emulate each and every one of these isolated detections. Rather the subsurface transport model attempts to mimic the large-scale overall behavior of contaminants in the subsurface. This means the model attempts to emulate those contaminants that are consistently present in a distributed sense in the subsurface. Therefore, for purposes of model calibration, these isolated detections were neglected.

For contaminants that also migrate in the gaseous phase, such as tritium, the conceptual model was expanded to include a dual-porosity approach in which the contaminants could also diffuse or advect into the low permeability basalt matrix from fractures within the basalt. However, the majority of water and contaminant movement still occurred within the fractures in the basalt. Influences on advective movement of gaseous phase contaminants from barometric pressure fluctuations at the surface, positive pressure air injection during drilling of wells in the SDA, and the effects of several vapor-vacuum extraction remedial activities were also considered. Advective flux of contaminants out of the simulation domain was allowed at perimeter locations in the model.

3.2.2.2 Simulation Code. The TETRAD code (Vinsome and Shook 1993) was used to simulate flow and contaminant transport. Documentation of the selection process is discussed in Becker et al., (1996). Verification and validation (Shook 1995; Magnuson 1996) were conducted to demonstrate the proficiency of the TETRAD simulator for use in modeling subsurface fate and transport at the SDA.

TETRAD has complete multi-phase (aqueous, gaseous, and oleic), multi-component simulation capabilities. TETRAD uses a block-centered finite-difference approach and has capabilities for local grid refinement, which were used extensively. The TETRAD simulator also includes dual porosity simulation capabilities. This feature was used to address gaseous phase movement in both the fracture and matrix portions of the fractured basalts composing the majority of the subsurface beneath the SDA.

Table 3-4. Soil-to-water distribution coefficients used in modeling (Dicke 1997b).

Element	Sediment K_d (range) mL/g	Comments
Am	450 (450 to 1,100)	Measured values
C	0.1 (0.1 to 1.5)	Site-specific values
Cl	0	Anionic and will not react with sediments
Cm	400 (400 to 1,000)	Americium analog
Co	1,000 (50 to 4000)	Site-specific values
Cs	1,000 (589 to 3255)	Site-specific values
Eu	400 (400 to 1,000)	Americium analog
H	0	Nonreactive
I	0.1 (0.02 to 5)	Literature values
Nb	500 (100 to 1,000)	Literature values
Ni	300 (60 to 2,000)	Literature values
Np	8 (1 to 80)	Literature values
Pu	5,100 (5,100 to 22,000)	Site-specific values
Ra	575 (88 to 1,890)	Literature values
Sr	60 (35 to 186)	Site-specific values
Tc	0	Site-specific values
Th	500 (200 to 3,000)	Literature values
U	6 (3.4 to 9)	Site-specific values
Ac	400 (400 to 1,000)	Americium analog
Pb	270 (30 to 1,000)	Analogs and literature
Pa	8 (1 to 80)	Neptunium analog

3.2.2.3 Model Implementation. To achieve a representative flow simulation, spatially variable thickness of the surficial sediments, sedimentary interbeds, and fractured basalts composing the subsurface were included in the modeling effort. Data from ninety-two wells in the SDA vicinity were used to generate the surfaces and thickness of each lithologic unit. These surfaces and thickness were then mapped onto a three-dimensional simulation grid that extended from land surface to the effective depth [76-m 249-ft)] of the SRPA in the vicinity of the SDA. The horizontal simulation domain extended from north of the SDA to the southern INEEL boundary (Figure 3-4). The numerical discretization is relatively fine in the immediate vicinity of the RWMC and is more course further from the facilities. The Big Lost River and outline of the spreading areas are include in the figure. Known gaps or locations of zero thickness in the sedimentary interbeds were also included in the lithologic representation.

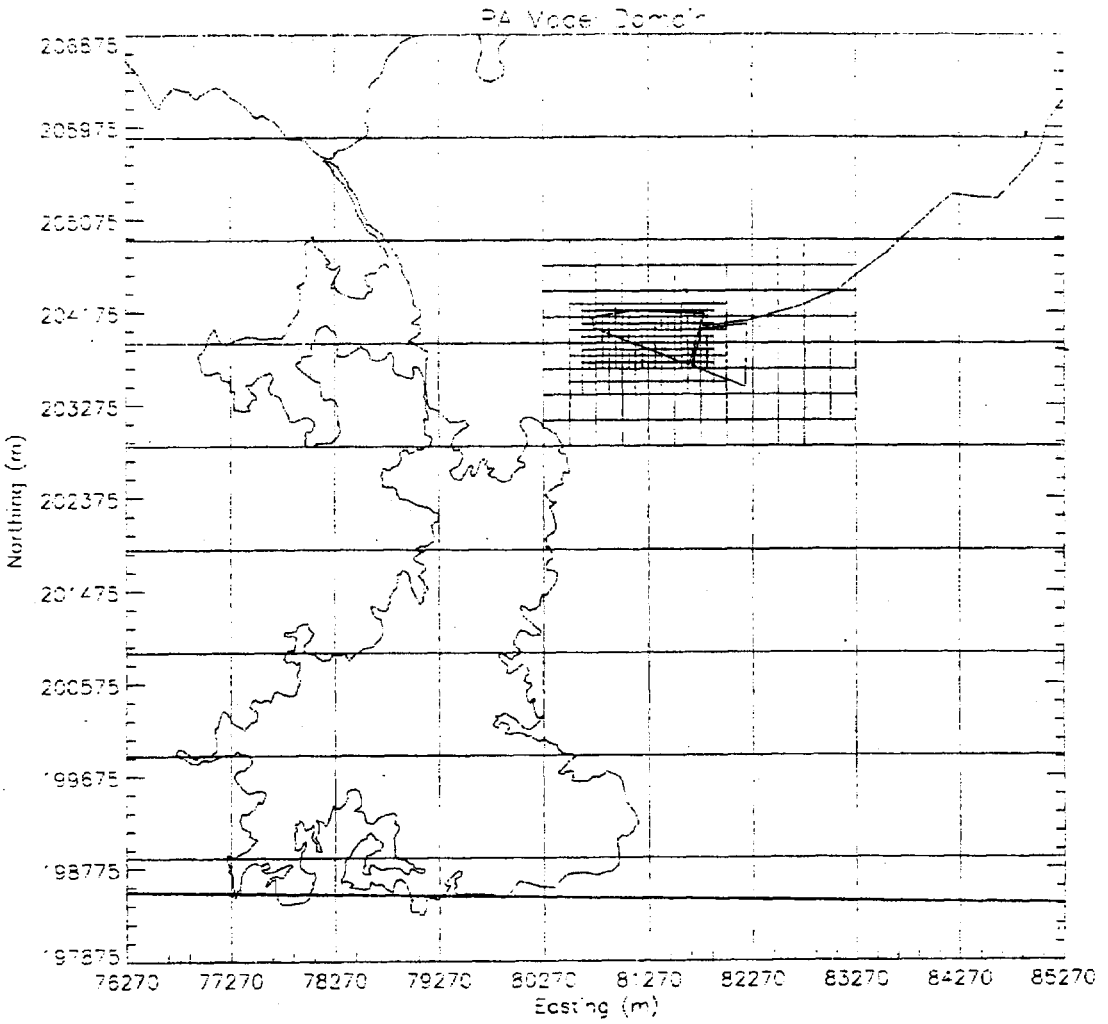

Figure 3-4. Domain of the SDA contaminant transport simulation model.

Results from a calibrated modeling study of infiltration using moisture monitoring within the SDA surficial sediments (Martian 1995) were used to define the spatially variable infiltration of water at land surface in the SDA. Martian selected three representative infiltration rates and assigned them to portions of the SDA based on similarity to observed infiltration results and surface topography (see Figure 3-5). Each of the low, medium, and high infiltration rates had a transient description. A constant time-weighted average of Martian's transient averaged rates was examined. A spatial average of the three infiltration rates is 8.5 cm/yr (3.3 in/yr). The time period for the flow-and-transport calibration simulations was from the beginning of 1952, the year waste was first buried in the SDA, until the end of April 1995, the end of the Martian infiltration simulation study. Estimated amounts of water from the three historical flooding events (1962, 1969, and 1983) were superimposed on both the transient and constant infiltration surface-boundary conditions.

Time-dependent mass release histories for each radionuclide from the source term model (Section 3.2.1) were input spatially into the source area of the subsurface transport model (Figure 3-1). The source release terms were also distributed vertically at each location beginning from a depth of 1.5-m (5-ft) down to the bottom of the surficial sediments. The 1.5-m (5-ft) depth was used to represent clean overburden above the waste. The depth to the bottom of the surficial sediments varied spatially and ranged from 3.0 to 6.25 m (10 to 20 ft) below land surface except where the active low-level waste pit was excavated into the upper basalt to a total depth below land surface of 9.0 m (30 ft).

The water and contaminant movement within the fractured basalts of the vadose zone was simulated as well. A hydraulic description of the water movement in fractured basalt was based on the inverse modeling study (Magnuson 1995) of the large-scale infiltration test (LSIT) conducted near the SDA (Wood and Norrell 1996). Simulation of flow in both the basalt and sediments allows the model to capture horizontal spreading of the water and contaminants in the vadose zone. Previous modeling efforts related to migration of waste at the SDA, including the RWMC LLW Radiological PA (Maheras et al., 1994), conservatively assume instantaneous movement of water and dissolved contaminants through the fractured basalt portions of the vadose zone.

Both the vadose zone and the aquifer regions were included in a single simulation domain. Combining the vadose zone and aquifer portions of the subsurface within a single domain eliminated the need for a numerical interface between separate vadose zone and aquifer models that would impose artificial numerical constraints between the two domains due to partitioning of gaseous phase contaminants from the vadose zone into the aquifer. Aquifer boundary heads were interpolated from the measured 1994 water levels and were assumed to be representative of long-term steady-state conditions.

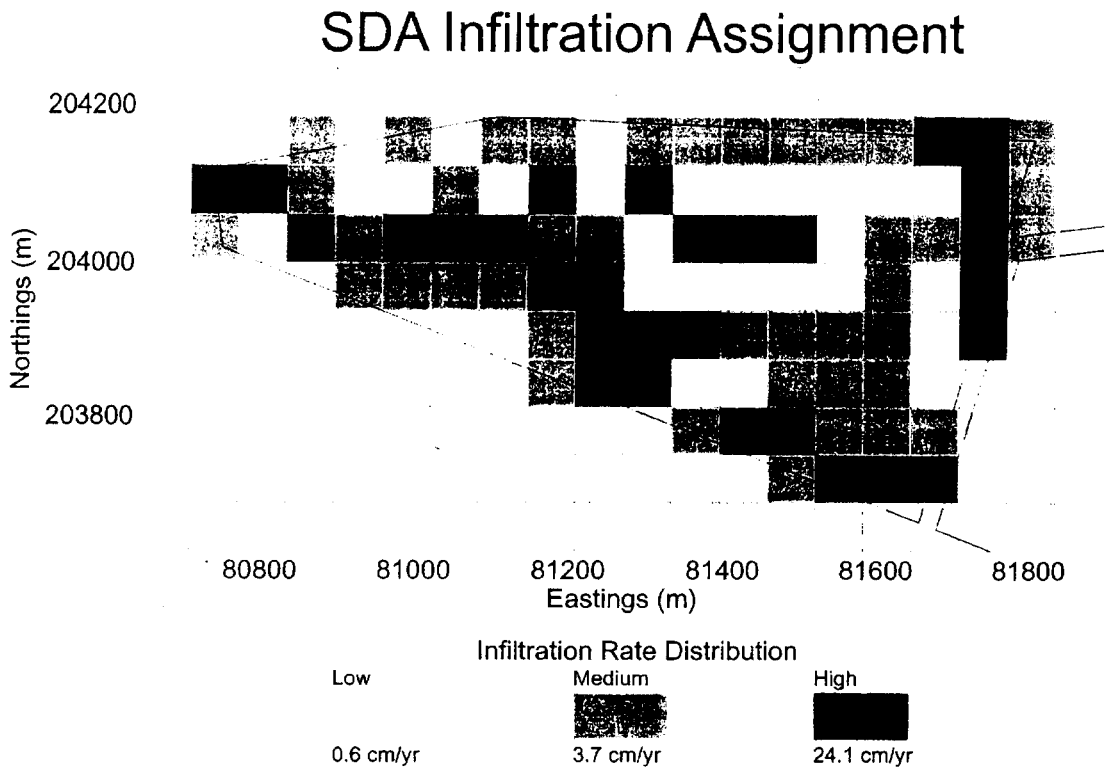

Figure 3-5. Assignment of variable surface infiltration inside the SDA.

3.2.2.4 Subsurface Model Calibration. The adequacy of the calibration obtained in the subsurface modeling was variable. The amount of data available for calibrating the vadose zone flow model was limited. While the model results mimicked the character of the vadose zone data, there was only a partial agreement between the simulated and limited observed results. Computational limitations in the amount of discretization that could be incorporated and adequacy of the surface infiltration description were identified as two possible reasons for only achieving a limited calibration. The calibration of the simulated water levels to measured 1994 aquifer water levels showed good agreement.

Calibration of dissolved-phase transport assumes that there was a contribution from SDA wastes to observed nitrate concentrations in the aquifer downgradient from the SDA. There were no nitrate sampling data available from the few perched water samples in the vadose zone beneath the SDA. There was, however, an indication of slightly increased nitrate concentration downgradient from the SDA (Burgess 1996; Orr and Cecil 1991). An estimated local background concentration of 700 μg-N/L (Burgess 1996) was assumed to be correct. The dissolved-phase transport model was then calibrated to that portion of the observed aquifer nitrate concentrations above the estimated local background concentration. Since the identification of a nitrate source from the SDA is questionable, assuming that a nitrate source did cause the observed concentrations above a local background is conservative from the standpoint of assessing dissolved-phase transport. If there is in fact not a nitrate contribution to the aquifer from the SDA and the calibrated model shows there is, the model then predicts more rapid transport than is actually occurring which is generally conservative. The calibration to nitrate concentrations above the local background did show reasonable agreement. Further comparisons of the vadose zone field data and the C-14 simulations indicate that the model is predicting C-14 transport at a higher rate than is observed.

The combined gaseous- and aqueous-phase transport model was calibrated using carbon tetrachloride concentrations measured in an extensive vapor-phase-monitoring network and in the groundwater. This calibration was very successful in that good agreement was obtained between vadose zone soil gas concentration profiles and time histories. Good agreement was also obtained between simulation and observed carbon tetrachloride concentrations in the aquifer.

3.2.3 Predictive Simulations

Following the flow and transport calibration effort, the model was used to predict contaminant fate and transport. Becker et al. (1998) simulated 53 total contaminants (radiological and nonradiological) with upper-bound inventory estimates. The CA used the results of this modeling to identify the contaminants of potential concern for the CA. Because the PA is a subset of the CA, these same contaminants were identified as the PA contaminants of concern. The PA contaminants of concern are C-14, Cl-36, I-129, Np-237, U-234, and U-238. These six radionuclides and the necessary parents (Pu-242, Pu-238, and Am-241) were re-simulated for the Performance Assessment with updated waste disposal and projected inventories.

Predicted model concentrations at a depth of 12 m (40 ft) within the saturated portion of the simulation domain that corresponded to the SRPA were used to calculate doses. There were effectively seven [8m (26 ft) thick] vertical saturated grid blocks representing the aquifer in the flow and transport simulations. The 12-m (40-ft) depth corresponded to the second saturated grid block from the top of the aquifer, which extended from 8 to 16 m (26 to 52 ft). The existing monitoring wells at the SDA are generally screened in this same interval because it was the first productive zone encountered during drilling. It is assumed that this same vertical interval will supply the majority of water for a hypothetical groundwater well. The locations where dose is calculated are shown in Figure 3-6. Essentially, a series of receptor "fences", beginning 100-m downgradient of the SDA facility boundary, are used to estimate dose. Downgradient in this case is generally to the south of the SDA for both the simulations and for the general understanding of the flow direction in the aquifer beneath the SDA. Based on water level time histories of wells in the SDA vicinity, there are times when the flow direction within the aquifer may be substantially different.

For each point in time during and after the 1,000-yr-compliance period, the location of maximum dose along the receptor "fences" is calculated. This means that the locations can and do change along a "fence" over time. In addition to the receptor "fences" in Figure 3-6, doses were calculated along the southern INEEL boundary approximately 5,500-m downgradient.

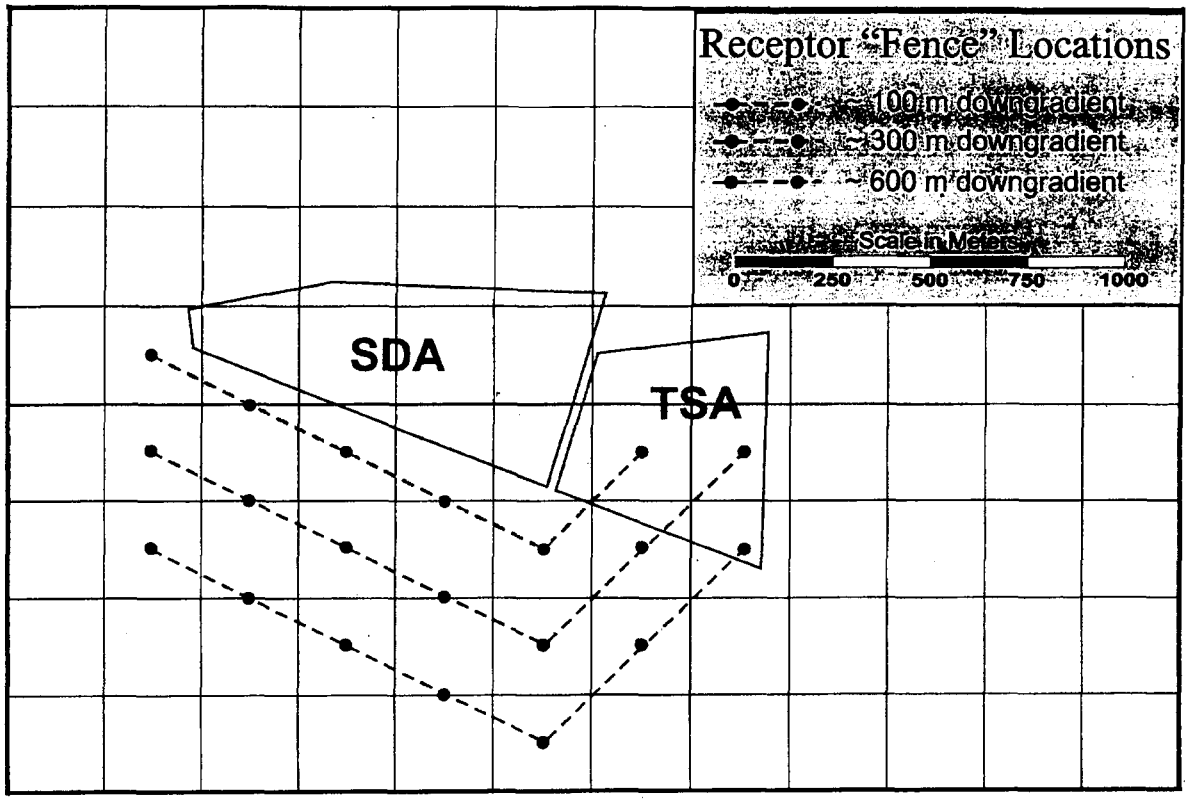

Figure 3-6. Numerical grid locations from which the peak aquifer concentrations were taken.

The following list contains the assumptions that were necessary to perform the subsurface pathway flow and transport simulations. The list is modified from Magnuson and Sondrup (1998). The few modifications were necessary because of the addition of an infiltration-reducing cap in the year 2021.

- This cap, because of its simple design is assumed to be effective in perpetuity. Subsidence events will cease within the 100-yr period of institutional control and can therefore be corrected through a maintenance program.
- The surficial sediments and sedimentary interbeds have spatially variable lithologic surfaces and thickness that influence water and contaminant movement.
- Interbeds below the 240-ft interbed are thin and discontinuous and do not significantly affect flow and transport in the vicinity of the SDA.
- Hydrologic properties within lithologic units are homogenous.
- Flow in the fractured porous basalts is controlled by the fracture network and adequately represented as equivalent to a high-permeability, low-porosity porous medium.
- The field-scale hydraulic properties for all fractured basalts are adequately described by the inverse modeling performed by Magnuson (1995) for the large-scale infiltration test (LSIT).

- Controls on water movement in the aquifer are consistent with the controls on water movement in the fractured basalts in the vadose zone.

- Water movement in the aquifer is steady state.

- Influences of discharges of Big Lost River water to the spreading areas on flow within the vadose zone or the aquifer in the immediate vicinity of the SDA are neglected.

- Water levels corrected for borehole deviations from 1994 are adequate for calibrating the SRPA flow model and are representative of long-term steady-state conditions.

- A region of continuous low permeability exists in the SRPA southwest of the SDA, based on pumping tests of wells in the vicinity of the SDA.

- The effective depth of the SRPA is 76 m, the same values as in the RWMC LLW Radiological PA (Maheras et al, 1994) and the Composite Analysis (McCarthy et al, 2000). This estimated thickness was originally developed by Robertson (1974) and has been used extensively since that time.

- Contaminants that have both aqueous- and gaseous-phase components are adequately simulated with a dual-porosity representation for the fractured basalt portions of the subsurface.

- Field-measured concentrations of subsurface contaminants of concern are generally representative and valid based on data quality requirements associated with sampling activities. Single isolated detections of contaminants are anomalous and not representative.

- The DUST source term model adequately describes the release of dissolved- and gaseous-phase contaminants.

- Advection, dispersion, diffusion, sorption, and radioactive decay are the only processes that influence contaminant movement in the subsurface at the SDA. Degradation of VOCs and other chemicals was not included.

- Division of the disposed wastes into three time-dependent waste streams (pre-1971, 1971-1984, and post-1984) applied spatially across the SDA is adequate for assessing fate and transport.

- Fine-grained sediment coatings and chemical alteration products on the surfaces of the basalt fractures control the sorption of aqueous phase contaminants moving within the fractured basalt. The basalt matrix has no interaction with contaminant movement in the fractures. Both assumptions apply equally to fractured basalts in both the vadose zone and the SRPA.

- The sediment Kd values determined by Dicke (1997a) are the most accurate for fate and transport modeling.

- Partitioning of contaminants between phases is linear and reversible.

- The local background nitrate contribution from upgradient sources is 700 μg-N/L.

- Nitrate concentrations in the aquifer above this background concentration are an adequate target for calibrating the aqueous-phase transport model.

- Calibration from the start of waste burial at the SDA in 1952 until April 1995 is adequate to make predictions indefinitely into the future provided uncertainties in the SDA subsurface model are acknowledged. Indefinitely into the future in this case means 10,000 years, which captures the peak dose for most of the radionuclides.

- Carbon tetrachloride gaseous-phase concentrations in the vadose zone and aqueous-phase concentrations in the SRPA are adequate for calibrating the combined aqueous- and gaseous-phase transport model.

- Volatile organic contaminants (VOC) are simulated as if they are released as nonaqueous-phase liquids that rapidly partition into aqueous and gaseous phases. If VOC releases were rapid enough, a nonaqueous-phase liquid would occur in the simulations.

- Calibration of VOC transport was performed using only one organic component, carbon tetrachloride, and did not consider the effect of the presence of other VOCs on partitioning and advective transport. (This calibrated VOC model was then used to simulate tritium migration.)

- The SDA was the only source of carbon tetrachloride for the VOC calibration.

Simulated concentrations at a depth of 12 m which represent a grid block over the interval from 8 to 16 m in the aquifer are representative of water quality that would be produced from a well screened over that interval.

3.3 Conceptual Model for Atmosphere and Intruder Pathways

The following is a brief description of the conceptual model used for the intruder and atmospheric transport scenarios. For the performance assessment analyses, the RWMC SDA was modeled for disposal of LLW in pits and soil vaults from 1984 to 2020, at which time the SDA was closed. Upon closure, a thick soil barrier, which includes a vegetative cover, was emplaced over the operational cover and maintained during the period of institutional control. The total thickness of the cover at closure is 5 m. This maintenance includes keeping the vegetative cover intact and preventing animal burrowing. After the institutional control period, no maintenance is performed on the cover, and erosion is assumed to occur down to the existing RWMC grade. At the time of maximum erosion, this results in 2.4 m of cover remaining over the waste for pits and 3.3 m of cover remaining over the soil vaults. Figures 3-7 and 3-8 present the conceptual profile of a pit and a soil vault.

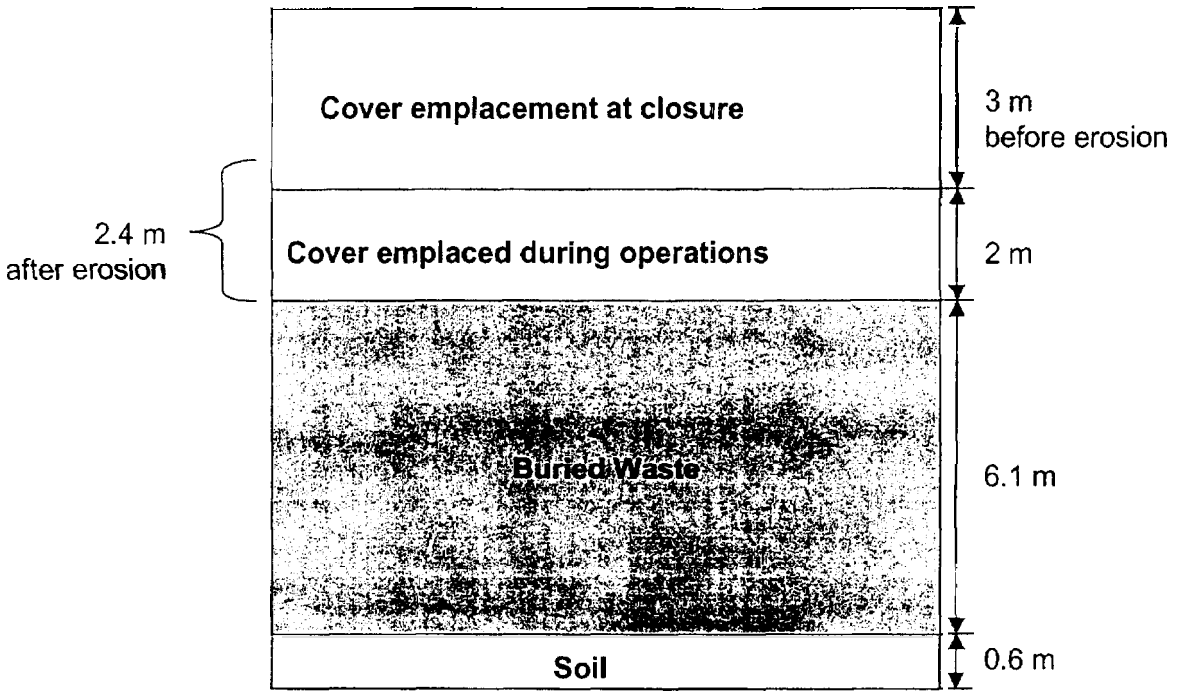

Figure 3-7. Conceptual profile of pits.

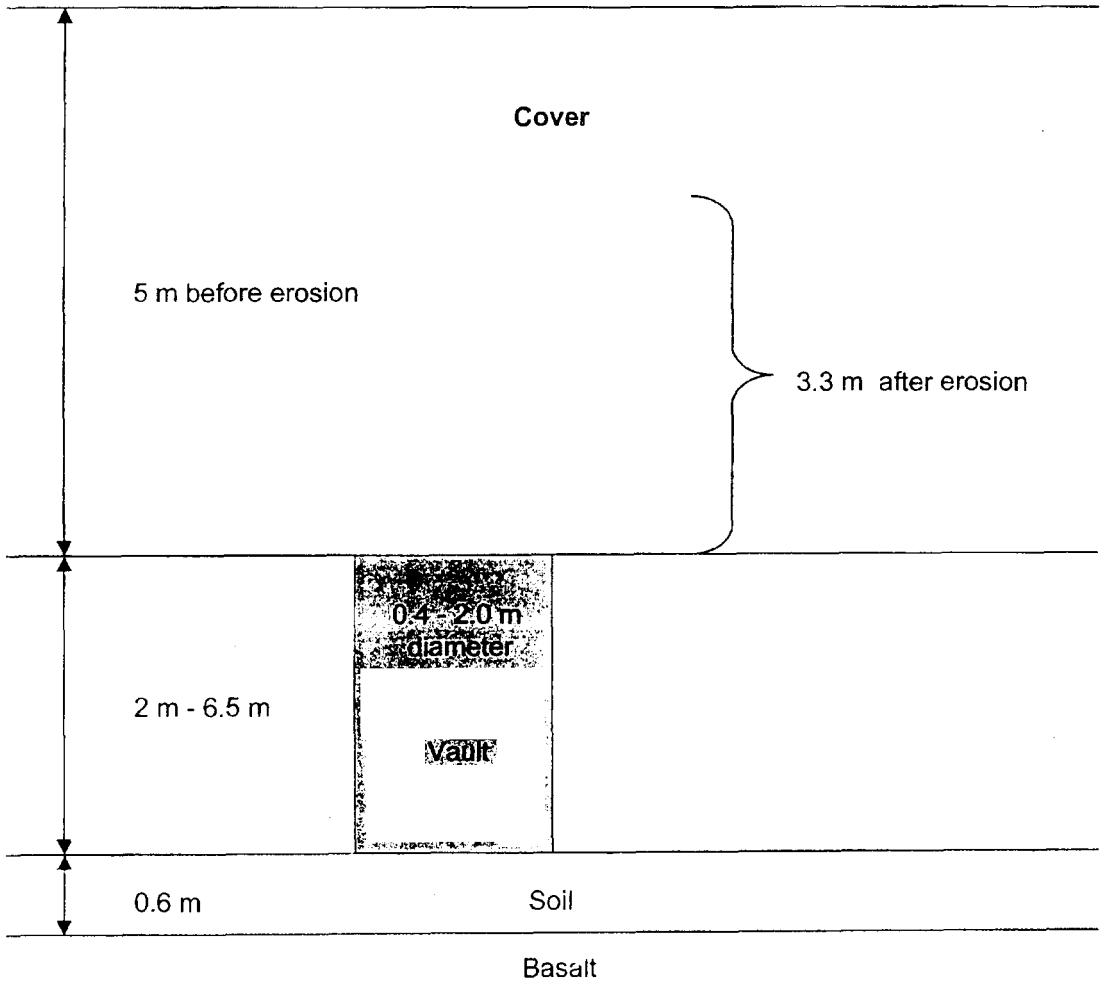

Figure 3-8. Conceptual profile of a soil vault.

3.4 Atmospheric and Intruder Pathways and Scenarios

Exposure pathways are the link between contaminated environmental media and the exposure of a receptor. Figure 3-9 summarizes the exposure pathways from LLW disposed of in the RWMC SDA. This diagram does not include processes that recycle radionuclides, such as plant death and decay, because these processes tend to dilute the amount of radioactive material available for uptake when compared to direct uptake pathways.

Environmental monitoring has been performed at the RWMC since 1960, and special studies are also periodically conducted. The Radiological and Environmental Sciences Laboratory (RESL) conducted radioecological studies at and around the RWMC until 1997. Many of the RESL studies focused on radionuclide transport via biota. The results of the monitoring and special studies indicate that the greatest potential for the transport of radionuclides to a member of the public is via atmospheric transport of resuspended soil and groundwater transport of radionuclides leached from buried waste. Therefore, this performance assessment focuses on these two routes of exposure for dose assessments for members of the public. For intruders, direct exposure to the waste is assumed, either through excavation or drilling. For excavation and drilling, pathways are evaluated and doses are calculated from ingestion, inhalation, and external exposure to radioactive material.

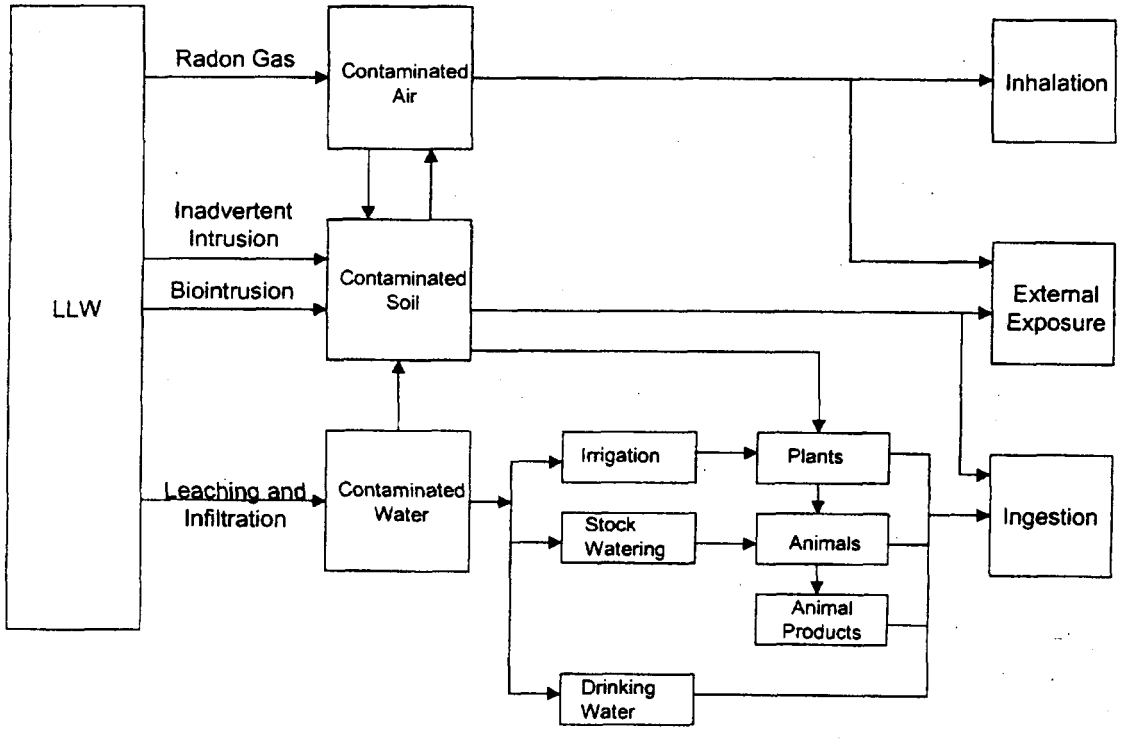

Figure 3-9. Exposure pathways at the RWMC.

Two general types of scenarios are evaluated in this performance assessment: (1) doses to members of the public, and (2) doses to inadvertent intruders (see Figure 3-10). Doses to members of the public are evaluated for two scenarios: atmospheric transport, which is discussed below, and groundwater transport, which is discussed in Sections 3.2.2 and 3.2.3. To meet the requirements in DOE Order 435.1, doses to intruders are also evaluated for two scenarios: acute exposures and chronic exposures. The receptors for the member of the public dose assessments are located at the INEEL Site boundary during operations and institutional control and at 100 m from the RWMC boundary during post-institutional control. The intruder is assumed to reside on the RWMC SDA. The following sections describe the atmospheric, all-pathways, intruder, and groundwater protection scenarios used to evaluate impacts.

3.4.1 Atmospheric Scenario

3.4.1.1 Operational and Institutional Control Periods. This section describes the methodology and data used to calculate doses from atmospheric emissions from the RWMC during the operational and institutional control periods. These doses are based, in part, on the emissions dose assessments performed for the INEL National Emission Standard for Hazardous Air Pollutants (NESHAP) Annual Report (DOE 2000).

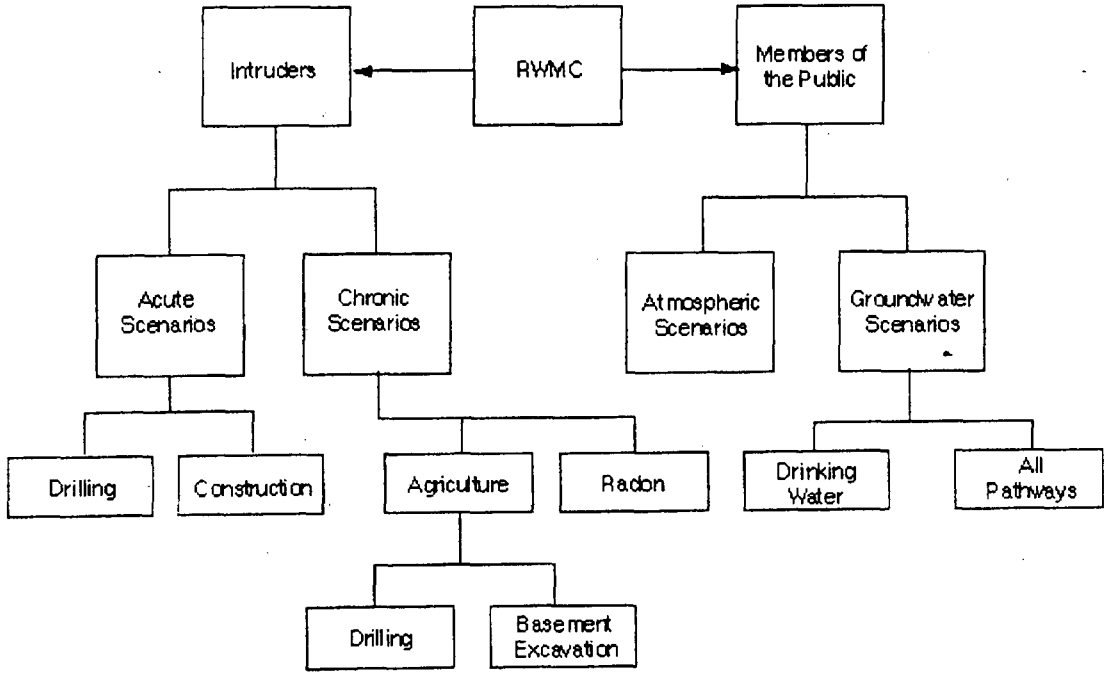

Figure 3-10. Scenarios at the RWMC.

Current releases from the RWMC, as reported in DOE (2000) include specific stack release points [the Organic Contaminant Vadose Zone (OCVZ) thermal oxidation units, the Drum Vent Facility, and Processing Tent] and diffuse sources. The diffuse sources include resuspension of contaminated surface soil and the diffusion of tritium and C-14 from buried waste. During the operational and institutional control periods, the RWMC will be actively maintained and monitored. Therefore, it is reasonable to postulate that soil contamination levels will not be higher than current levels. DOE (2000) provides the existing soil contamination levels at the RWMC and the areal extent of this contamination. The radionuclide soil concentrations at contaminated areas were estimated based on sampling studies or field survey measurements. The areal extent of each area was also estimated based on field observations and measurements. These data were used to estimate an annual release rate for each radionuclide in units of curies per year and to calculate a dose to the maximally exposed individual at the INEEL boundary (DOE 2000).

The doses due to releases of tritium and C-14 from the RWMC that were reported in DOE (2000) were not used for the PA because the estimates are less conservative than those predicted by the DUST model. Instead, the fluxes from the DUST model were assumed to diffuse upwards from the waste through the surface into the atmosphere (see Section 3.4.1.3). The ISCST3 model (EPA 1995) was then used to disperse the gases and predict the concentrations at the location of the maximally exposed individual. The dose to that individual was calculated using an annual breathing rate of 8030 m^3 and the maximum inhalation dose conversion factors for tritium and C-14 found in the RESRAD dose factor library.

As required for NESHAP compliance dose assessments, the receptor location for the operational and institutional control periods was located at the point of the maximally exposed individual at Frenchman's Cabin, about 8 km SSW of the RWMC outside the INEEL boundary (DOE 2000). The atmospheric data, environmental data, and the computer code used in the analyses are also discussed in DOE (2000).

3.4.1.2 Biointrusion. This section describes the methodology used to calculate doses from atmospheric emissions of radionuclides brought to the surface by biointrusion of the RWMC SDA after institutional control This contaminated surface soil was blown offsite to a member of the public 100 m from the boundary of the RWMC SDA. This hypothetical receptor ate contaminated food, was immersed in contaminated air, breathed contaminated air, and was exposed to contaminated ground surfaces.

The scenario used for this analysis started with the LLW inventory disposed of in the RWMC LLW disposal locations from 1984 to 1999 and was augmented with the forecasted additions for 2000 to 2020 (see Appendix B). A portion of the inventory was brought to the surface through biointrusion and distributed over the RWMC, forming a large area source of radioactive material that could be resuspended by wind.

The contaminated material was then blown offsite to a hypothetical member of the public located 100 m from the RWMC. The receptor was located at the 50-m grid point outside the RWMC that yielded the largest annual air concentration at 100 m from the RWMC, using a ground-level release and meteorological data collected from 1995 to 1999 at the Central Facilities Area (CFA) and the ISCST3 air dispersion model (Version 99155) (EPA 1995). The ISCST3 code was set in deposition mode so that results were in terms of quantity of radionculide deposited.

For this analysis, the RESRAD computer code (Version 5.95), developed for implementing the U.S. Department of Energy's residual radioactive material guidelines (Yu 1993), was used to model the doses resulting from RWMC atmospheric releases. From the ISCST3 output, the maximum amounts deposited 100 m outside the RWMC were determined and the results were used as a source term for

RESRAD. The RESRAD code uses the concentrations of radionuclides in soil to estimate doses. The output from RESRAD is the EDE, which includes the 50-year committed effective dose equivalent (CEDE) from internal exposure through the ingestion and inhalation pathways and the external EDE from ground deposition and air immersion. Yu et al (1993) completely describes the RESRAD computer code. The assessments done for operational and institutional control periods (DOE 1999) and RESRAD use the same pathways.

Inhalation doses were calculated based on exposure to contaminated air for 1 year (8760 hours). The inhalation rate, 8030 m^3/yr, presented in ICRP-23 as the inhalation rate for Reference Man (ICRP 1975) was used.

Ground surface doses were calculated assuming 100 years of buildup of radionuclides in the surface soil because of atmospheric deposition. The shielding factor of 0.7 was adapted from NRC (1977) and corresponds to the shielding factor used for the maximally exposed individual.

Air immersion doses were calculated based on exposure to contaminated air for 1 year, using the shielding factors of 0.7, as in the ground surface analyses (see NRC 1977).

Ingestion doses were calculated based on the consumption of contaminated produce, leafy vegetables, milk, and meat. The conceptual model for ingestion doses begins with radionuclides that are deposited on forage, soil, produce, and leafy vegetables. Radionuclides deposited on forage are subsequently transferred through the food chain to meat and milk and then to humans. Radionuclides deposited on produce and leafy vegetables are also consumed by humans. Radionuclides deposited on soil are transferred to forage, produce, and leafy vegetables through the mechanism of root uptake and then transferred to humans through ingestion of contaminated meat, milk, produce, and leafy vegetables. The parameters used to calculate food chain doses in Maheras et al (1994) were used to the extent possible. RESRAD default values were used for parameters not previously identified by Maheras et al (1994, 1997).

A diet developed by Rupp (1980) and based on a 1965 U.S Department of Agriculture (USDA) survey was used (see Table 3-5). The Rupp diet was the default diet used in the EPA's NESHAPs Environmental Impact Statement (EPA 1989). Dietary fractions representative of rural agricultural areas were used (EPA 1989). Based on the data in EPA (1989), 70% of the receptor's vegetables and produce, 40% of the milk, and 44% of the meat were produced locally.

The dose conversion factors (DCFs) and elemental transfer factors used in this analysis are the default values from the RESRAD library. The RESRAD code uses the most conservative dose conversion factors contained in DOE (Yu 1993).

Two biointrusion mechanisms were examined as potential ways to bring contaminated material to the surface: intrusion by burrowing animals and intrusion by plant roots. Groves and Keller (1983) identified 10 species of small mammals nesting on or near the RWMC. Four species were the most numerous: deer mice (*Peromyscus maniculatus*), montane voles (*Microtus montanus*), Ord's kangaroo rats (*Dipodomys ordii*), and Townsend's ground squirrels (*Spermophilus townsendii*). Reynolds and Wakkinen (1987) studied the burrow depths of these four species in undisturbed soils and the maximum reported burrow depth for undisturbed soil was 138 cm for a Townsend's ground squirrel. A 1988 study by Reynolds and Laundre examined the burrow depths of the same species in both disturbed and undisturbed soils on the INEEL. The maximum burrow depth in disturbed soils documented in Reynolds and Laundre (1988) was 140 cm was for a Townsend's ground squirrel. None of the deer mice burrows extended past 60 cm, none of the montane vole burrows extended past 70 cm, and none of the Ord's kangaroo rat burrows extended past 100 cm.

Table 3-5. Human diet used in the performance assessment.

Food product	Rupp diet
Produce (kg/yr)	176
Leafy vegetables (kg/yr)	18
Milk (L/yr)	112
Meat (kg/yr)	85

At maximum erosion, there is 240 cm of cover left over the pits and trenches and 330 cm of cover left over the soil vaults. Based on the site-specific studies in Reynolds and Wakkinen (1987) and Reynolds and Laundre (1988) that report burrow depths are not observed in undisturbed or disturbed soils at the INEEL greater than 140 cm deep, intrusion by burrowing small mammals is highly unlikely and was removed from further consideration. The authors acknowledge that investigators at other sites have observed different results for other species of small mammals (e.g., McKenzie et al. 1982). These other studies were considered in evaluating intrusion by the burrowing small mammal pathway; however, preference was given to the site-specific studies based on the guidance provided in Dodge et al. (1991).

In contrast to burrowing mammals, harvester ants (*Pogonomyrmex salinus*) burrow deep enough to encounter the waste. For example, Blom et al. (1991) states that harvester ants have been found as deep as 2.7 m in Wyoming and at the Hanford Site. To account for the intrusion of harvester ants into the waste, a model similar to that in Kennedy et al. (1985) was constructed. In contrast to burrowing small mammals, no site-specific data for harvester ant burrow depths exist; therefore, data from Kennedy et al. (1985) were used in the model.

The model was based on harvester ants burrowing into the waste and bringing contaminated material to the surface. The volume of contaminated material that a single harvester ant colony brought to the surface was calculated using the burrow volume and the fraction of the burrow that was deep enough to encounter the waste. Because the waste was at depths greater than 2 m below the surface at maximum erosion, 5% of the burrow volume was estimated to encounter the waste (see Kennedy et al. 1985). An average burrow volume per colony of 0.002 m^3 was also obtained from Kennedy et al. (1985). The resulting volume of contaminated material was multiplied by the radionuclide concentration in the waste to yield the activity that a single harvester ant colony could bring to the surface. This result was multiplied by the average harvester ant colony density and the surface area of the pits and soil vaults to yield the total activity brought to the surface:

Activity on the surface (Ci) = waste concentration (Ci/ m^3) x

burrow volume (m^3 /colony) x fraction of burrow in waste x

colony density (colonies/ m^2) x surface area (m^2).

Based on data for harvester ant colony densities in big sagebrush (*Artemisia tridentata*) communities on the INEEL (Blom et al. 1991), a density of 35.6 colonies/10,000 m^2 was used. This represents the mean density over five locations on the INEEL. For pits[c] and soil vaults,[d] surface areas of 12,000 and 890 m^2 were calculated, respectively.

---

c. The volume of waste in the pits was 75,600 m^3 and the waste thickness was 6.1 m, which yielded a surface area of 12,000 m^2.

The total activity brought to the surface through harvester ant burrowing was then dispersed in the environment and blown to a hypothetical receptor located 100 m from the RWMC. While this is a conservative assumption, it puts an upper bound on the material that a receptor could be exposed to through the atmospheric pathway.

The potential for biointrusion by plant roots was also evaluated. Elevated concentrations of radionuclides in plant species growing on the RWMC have been observed (Arthur 1982). These elevated concentrations were observed in areas where 0.6 to 1.8 m of cover was present over the waste. Reynolds and Fraley (1989) studied root profiles near the RWMC and determined the maximum rooting depth for big sagebrush (*Artemisia tridentata*) was 225 cm, for green rabbitbrush (*Chrysothamnus vicidiflorus*) was 190 cm, and for Great Basin wild rye (*Leymus cinereus*) was 200 cm.

Based on the site-specific data in Reynolds and Fraley (1989), biointrusion by plant roots of pits and soil vaults may be possible. However, biointrusion by plant roots of soil vaults is less likely because of increased cover depth.

To estimate the amount of radioactive material that plant roots could bring to the surface, a model similar to those used in GENII (Napier et al. 1988) and Kennedy et al. (1985) was constructed. First, the dominant plant species in terms of absolute cover were determined. Anderson and Inouye (1988) found that big sagebrush has an absolute cover of 13%, green rabbitbrush has an absolute cover of 4.3%, and Great Basin wild rye has an absolute cover of 0.013% at the INEEL. Russian thistle, another potentially deep rooted species, had an absolute cover of 0.005%. Because big sagebrush is the dominant plant species, estimates of biointrusion were based on big sagebrush data.

The aboveground biomass of big sagebrush was estimated to be 46 g/m^2 using INEEL-specific data from Fraley (1978). Because the waste is at depths greater than 2 m below the surface at maximum erosion, 5% of the plant roots were estimated to encounter the waste (see Kennedy et al. 1985). The activity brought to the surface by plants was estimated by multiplying the radionuclide concentration in the waste by the concentration ratio (CR), the fraction of the roots that can encounter the waste, the biomass, and the area of the pits or soil vaults.

$$\textit{Activity on the surface (Ci)} = \textit{waste concentration (Ci/ m}^3\textit{)} \times \frac{1}{\textit{soil bulk density (g/ m}^3\textit{)}} \times \textit{fraction of roots in waste} \times CR\left[\frac{\textit{Ci/g(plants)}}{\textit{Ci/g(waste)}}\right] \times \textit{biomass (g/ m}^2\textit{)} \times \textit{area (m}^2\textit{)}.$$

Dry weight CRs for pasture from Baes et al. (1984) were used. CRs for uptake by cheatgrass and tumbleweed (Russian thistle) of neptunium, plutonium, americium, and curium were also examined and found to be in reasonable agreement (i.e., within an order of magnitude) of the CRs from Baes et al. (1984) (see Price 1972).

---

d. The volume of waste in the soil vaults was 2,700 m^3 and the waste thickness was 3.05 m, which yielded a surface area of 890 m^2.

The total activity brought to the surface through plant uptake was then dispersed in the environment and blown to a hypothetical receptor 100 m from the RWMC. This implies that the entire big sagebrush aboveground biomass was converted to a dispersible form. While this is a conservative assumption, it puts an upper bound on the material that a receptor could be exposed to through the atmospheric pathway.

Doses because of harvester ant burrowing and plant uptake were calculated at various points in time after site closure, beginning in 2120 and continuing to 10,000 years after site closure. The year 2120 corresponds to the beginning of the post-institutional control period and is the earliest time that biointrusion could occur during the post-institutional control period. This is also the time when the maximum fission product and activation product inventory is available for biointrusion because fission and activation products do not contain long-lived decay series with substantial progeny ingrowth. This time were chosen to determine if there were any long-lived actinide decay series that could yield large doses because of progeny ingrowth over long time frames. One million years corresponds to the time when most long-lived decay series have achieved a substantial fraction of secular equilibrium and was addressed in the previous performance assessment and addendum (Maheras et al 1993, 1997). However, it was not assessed in this technical revision because: 1) it is unreasonable to expect environmental conditions to remain constant over this enormous time frame, and 2) for consistency with the composite analysis, which only projects doses from subsurface pathways through the year 12000.

The fraction of the root or burrow system that contacted the waste did not change as the amount of cover over the waste changed because of erosion. This fraction was held constant over time because the data in Kennedy et al. (1985) do not permit further refinement of the depth profile at depths greater than 2 m. Because the minimum depth to waste at maximum erosion was 2.4 m, the data for the fraction of the root or burrow system at 2 m were applied to all depths greater than 2 m. This approach is conservative because there is undoubtedly a depth-dependent root or burrow profile at depths greater than 2 m that would result in less biointrusion as the depth to the waste increases. However, this approach eliminates the need to consider the erosion rate in the calculations, and maximum dose can be calculated by performing a few representative assessments. In addition, every burrow system or plant over the pits was assumed to contact the waste; this is also a conservative approach.

3.4.1.3 Gaseous Releases of Tritium and Carbon-14. The purpose of this analysis was to estimate the doses from gaseous releases of H-3 and C-14. The H-3 and C-14 release rates were calculated by the DUST model used to estimate flux rates from the sources. Instead of H-3 and C-14 moving downward with water, H-3 and C-14 were assumed to move upward as gases and were transported to receptors downwind of the RWMC. Doses were evaluated for two time periods: (1) the operational and institutional control periods, where the receptor was an actual residence located 8000 m south-southwest from the RWMC at the INEEL Site boundary and (2) the post-institutional control period, where the receptor was located at the RWMC. During each of these periods, the peak release rates for H-3 and C-14 were used.

During the operational and institutional control time periods, the peak release rate for C-14 was 0.258 Ci/yr, and the peak release rate for H-3 was 3860 Ci/yr. The release rates were input into the ISCST3 air dispersion code (EPA 1995), which calculated air concentrations at the INEEL boundary receptor location. The receptor was assumed to breathe this concentration, at an inhalation rate of 8030 m^3 per year. The resultant dose was calculated using the maximum dose conversion factors for inhalation for tritium and C-14 provided in the RESRAD dose conversion factor library.

During the post-institutional control period, the peak release rate for C-14 was 4.88×10^{-3} Ci/yr, and the peak release rate for H-3 was .145 Ci/yr. The RESRAD code was used to evaluate releases of ^{3}H and ^{14}C, which are modeled differently from the other solid radionuclides in the code due to their special

characteristics. In order to use RESRAD, which requires soil concentrations of radionuclides, the annual flux rates were first converted to area release rates (Ci/m^2), and then to soil concentrations (pCi/m^3), using the depth of the waste (m) and a soil density of 1.5 g/cm^3. The entire source was released to the air during the year by assuming an annual evasion rate (flux) equal to the soil concentration. For this scenario, the receptor was conservatively situated directly over the waste.

3.4.1.4 Radon Flux. The purpose of this analysis was to estimate the radon flux from the surface of the RWMC to demonstrate compliance with the 20 pCi/m^2-s standard contained in Subpart Q of 40 CFR 61. As with the chronic intruder radon scenario, the RESRAD computer code (Yu et al 1993) was used to estimate the surface radon flux. The methods and data used to estimate the radon flux were identical to the methods and data used to estimate the chronic intruder radon doses, except that a building was not included in the analysis. These methods and data are presented in Section 3.4.3.4.

3.4.2 All-Pathways Scenario

The methodology used to calculate the all-pathways dose was based on the methodology presented in NRC (1977) and Peterson (1983). This all-pathways scenario assumed that a receptor drank contaminated groundwater, ate leafy vegetables and produce that were irrigated with contaminated groundwater, and consumed milk and meat from animals that consumed contaminated water and pasture grass irrigated with contaminated groundwater. The scenario assumed that groundwater was used for drinking, watering beef and milk cattle, and irrigating crops and pasture. Radionuclide concentrations as a function of time at the receptor well that were calculated using the hydrological transport model described in Section 3.2 were used as input to this model. The receptor was located at the INEEL Site boundary during the operational and institutional control periods, based on guidance from DOE-HQ.[e] During this time, the INEEL Site boundary is maintained, and access by the public is not allowed. During post-institutional control, the receptor was located 100 m downgradient of the RWMC facility boundary. Table 3-6 contains the parameter values used in the all pathways dose calculation.

The dose from human consumption of drinking water was calculated using

$$D = C_{GW} \times U_W \times DCF \times \frac{10^{-6}\ \mu Ci}{pCi} \times \frac{1{,}000\ mrem}{rem}$$

where

D = dose (CEDE) from one year's consumption of contaminated media, in this case groundwater (mrem/yr)

C_{GW} = radionuclide concentration in groundwater (pCi/L)

U_W = human consumption rate of water (L/yr)

DCF = ingestion dose conversion factor (rem/μCi).

---

e. Letter from S. P. Cowan to J. T. Case, June 20, 1996, "Groundwater Compliance for the Low-Level Waste Radiological Performance Assessment for the Radioactive Waste Management Complex at the Idaho National Engineering Laboratory."

Table 3-6. Parameter values used in the all pathway dose calculation.

Parameter	Value	Reference
U_W	258 L/yr	Yang and Nelson (1984)
Q_W (beef cattle)	50 L/day	NRC (1977)
Q_W (milk cattle)	60 L/day	NRC (1977)
Q_F (beef cattle, dry weight)	12 kg/day	NCRP (1984)
Q_F (milk cattle, dry weight)	16 kg/day	NCRP (1984)
U_B	85 kg/yr	Rupp (1980)
U_M	112 L/yr	Rupp (1980)
U_P	176 kg/yr	Rupp (1980)
U_{LV}	18 kg/yr	Rupp (1980)
I	8.47 L/m^2-day	Site specific
k	0.025 mm^{-1}	Peterson (1983)
r/Y_v (leafy veg, wet weight)	0.076 m^2/kg	Calculated from Baes and Orton (1979) and Baes et al. (1984)
r/Y_v (produce, wet weight)	0.032 m^2/kg	Calculated from Baes and Orton (1979) and Baes et al. (1984)
r/Y_v (pasture, dry weight)	2.0 m^2/kg	Calculated from Baes and Orton (1979) and Baes et al. (1984)
P (dry weight)	225 kg/m^2	DOE (1987)
t_i	90 day	Site specific
t_b	365 day	Site specific
f_1	0.25	Site specific
T (leafy veg)	1.0	Ng et al. (1978)
T (produce)	0.1	Ng et al. (1978)
DF (leafy veg)	0.5	Ng et al. (1978)
DF (produce)	1.0	Ng et al. (1978)
FV	0.7	EPA (1989)
FB	0.442	EPA (1989)
FM	0.399	EPA (1989)

The dose through water ingestion by beef and milk cattle assumes that cattle drink contaminated water. The receptor is then assumed to drink milk and eat meat from the cattle that drank the contaminated water. Meat and milk were treated separately. The dose was calculated using

Meat:

$$D = C_{GW} \, x \, Q_W \, x \, F_f \, x \, U_B \, x \, DCF \, x \frac{10^{-6} \, \mu Ci}{pCi} \, x \frac{1{,}000 \, mrem}{rem} \, x \, FB$$

Milk:

$$D = C_{GW} \, x \, Q_W \, x \, F_m \, x \, U_M \, x \, DCF \, x \frac{10^{-6} \, \mu Ci}{pCi} \, x \frac{1{,}000 \, mrem}{rem} \, x \, FM$$

where

Q_W = consumption rate of water by beef or milk cattle (L/day)

F_f = meat transfer coefficient (day/kg)

U_B = human consumption rate of meat (kg/yr)

FB = fraction of beef produced locally (unitless)

F_m = milk transfer coefficient (day/L)

U_M = human consumption rate of milk (L/yr)

FM = fraction of milk produced locally (unitless).

The dose to humans from ingestion of contaminated leafy vegetables and produce was calculated assuming two contamination routes: direct deposition of contaminated irrigation water on plants and deposition of contaminated irrigation water on soil followed by root uptake by plants. Leafy vegetables and produce were treated separately. The dose through direct deposition was calculated using

Leafy Vegetables - Direct Deposition:

$$D = \frac{C_{GW} \, x \, I \, x \, r}{Y_v} \, x \frac{1 - e^{-(\lambda_r + kI)t_i}}{\lambda_r + kI} \, x \, U_{LV} \, x \frac{10^{-6} \, \mu Ci}{pCi} \, x \, DCF \, x$$

$$x \frac{1{,}000 \, mrem}{rem} \, x \, DF \, x \, T \, x \, FV$$

Produce - Direct Deposition:

$$D = \frac{C_{GW}\, x\, I\, x\, r}{Y_v} x \frac{1 - e^{-(\lambda_r + kI)t_i}}{\lambda_r + kI} x\, U_P\, x \frac{10^{-6}\ \mu Ci}{pCi} x\, DCF\, x$$

$$x \frac{1{,}000\ mrem}{rem} x\, DF\, x\, T\, x\, FV$$

where

I	=	irrigation rate (L/m^2-day)
r	=	interception fraction (unitless)
Y_v	=	agricultural yield (kg/m^2, wet weight)
λ_r	=	radioactive decay constant (per day)
k	=	washoff constant (mm^{-1})
t_i	=	irrigation time (day).
U_{LV}	=	human consumption rate of leafy vegetables (kg/yr)
DF	=	fraction of activity remaining after preparation and processing (unitless)
T	=	translocation factor (unitless)
FV	=	fraction of leafy vegetables and produce produced locally (unitless)
U_P	=	human consumption rate of produce (kg/yr).

The product kI is also known as the weathering rate constant because of washoff (Peterson 1983). This quantity describes the rate at which material is removed from plant surfaces by water and is analogous to λ_e, the weathering rate constant used in nonirrigation situations. The value of kI was calculated using

$$kI = 0.025\ mm^{-1} x \frac{8.47\ L}{m^2 - day} x \frac{1\ m^3}{1{,}000\ L} x \frac{1{,}000\ mm}{1\ m} = 0.212/day\ .$$

The dose from deposition of contaminated irrigation water on soil followed by root uptake by plants and human consumption of plants was calculated using the following equations. Credit was not taken for leaching of radionuclides from the root zone of plants.

Leafy Vegetables - Root Uptake:

$$D = \frac{C_{GW} \, x \, I \, x \, f_I}{P} \, x \, \frac{1 - e^{-\lambda_r t_b}}{\lambda_r} \, x \, CR \, x \, U_{LV} \, x \, \frac{10^{-6} \, \mu Ci}{pCi} \, x$$

$$x \, DCF \, x \, \frac{1{,}000 \, mrem}{rem} \, x \, FV$$

Produce - Root Uptake:

$$D = \frac{C_{GW} \, x \, I \, x \, f_I}{P} \, x \, \frac{1 - e^{-\lambda_r t_b}}{\lambda_r} \, x \, CR \, x \, U_P \, x \, \frac{10^{-6} \, \mu Ci}{pCi} \, x$$

$$x \, DCF \, x \, \frac{1{,}000 \, mrem}{rem} \, x \, FV$$

where

f_I = fraction of the year that crops are irrigated (unitless)

P = areal density [kg (dry weight soil)/m^2]

CR = concentration ratio [pCi/kg (wet weight plant) ÷ pCi/kg (dry weight soil)]

t_b = build-up time for radionuclides in soil (day).

The dose to humans from ingestion of contaminated animal products was also calculated assuming two contamination routes: direct deposition and root uptake; meat and milk were treated separately. All food (pasture or stored feed) eaten by cattle was assumed to be contaminated. The dose through direct deposition was calculated using

Meat - Direct Deposition:

$$D = \frac{C_{GW} \, x \, I \, x \, r}{Y_v} \, x \, \frac{1 - e^{-(\lambda_r + k\dot{I}) t_i}}{\lambda_r + k\dot{I}} \, x \, Q_F \, x \, F_f \, x \, U_B \, x$$

$$x \, \frac{10^{-6} \, \mu Ci}{pCi} \, x \, DCF \, x \, \frac{1{,}000 \, mrem}{rem} \, x \, FB$$

Milk - Direct Deposition:

$$D = \frac{C_{GW} \, x \, I \, x \, r}{Y_v} \, x \, \frac{1 - e^{-(\lambda_r + kl)t_i}}{\lambda_r + kl} \, x \, Q_F \, x \, F_m \, x \, U_M \, x$$

$$x \, \frac{10^{-6} \, \mu Ci}{pCi} \, x \, DCF \, x \, \frac{1{,}000 \, mrem}{rem} \, x \, FM$$

where

Y_v = agricultural yield (kg/m^2, dry weight)

Q_F = animal consumption rate of pasture and feed [kg (dry)/day].

The dose through deposition on soil followed by root uptake was calculated using the following equations. As with produce and leafy vegetables, credit was not taken for leaching of radionuclides from the root zone of plants.

Meat - Root Uptake:

$$D = \frac{C_{GW} \, x \, I \, x \, f_1}{P} \, x \, \frac{1 - e^{-\lambda_r t_h}}{\lambda_r} \, x \, CR \, x \, Q_F \, x \, F_f \, x \, U_B \, x$$

$$x \, \frac{10^{-6} \, \mu Ci}{pCi} \, x \, DCF \, x \, \frac{1{,}000 \, mrem}{rem} \, x \, FB$$

Milk - Root Uptake:

$$D = \frac{C_{GW} \, x \, I \, x \, f_1}{P} \, x \, \frac{1 - e^{-\lambda_r t_h}}{\lambda_r} \, x \, CR \, x \, Q_F \, x \, F_m \, x \, U_M \, x$$

$$x \, \frac{10^{-6} \, \mu Ci}{pCi} \, x \, DCF \, x \, \frac{1{,}000 \, mrem}{rem} \, x \, FM$$

where

CR = concentration ratio [pCi/kg (dry weight plant) ÷ pCi/kg (dry weight soil)].

Equivalent water intake rates for all pathways were calculated using the above methodology and a spreadsheet. These rates were then input into GWSCREEN to perform all-pathways dose calculations.

Secondary and indirect pathways, such as inhalation of contaminated irrigation water, inhalation of contaminated dust, or external exposure from radionuclides deposited on the soil, were omitted from this scenario. These pathways were either not viewed as credible (e.g., a farmer standing under a center pivot irrigator while it was running and inhaling contaminated irrigation water) or would contribute relatively minor amounts when compared to direct pathways such as direct ingestion of contaminated water.

3.4.3 Intruder Scenarios

The following six types of inadvertent intruder scenarios were evaluated in this analysis and are summarized in this section:

1. Acute intruder drilling
2. Acute intruder construction
3. Chronic intruder drilling
4. Chronic intruder basement excavation
5. Chronic intruder radon
6. Chronic biointrusion.

The results from the acute drilling and acute construction scenarios were compared to the 500 mrem acute exposure standard in DOE Order 435.1. The results from the chronic drilling, chronic basement excavation, chronic radon, and chronic biointrusion scenarios were compared to the 100 mrem/yr continuous exposure standard in DOE Order 435.1. These scenarios were based on the scenarios developed and used by the NRC in 10 CFR 61 to evaluate the land disposal of radioactive waste (NRC 1981; NRC 1982; Oztunali and Roles 1986; Kennedy and Peloquin 1988).

The acute drilling, acute construction, chronic drilling, chronic basement excavation, chronic radon, and chronic biointrusion scenarios were evaluated for pits. For the soil vaults, the acute drilling, chronic drilling, chronic radon, and chronic biointrusion scenarios were evaluated. The acute construction scenario and the chronic basement excavation scenario were not evaluated for the soil vaults because a basement excavation would not contact the waste. The entire inventory in the pits and soil vaults was available for intrusion, but no depletion due to leaching was assumed. Although leaching will occur over time, this conservative assumption was made for excavation cases; during the drilling cases both the inventory still in the waste and the leached inventory would be contacted during intrusion. Therefore, leaching has no impact on the drilling intruder assessments.

Appendix B contains the inventory used in the intruder assessments. In all cases, the doses resulting from intrusion include the contributions from the decay and ingrowth of radioactive progeny. Figure 3-11 summarizes the pathways evaluated for each intruder scenario.

3.4.3.1 Acute Intruder Drilling Scenario. The acute drilling scenario assumed that an inadvertent intruder drilled a well into the contents of a soil vault or pit (see Figure 3-12). As in the NRC drilling scenario, the intruder was exposed to contaminated drill cuttings spread over the ground and to contaminated airborne dust. In the NRC drilling scenario, the intruder was exposed to contaminated drill cuttings in a mud pit. Interviews with local well drilling contractors in the Idaho Falls area indicated that drillers spread the cuttings over the ground and do not use mud pits (Seitz 1991); therefore, this site-specific deviation of the NRC drilling scenario was incorporated into the analyses. In addition,

spreading the cuttings over the ground yields higher doses than putting the cuttings in a mud pit because of decreased shielding. These cuttings were spread out over a 2,200 m^2 lot (Rogers and Hung 1987). This lot corresponds to about one-half of an acre; lots located outside the city limits of Idaho Falls are typically 1 to 3 acres. Therefore, a 2200 m^2 lot size is conservative for the local area surrounding Idaho Falls. The intruder was exposed to the contaminated cuttings for 160 hours (Seitz 1991), the time local Idaho Falls well drilling contractors state it would take to drill and develop a 22-in. diameter irrigation well.

Well drilling contractors in the Idaho Falls area reported that two types of wells are typically drilled: small diameter residential wells and large diameter irrigation wells. The small residential wells are typically 6 to 8 in. in diameter, serve a single residence, and also may provide enough water for a family garden and several cows. The large diameter irrigation wells are drilled to serve systems that irrigate hundreds of acres; the wells are located in the middle of farm fields, not near the farmer's residence. Therefore, a farmer would not drill an irrigation well to acquire water for his residence. Large diameter irrigation wells are currently drilled 18-in. in diameter, but drilling contractors thought 22-in. diameter irrigation wells would be drilled in the near future.

Based on the information obtained from Idaho Falls area drilling contractors, an acute drilling exposure could result from drilling either an 8-in. diameter residential well or a 22-in. diameter irrigation well. Because the doses for this scenario are directly proportional to the volume of contaminated cuttings brought to the surface, to provide bounding doses a 22-in. diameter irrigation well was evaluated. The time required to drill and develop a well (160 hours for a large irrigation well and 48 hours for a residential well) also provided bounding doses when an irrigation well was evaluated.

Based on a waste thickness of 6.1 m for pits, the 22-in. well results in 1.5 m^3 of contaminated cuttings being brought to the surface during the acute drilling scenario. Based on a waste thickness of 3 m, for soil vault rows, the 22-in. well results in 0.75 m^3 of contaminated cuttings being brought to the surface.

Intruder doses were calculated at various points in time after site closure. For pits and soil vaults, these times were 2120 (100 years after site closure), 3020, 5020, 7020, and 12020. In the construction and excavation scenarios, additional calculations were made at one million years to allow for secular equilibrium of radioactive daughter radionuclides with the long-lived actinide parent radionculides. Inhalation doses were calculated using the RESRAD computer code and were based on a dust loading of 1 mg/m^3 (EG&G Idaho 1984), representative of construction activities. The external dose rate was calculated using the MICROSHIELD 5.0 computer code. The source configuration was modeled as a 26.5-m radius disk, the radius of a circular 2,200 m^2 lot, with a receptor point 1 m above the plane at approximately waist height. The doses include exposure to radioactive progeny. No shielding factors were incorporated into the analyses.

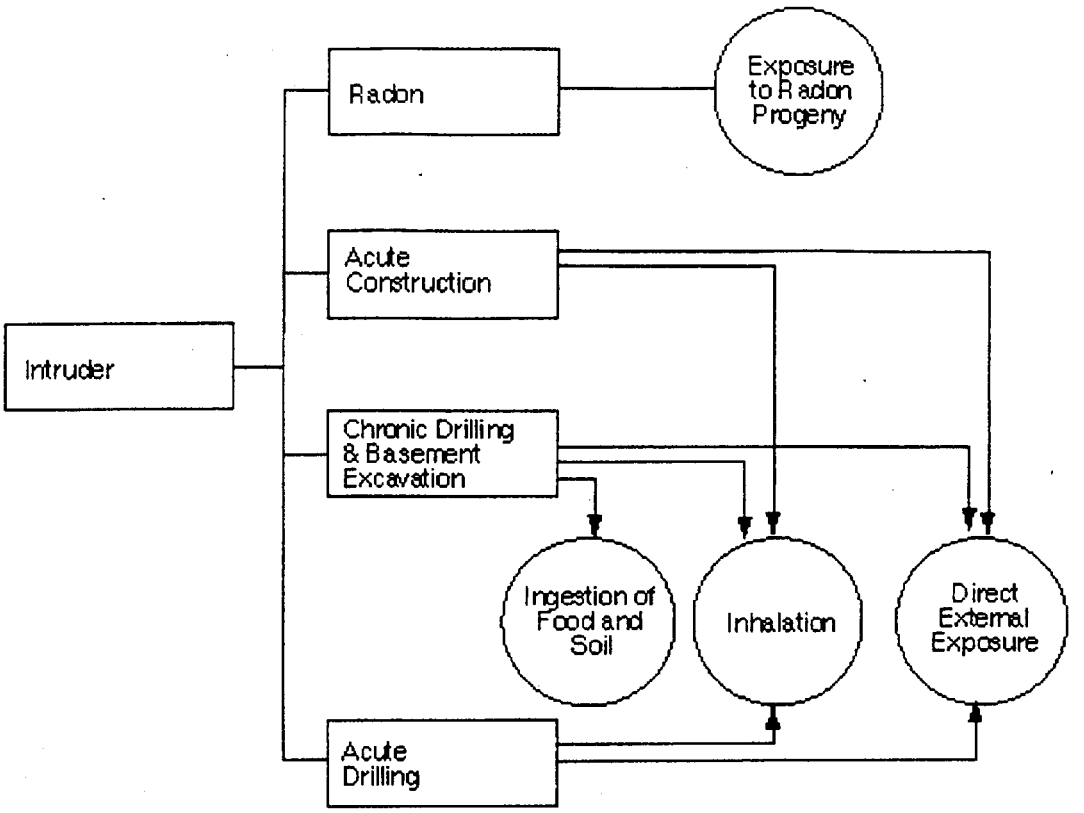

Figure 3-11. RWMC performance assessment intruder pathways.

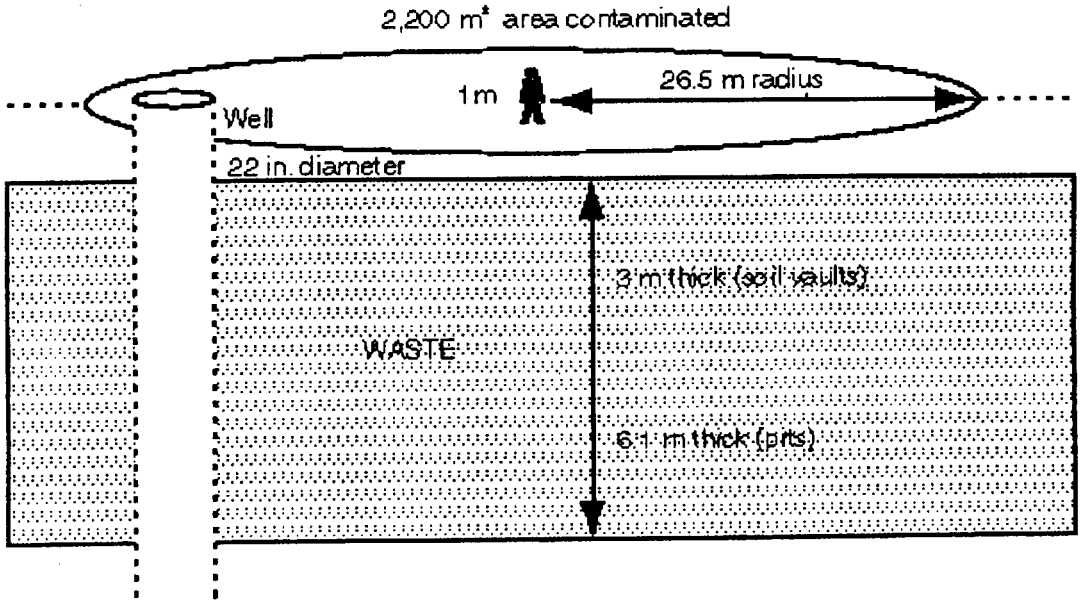

Figure 3-12. Acute intruder drilling scenario.

3.4.3.2 Acute Intruder Construction Scenario. The acute construction scenario assumes that an inadvertent intruder moves onto the RWMC SDA and excavates a basement in the waste (see Figure 3-13). The intruder is exposed to contaminated dust and contaminated waste in the bottom of the excavation. No ingestion doses are postulated for this scenario. This scenario is applicable to pits but not to soil vaults. Soil vaults have extra cover, which precludes intrusion into the waste by digging a basement. Because potatoes are a large cash crop in southeastern Idaho, the potential for an inadvertent intruder to dig a potato cellar was also considered. This scenario was dismissed because potato cellars are relatively shallow, approximately 1 m deep, and the intruder is unable to contact the waste during excavation. Because a basement excavation, which is 3 m deep, contacts the waste, the acute potato cellar construction scenario is bounded by the acute basement construction scenario.

Based on an interview with an Idaho Falls construction contractor, the exposure time for this scenario was 64 hours (Sussman 1993). This exposure time includes the time required to excavate the basement, pour the footings, form the basement walls, remove the forms, and backfill and grade the area around the basement. For the inhalation pathway, the dust loading was 1 mg/m^3 (EG&G Idaho 1984), representative of construction activities. For the external exposure pathway, the intruder stood directly on the exposed waste. This is conservative because an intruder would spend only a part of the time down inside the excavation. Shielding was not considered except for the self-shielding provided by the waste. The excavation was an 10×10-m area and 3-m deep (Rogers and Hung 1987). At the time of maximum erosion (the year 5020), 2.4 m of cover remains over the waste and the 3-m basement protrudes into the waste a distance of 0.6 m. The area of the basement corresponds to 1,100 ft^2, a reasonably-sized home in southeastern Idaho. The sides of the excavation will undoubtedly slope, but because of the small depth that the excavation penetrates the waste (0.6 m or less than 2 ft), sloping sides were not considered. Intruder doses were calculated at various points in time after site closure. Because of cover thickness, intrusion into the waste was not possible until about 3000 years after closure. To maximize doses, intrusion was postulated to start in 5020, which corresponds to the time of maximum. In addition, because the doses appeared to be increasing during the period from 1000 to 10,000 years after closure due to ingrowth of radioactive progeny, the doses at one million years was also calculated. One million years corresponds to the time when most long-lived decay series have achieved a substantial fraction of secular equilibrium.

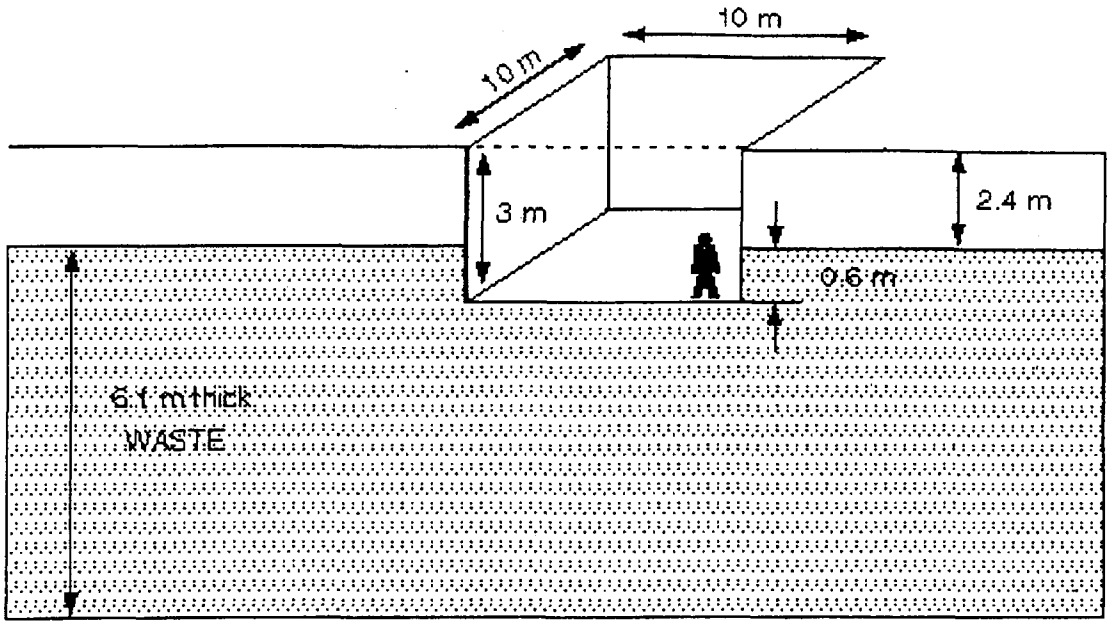

Figure 3-13. Acute intruder construction scenario.

RESRAD was used to model the inhalation pathway, and MICROSHIELD 5.0 was used to model the external exposure pathway. The source configuration was modeled as a volume source with infinite lateral extent with a receptor point 1 m above the source. In this configuration, the top of the volume source is the floor of the basement. This configuration does not account for the four 0.6-m vertical walls that surround the receptor. An evaluation of the doses from these walls found the doses to be two orders of magnitude less than the doses from the floor of the basement, and the doses from the walls were omitted from further calculations.

3.4.3.3 Chronic Intruder Drilling and Chronic Intruder Basement Excavation Scenarios. The chronic drilling scenario assumes that an inadvertent intruder moves onto the RWMC SDA and drills a residential well into the waste (see Figures 3-14 and 3-15). This scenario is applicable to both pits and soil vaults. The chronic basement excavation scenario assumes that an inadvertent intruder drills a residential well through the waste and also excavates a basement in the waste (see Figure 3-14). This scenario is applicable to pits, but not to soil vaults, because a basement excavation would not contact the waste in soil vaults.

In both the chronic drilling and chronic basement excavation scenarios, the contaminated material brought to the surface is spread around the site and mixed in the top 0.61 m of soil where crops are grown. The intruder breathes contaminated dust, eats contaminated food stuffs, inadvertently eats soil, and is directly exposed to contaminated ground surfaces.

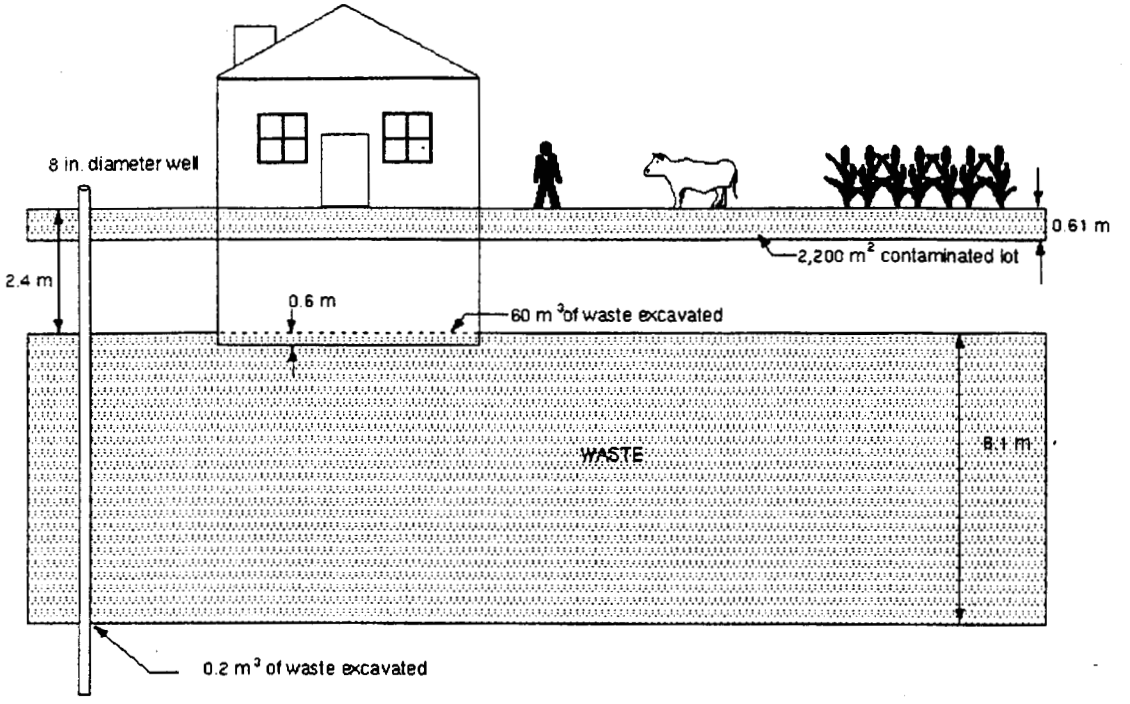

Figure 3-14. Chronic intruder drilling and chronic intruder basement excavation scenarios for pits.

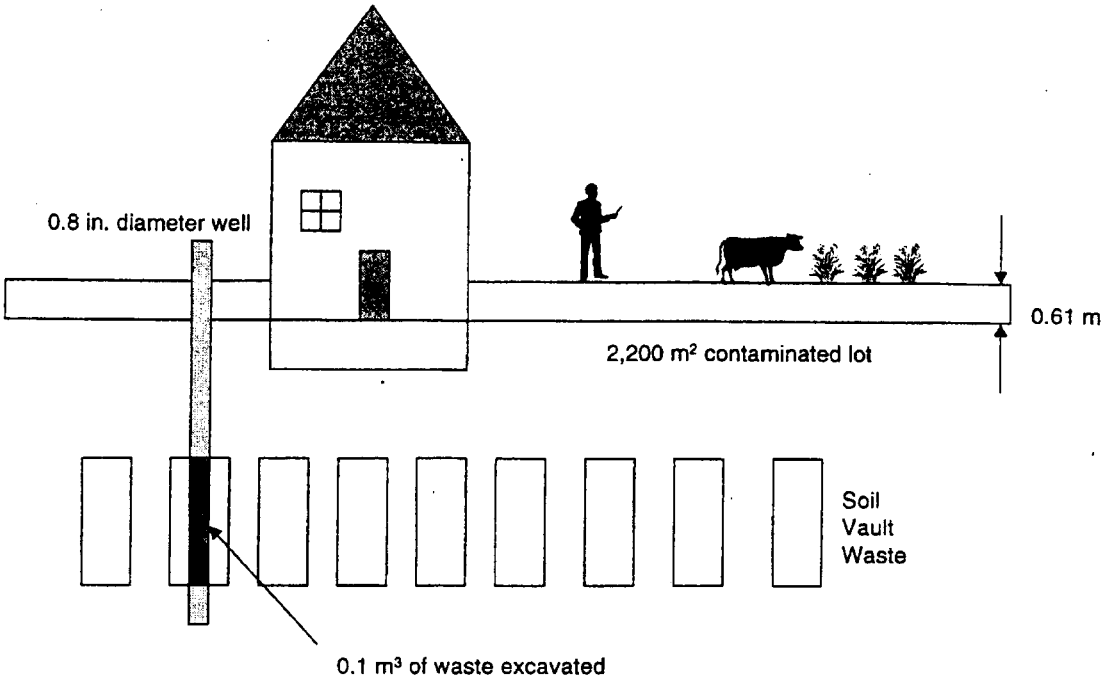

Figure 3-15. Chronic intruder drilling scenario for soil vaults.

The drilling portion of the scenarios evaluates an 8-in. residential well. This type of well serves a single residence and provides enough additional water for a family garden and several cows. As described in the acute drilling scenario, large diameter irrigation wells are drilled to serve large irrigation systems (hundreds of acres) that are located in the middle of farm fields, not near a farmer's residence. Therefore, in this residence/home garden scenario it is appropriate to evaluate a case where a farmer drills a small diameter residential well near his residence, not a large diameter irrigation well.

As discussed in the acute construction scenario, the basement excavation was 10 × 10 m in area and 3 m deep (Rogers and Hung 1987). As is the case in the acute construction scenario, the potential for an inadvertent intruder digging a potato cellar was considered. This scenario was dismissed because potato cellars are relatively shallow, approximately 1 m deep, and the intruder is able to contact more waste during basement excavation, approximately 3 m deep. Therefore, the amount of contaminated material brought to the surface through basement excavation exceeds the amount of contaminated material brought to the surface during potato cellar construction. Therefore, the doses from the chronic basement excavation scenario bound the doses from the chronic potato cellar construction scenario and eliminate the need for a chronic potato cellar construction scenario.

For the pits, drilling an 8-in. diameter residential well through the waste would bring 0.2 m^3 of waste to the surface, based on a 6.1-m waste thickness. For the pits at minimum cover thickness (maximum waste penetration), 2.4 m of cover is present over the waste, and 60 m^3 of contaminated waste could be brought to the surface[f] through basement excavation. Because an 8-in. diameter residential well is also drilled through the waste, an additional 0.2 m^3 of waste is brought to the surface, for a total of 60.2 m^3 of contaminated material on the surface.

For the soil vaults, intrusion by basement excavation is precluded by increased cover thickness (greater than 3 m). Well drilling was calculated to bring 0.1 m^3 of contaminated material to the surface based on a 3-m waste thickness and an 8-in. diameter residential well.

The exposure time was 1 year (8760 hours). For the dust inhalation pathway, the intruder spent 24 hours plowing and cultivating (1 mg/m^3 dust loading), 1200 hours conducing other farm activities (0.07 mg/m^3 dust loading), and 7536 hours conducting other activities, which result in a dust loading of 0.05 mg/m^3 (EG&G Idaho 1984). This results in a time-weighted average dust loading of 5.53E-8 kg/m^3. The waste was spread out over a 2,300 m^2 lot (Rogers and Hung 1987). The 2,200-m^2 (0.5-acre) lot is conservative because lots outside of Idaho Falls are typically 1 to 3 acres. The waste was mixed to a depth of 0.61 m. The mixing depth of 0.61 m was based on using a deep tilling plow to increase the depth of the root zone and to break up soil compaction. These plows are also used in areas of southeast Idaho with highly erodible soils to minimize erosion. Deep tilling plows have shanks that till to a depth of 24 inches (0.61 m) and are sold at Idaho Falls implement dealers.

The RESRAD computer code was used to model the inhalation and food chain doses. Crops were grown onsite in a family garden that contained contaminated soil. Yu et al. (1993) provides details on the food chain pathway methodology used in RESRAD. The contaminated soil was mixed and diluted with uncontaminated excavated soil and surface soil (Rogers et al. 1982). Dietary fractions representative of rural agriculture areas were used (EPA 1989). Based on the data in EPA (1989), 70% of the intruder's vegetables and produce, 40% of the intruder's milk, and 44% of the intruder's meat were assumed to be produced locally. Because 2200 m^2 is a relatively small lot that cannot fully support beef cattle or milk

---

f. A 3-m excavation depth and a 2.4-m cover thickness results in a 0.6 m penetration of the waste. Based on an area of 10 × 10 m, the volume brought to the surface is 60 m^3 (0.6 × 10 × 10 m).

cows, the consumption rate of contaminated pasture was adjusted to reflect the maximum amount of feed that could be produced on the lot, assuming three cuttings of hay per year and a yield of 0.7 kg/m^2 (wet weight). Stored feed was assumed to be uncontaminated. Based on a total consumption rate of 12 kg/day (dry weight) for beef cattle and 16 kg/day (dry weight) for milk cows and a dry to wet weight conversion factor of 0.2, 9% of the total pasture eaten by the animal was contaminated. The consumption rate for contaminated pasture was 5.4 kg/day (wet weight) for beef cattle and 7.2 kg/day (wet weight) for milk cows.

$$0.7 kg/m^2 \text{ (wet wt.)} \times 3 \text{ cuttings hay/yr} \times 2{,}200 m^2 = 4{,}620 \text{ kg/yr (wet wt.)} \quad (3\text{-}47)$$

$$\frac{12 \text{ kg/d}}{0.2} \times 365 \text{ d/yr} = 21{,}900 \text{ kg/yr (beef cattle, wet wt.)} \quad (3\text{-}48)$$

$$\frac{16 \text{ kg/d}}{0.2} \times 365 \text{ d/yr} = 29{,}200 \text{ kg/yr (milk cattle, wet wt.)} \quad (3\text{-}49)$$

$$\text{Total} = 21{,}900 \text{ kg/yr} + 29{,}200 \text{ kg/yr} = 51{,}100 \text{ kg/yr (wet wt.)} \quad (3\text{-}50)$$

$$\frac{4{,}620 \text{ kg/yr}}{51{,}100 \text{ kg/yr}} = 0.090 \quad (3\text{-}51)$$

$$\frac{12 \text{ kg/d}}{0.2} \times 0.090 = 5.4 \text{ kg/d (beef cattle, wet wt.)} \quad (3\text{-}52)$$

$$\frac{16 \text{ kg/d}}{0.2} \times 0.090 = 7.2 \text{ kg/d (milk cattle, wet wt.)} \quad (3\text{-}53)$$

Human consumption rates were derived from the diet developed in Rupp (1980), based on a 1965 USDA survey. The Rupp diet was the default diet used in the EPA's NESHAPs Environmental Impact Statement (EPA 1989). The inhalation rate evaluated was 8030 m^3 /yr. Consumption of contaminated soil by adults was incorporated into the scenario using a consumption rate of 10 mg/day (Konz et al. 1989).

External exposures were calculated using the computer code MICROSHIELD 5.0. The intruder was exposed to waste excavated from the basement and spread around a home site (2,200 m^2) to a depth of 0.61 m. The source configuration was modeled as a 26.5-m radius disk, with a thickness of 0.61 m. The receptor point was 1 m above the plane (see Figures 3-16 and 3-17).

The excavated waste was diluted and mixed with uncontaminated soil during excavation. The exposure time was 1 year (8760 hours). The shielding factor evaluated was 0.7. The 0.7 shielding factor is from NRC (1977) and corresponds to the shielding factor used for the maximally exposed individual.

For pits and soil vaults, the chronic drilling scenario was evaluated at 2120, 3020, 5020, 7020, and 12020. For pits, the chronic basement excavation scenario was postulated to start in 5020, which corresponds to the time of maximum erosion. The chronic basement excavation scenario was also evaluated at 7020 and 12020. In addition, because the doses appeared to be increasing during the period from 1000 to 10,000 years after closure, due to ingrowth of radioactive progeny, the doses at one million years was also calculated. One million years corresponds to the time when most long-lived decay series have achieved a substantial fraction of secular equilibrium. One million years corresponds to the time when most long-lived decay series have achieved a substantial fraction of secular equilibrium.

3.4.3.4 ***Chronic Intruder Radon Scenario.*** Two scenarios were considered for calculating chronic radon doses: excavation over pits and excavation over soil vaults (Figures 3-16 and 3-17). The scenarios were based on an intruder excavating a 10 x 10 x 3-m basement over the waste and constructing a 10 x 10 x 3-m house over the basement. The intruder was exposed to Rn-222 and its short-lived progeny (Po-218, Pb-214, Bi-214, and Po-214) while in the basement and house. The data in Konz et al. (1989) were used to estimate that an individual spent 115 h/week or 68% of their time indoors. This represents the time spent at home and indoors. For soil vaults, the analysis was based on excavating a basement over a row of five soil vaults, each with the diameter of 2 m, separated by 0.6 m of clean soil. This is the maximum number of 2-m diameter soil vaults that can fit in the area of a 10 x 10-m basement.

The RESRAD computer code (Gilbert et al. 1989) was used to perform the dose assessments. The RESRAD output also provides the radon flux from the surface, which was compared to the 20 pCi/m2s standard contained in 40 CFR 61 Subpart Q. Site-specific geometry parameters (such as waste layer thickness and cover thickness) were used in the analyses. The data for the properties of the concrete used in the basement foundation were obtained from two instrumented basement structures located at Colorado State University in Fort Collins, Colorado (Gadd 1993).

The Colorado State University structures were constructed and instrumented for research into the transport, entry, and accumulation of radon in residential structures (Ward et al. 1993). The structures were built using standard residential construction techniques and concrete. For example, the concrete was selected from three Fort Collins-area concrete distributors, based on the lowest cost. The concrete aggregate was surveyed to ensure that it did not contain excessive quantities of Ra-226, which would confound soil radon entry measurements.

Although the outside of a foundation is typically water proofed in the Western United States, water proofing was not applied to the basement structure. The walls and floor were constructed slightly thinner than standard because the structural support for a full upper story was not required and to increase the diffusion of radon into the basement from the surrounding soil to minimize radon measurement problems. The basement structures were instrumented to measure indoor-soil pressure differentials; soil gas Rn-222 concentrations; air permeability; soil moisture; and indoor, outdoor, and subslab Rn-222 concentrations (Gadd 1993).

The Colorado State University data (see Table 3-7) were used because they represent residential concrete and construction techniques used in the Western United States, and they were collected under rigorous and known conditions. RESRAD does not model basement and first floor radon exposures separately. Therefore, a total room height of 6 m was used to account for first floor and basement exposures.

Table 3-7 lists the U-238, U-234, Th-230, and Ra-226 concentrations in the year 2020 (site closure). Radon doses were evaluated at 3000, 5000, and 10,000 years after site closure.

Table 3-7. Data used in the chronic intruder-radon scenario.

Parameter	Pits	Soil vaults
Basement depth	3 m	3 m
First floor height[a]	3 m	3 m
Total porosity	0.487	0.487
Volumettic water content	0.33	0.33
Soil density	1.5 g/cm^3	1.5 g/cm^3
U-238 concentration in 2020	175 pCi/g	279 pCi/g
U-234 concentration in 2020	38.8 pCi/g	1.67 pCi/g
Th-230 concentration in 2020	0.618 pCi/g	3.35E-4 pCi/g
Ra-226 concentration in 2020	14 pCi/g	1.94E-6 pCi/g
Ra-226 concentration at time of maximum dose	14 pCi/g	1.94E-6pCi/g
Waste area	12,400 m^2	15.7 m^2 [b]
Waste thickness	6.1 m	3.05 m
Cover thickness	3 m	3.3 m
Uranium leach rate	7.6E-6/yr[c]	1.5E-5/yr[c]
Thorium leach rate	7.6E-6/yr[c]	1.5E-5/yr[c]
Radium leach rate	1.5E-4/yr[d]	3.1E-4/yr[d]

	Colorado State University value
Diffusion coefficient	2.5E-8 m^2/S
Emanation fraction	0.17
Thickness of building foundation	0.10m
Density of building foundation	2.1 g/cm^3
Total porosity of building foundation	0.13
Volumetric water content of building foundation	0.13[f]

a. A total room height of 6 m was used.

b. Based on five 2-m diameter soil vaults.

c. Based on a K_d Of 1,000 mLg and an infiltration rate of 0.070 m/yr.

d. Based on a K_d of 50 mLg and an infiltration rate of 0.070 m/yr.

e. Source: Gadd (1993).

f. Calculated based on I 00% saturation of concrete. Because a diffusion coefficient was entered, this parameter is not used by RESRAD.

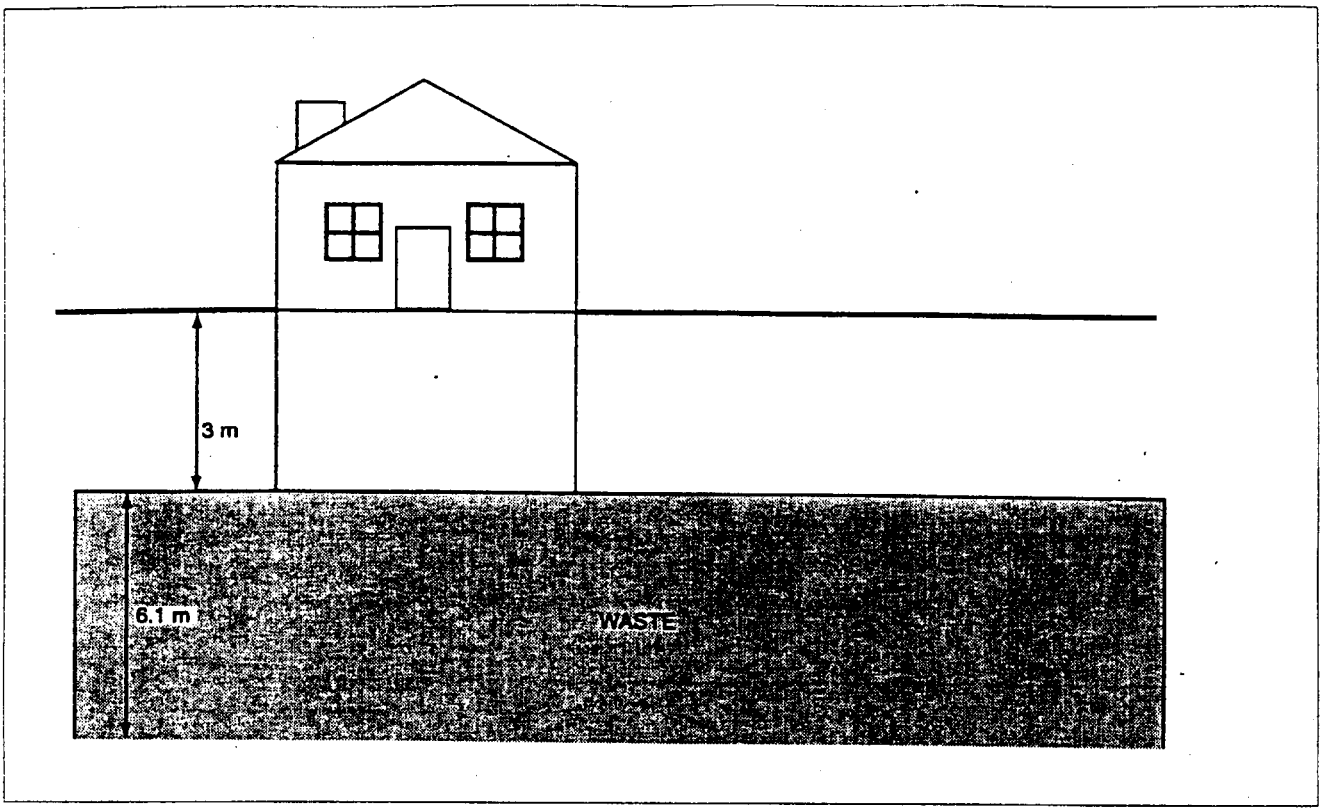

Figure 3-16. Chronic radon scenario for pits.

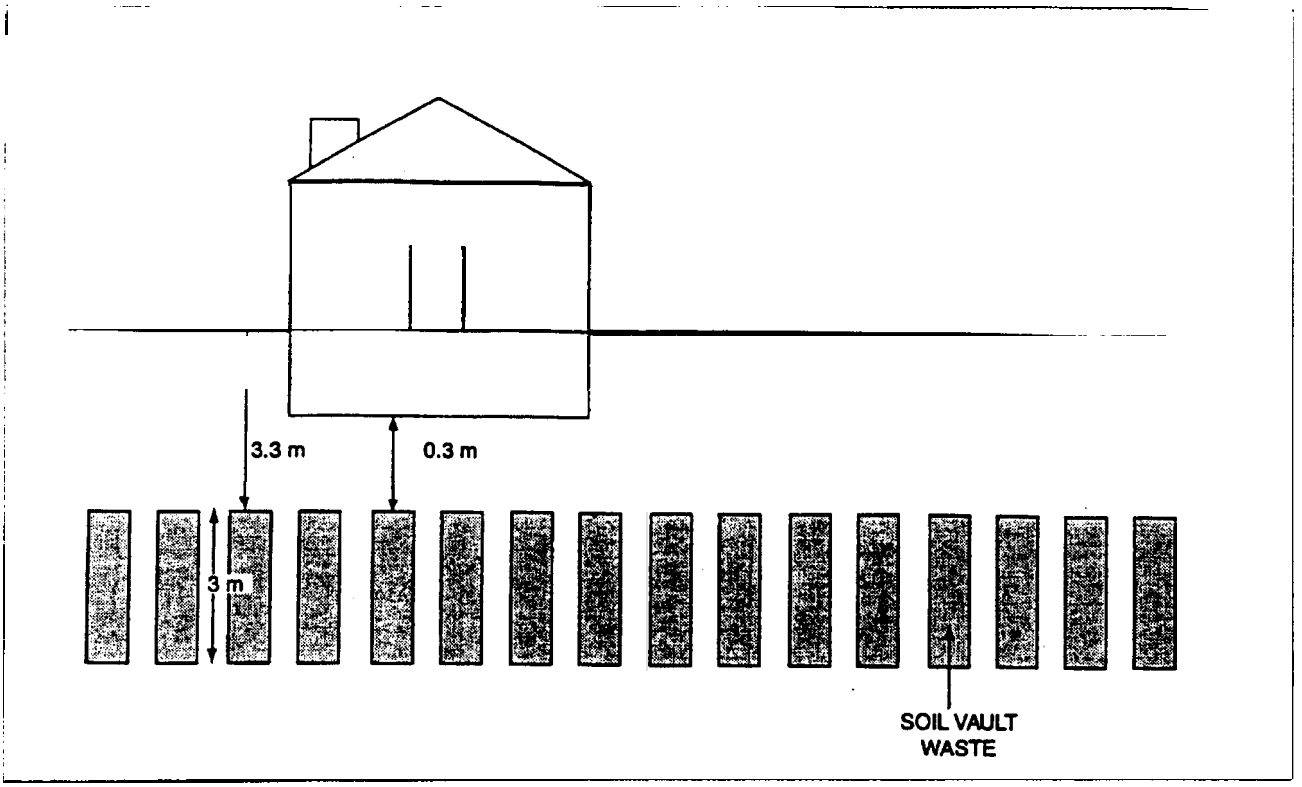

Figure 3-17. Chronic radon scenario for soil vaults.

4. RESULTS OF ANALYSES

This chapter presents the projected impacts for each pathway, the sensitivity and uncertainty related to the impacts, and an integration and interpretation of the results.

4.1 Projected Impacts

Section 4.1 presents projected impacts for the atmospheric, all pathways, intruder, and groundwater protection analyses. The impacts are presented based on a time of compliance of 1000 years. However, if the peak impacts occur beyond 1000 years (up until 10,000 years) they are also presented.

Previous analyses (Maheras et al 1994, 1997) used the GENII model for the assessment of doses associated with atmospheric releases and intruder scenarios. RESRAD was used for current analysis. A comparison of RESRAD and GENII was made via a benchmarking exercise described in Appendix C. In this exercise parameter values used in the GENII calculations were applied to the RESRAD code.

4.1.1 Atmospheric

Based on the dose assessments in the *1992 INEL National Emission Standard for Hazardous Air Pollutants Annual Report* (DOE 1993), the emissions from contaminated soil areas at the RWMC yielded a dose of 5.7E-6 mrem/yr during the operational and institutional control periods. Gaseous emissions of H-3 and C-14 during the operational and institutional control periods yielded a dose of 0.003 mrem/yr. When these doses were combined with the dose from existing monitored and unmonitored emission points at the INEEL and existing diffuse sources at other areas of the INEEL (DOE 2000), a dose of 0.0086 mrem/yr was calculated (see Table 4-1). This dose was well below the 40 CFR 61 Subpart H standard of 10 mrem/yr.

Post-institutional control doses represent the doses through the ingestion, inhalation, and external exposure pathways. During the post-institutional control period, biointrusion by plant roots and harvester ants was used as the mechanism to move radioactive material to the surface, which was then transported to a receptor via the atmosphere. For both pits and soil vaults, the maximum doses occurred in the year 2120, at the end of institutional control. The dose for pits was estimated to be 0.033 mrem/yr, and the doses for soil vaults was calculated to be 0.11 mrem/yr. The dominant dose contributor for the pits was Cs-137, and the dominant dose contributors for the soil vaults were Cs-137 and Ni-63.

Gaseous emissions of H-3 and C-14 during the post-institutional control period yielded a dose of 0.41 mrem/yr. When these doses were combined with the dose from existing monitored and unmonitored emission points at the INEEL and existing diffuse sources at other areas of the INEEL (DOE 1993), a dose of 0.53 mrem/yr resulted (see Table 4-1). These doses were well below the 40 CFR 61 Subpart H standard of 10 mrem/yr.

Table 4-1. Atmospheric impacts.

Time period	EDE (mrem/yr)
Operational and institutional control	
INEEL baseline[a]	0.0056
Contaminated soil areas at the RWMC[b]	5.7E-6
Gaseous H-3 and C-14[c]	0.003
Total	0.0086
Post-institutional control	
INEEL baseline[a]	0.0056
Pits	5.7E-6
Soil vaults	0.11
Gaseous H-3 and C-14	0.34
Total	0.46
Radon Flux	
Pits	0.37 pCi/m^2-s
Soil vaults	0.00005 pCi/m^2-s
Total	0.37 pCi/m^2-s

a. Includes doses from Continuously Compliance Monitored Release Points, Other Release Points, and Diffuse Sources at the INEEL reported in DOE (2000). Does not include the RWMC Diffuse Source reported in DOE (2000).
b. Reported in DOE (1993).
c. Calculated using flux rates from DUST.

Based on a time of compliance of 1000 years, the peak radon flux was 0.37 pCi/m^2-s for pits and 0.00005 pCi/m^2-s for soil vaults. The combined radon flux, 0.37 pCi/m^2-s, was well below the 40 CFR 61 Subpart Q standard of 20 pCi/m^2-s and occurred immediately after institutional control ceased in the year 2021. The peak radon flux was associated with Ra-226 disposed in pits.

4.1.2 All-Pathways

For members of the public, groundwater was the primary pathway of concern. The maximum all-pathways doses were calculated for three time periods; operational and institutional control (1984 – 2120), the post-institutional control (1984 – 3000), and long term post-institutional control period (through year 12,000). During the operational period, 1984 – 2020, an average infiltration rate of 7.6 cm/yr was used to calculate the release rate from the waste and an average infiltration rate of 8.5 cm/yr was used to define the infiltration rate throughout the area of the SDA. (See Figure 3-1 and 3-5.) At the end of institutional control in 2020, the infiltration rate was reduced to 1 cm/yr to simulate the placement of a cap over the disposal facility. This infiltration rate is approximately equal to the infiltration rate

through undisturbed soils in the vicinity of the SDA. Therefore, it was assumed that a 1-cm/yr-infiltration rate could be maintained in the future.

During the operational and institutional control periods, 1984 through 2120, the member of the public was assumed to be located at the INEEL Site boundary, 5500-m south of the RWMC facility boundary. As shown in Table 4-2, the all-pathways dose through groundwater for this member of the public was estimated to be 0.002-mrem/yr, in the year 2120. This is less than 0.01% of the 25-mrem/yr standard. The primary radionuclides of concern during the operational and institutional control periods are C-14, Cl-36, and I-129.

Table 4-2. Predicted maximum SDA radionuclide all-pathways dose (mrem/yr) for the 100-yr institutional control period.

Radionuclide	Peak Time and Magnitude of Maximum all-pathways dose at INEEL boundary up to year 2020	
	Date	Dose
	Year	mrem/year
C-14	2120	1.08E-03
Cl-36	2120	8.69E-04
I-129	2120	1.98E-04
Np-237	2120	8.61E-11
U-234	2120	2.87E-09
U-238	2120	6.08E-09
Total Dose	2120	2.15E-03

During the post-institutional control period from 2120 through 3000, the member of the public was assumed to be located at 100 m, 300 m, 600 m, or the boundary of the INEEL south of the SDA. The results of the simulations are shown in Figures 4-1, 4-3, 4-5, and 4-7 and Table 4-3. The all-pathways dose through groundwater for these members of the public at the receptor location were estimated to be:

- 5.5-mrem/yr in the year 2521 at 100-m (22% of the 25-mrem/yr standard),
- 0.87-mrem/yr in the year 2570 at 300-m (3.5% of the 25-mrem/yr standard),
- 0.38-mrem/yr in year 2521 at 600-m (1.5% of the 25-mrem/yr standard), and
- 0.017-mrem/yr in year 2496 at the INEEL site boundary (0.07% of the 25-mrem/yr standard).

During the post-institutional control period from 2120 through 3000, the primary radionuclides of concern are C-14, Cl-36, and I-129.

During the long term post-institutional control period from 2120 through 12,000, the member of the public was also assumed to be located at 100 m, 300 m, 600 m, or the boundary of the INEEL south of the SDA. The results of the simulations are shown in Figures 4-2, 4-4, 4-6, and 4-8 and Table 4-4. During the post-institutional control period from 2120 through 12,000, there are two dose peaks of

interest. The first is the dose peak captured in the post-institutional control period between year 2120 and 3000 and has been discussed above. The second and larger peak is the dose peak in about 10,000 years, from the actinide disposals. The all-pathways groundwater dose for these members of the public were estimated to be:

- 15.9-mrem/yr in the year 12,010 at 100-m (64% of the 25-mrem/yr standard),
- 2.34-mrem/yr in the year 12,010 at 300-m (9% of the 25-mrem/yr standard),
- 1.11-mrem/yr in year 11,360 at 600-m (4% of the 25-mrem/yr standard), and
- 0.05-mrem/yr in year 11,360 at the INEEL site boundary (0.2% of the 25-mrem/yr standard).

During this period, the primary radionuclides of concern are U-238 and U-234.

The sensitivity of the results to a variety of parameters is discussed in Section 4.2. The parameters evaluated include the infiltration rates, Kd values, and aquifer velocity.

Table 4-3. Predicted maximum SDA radionuclide all-pathways dose (mrem/yr) for the 1,000-yr-compliance period (from year 2120 – 3000).

	Peak Time and Magnitude of Maximum All-pathways Dose Down-gradient from SDA							
	Receptor at 100-m		Receptor at 300-m		Receptor at 600-m		Receptor at INEEL Boundary	
Nuclide	Date	Dose	Date	Dose	Date	Dose	Date	Dose
	Year	mrem/year	Year	mrem/year	Year	mrem/year	Year	mrem/year
C-14	2546	3.74E+00	2696	5.80E-01	2570	2.59E-01	2521	1.13E-02
Cl-36	2371	1.05E+00	2446	1.72E-01	2396	7.26E-02	2346	3.07E-03
I-129	2546	9.56E-01	2570	1.44E-01	2570	6.55E-02	2521	2.93E-03
Np-237	2999	5.12E-05	2999	2.22E-05	2999	8.93E-06	2999	6.51E-07
U-234	2999	1.75E-03	2999	6.68E-04	2999	2.06E-04	2999	1.64E-05
U-238	2999	5.51E-03	2999	2.18E-03	2999	7.31E-04	2999	5.67E-05
Total Dose	2521	5.49E+00	2570	8.75E-01	2521	3.83E-01	2496	1.66E-02

Table 4-4. Predicted maximum SDA radionuclide all-pathways dose (mrem/yr) for the 10,000-yr-simulation period (from year 2120 – 12,000).

Nuclide	Peak Time and Magnitude of Maximum All-pathways Dose Down-gradient from SDA							
	Receptor at 100-m		Receptor at 300-m		Receptor at 600-m		Receptor at INEEL Boundary	
	Date	Dose	Date	Dose	Date	Dose	Date	Dose
	Year	mrem/year	Year	mrem/year	Year	mrem/year	Year	mrem/year
C-14	2546	3.74E+00	2696	5.80E-01	2570	2.59E-01	2521	1.13E-02
Cl-36	2371	1.05E+00	2446	1.72E-01	2396	7.26E-02	2346	3.07E-03
I-129	2546	9.56E-01	2570	1.44E-01	2570	6.55E-02	2521	2.93E-03
Np-237	12010	3.27E-01	12010	4.79E-02	12010	2.46E-02	12010	1.11E-03
U-234	12010	2.69E+00	12010	3.95E-01	11360	1.89E-01	11360	8.65E-03
U-238	12010	1.28E+01	12010	1.88E+00	11360	8.96E-01	11360	4.12E-02
Total Dose	12010	1.59E+01	12010	2.34E+00	11360	1.11E+00	11360	5.12E-02

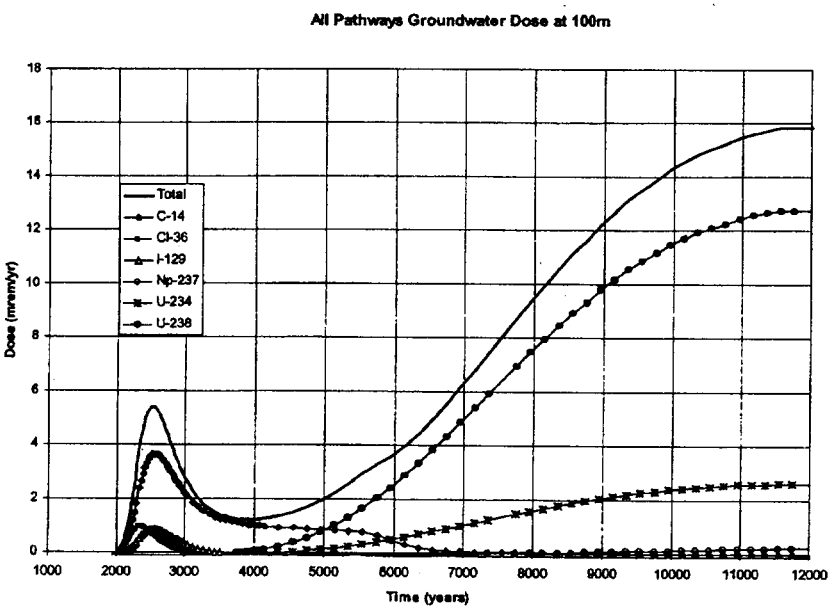

Figure 4-1. Simulated PA contaminant all-pathways groundwater dose at the 100-m receptor fence during the 1,000-yr-compliance period.

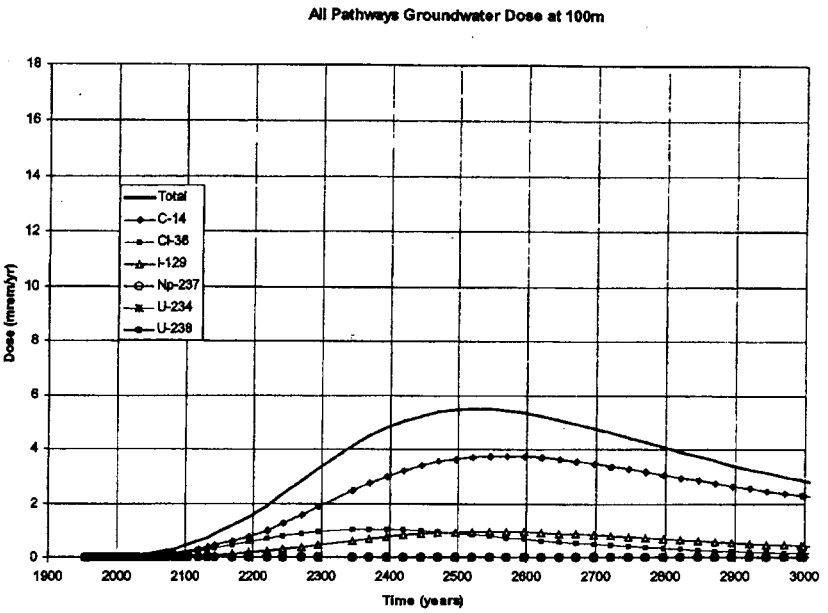

Figure 4-2. Simulated PA contaminant all-pathways groundwater dose at the 100-m receptor fence during the 10,000-yr. simulation period.

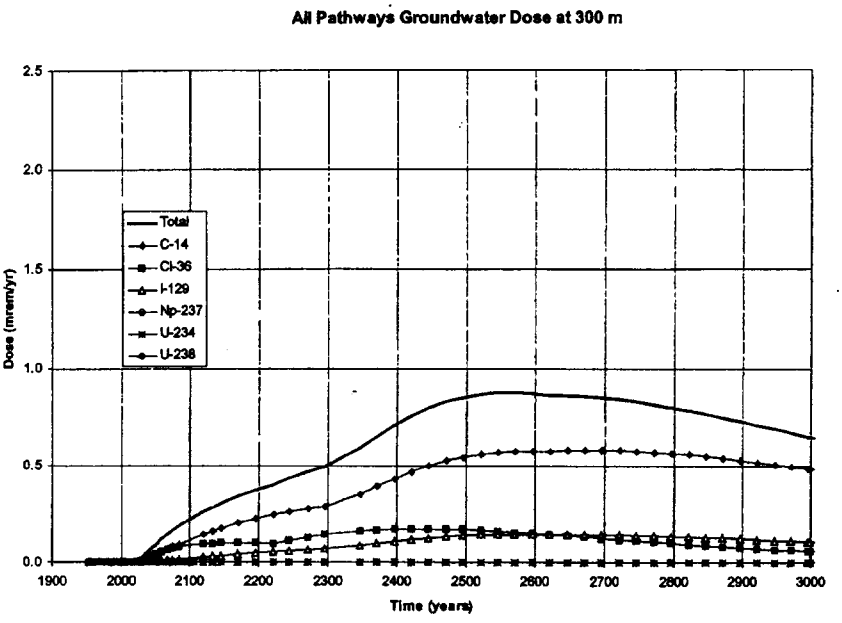

Figure 4-3. Simulated PA contaminant all-pathways groundwater dose at the 300-m receptor fence during the 1,000-yr-compliance period.

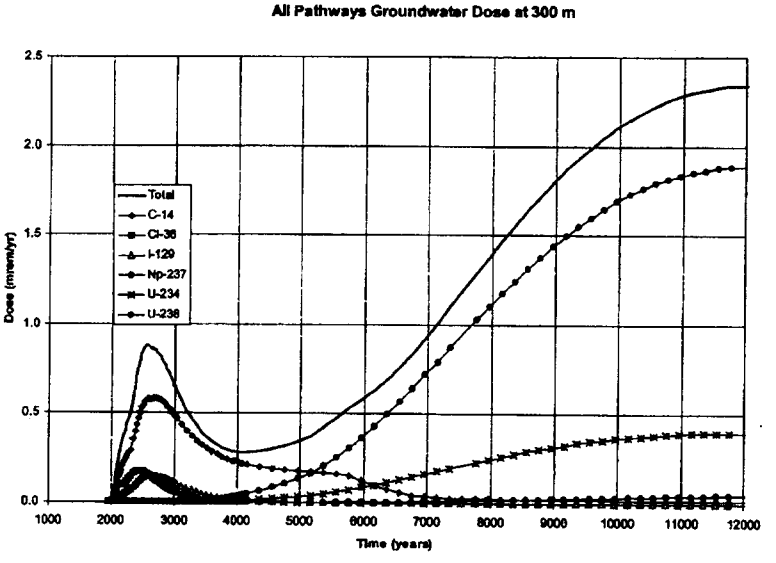

Figure 4-4. Simulated PA contaminant all-pathways groundwater dose at the 300-m receptor fence during the 10,000-yr. simulation period.

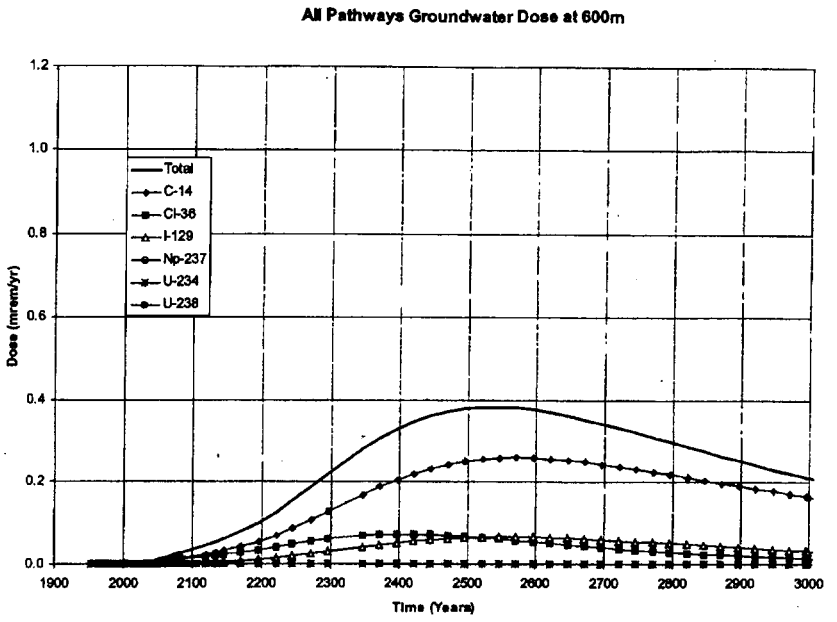

Figure 4-5. Simulated PA contaminant all-pathways groundwater dose at the 600-m receptor fence during the 1,000-yr-compliance period.

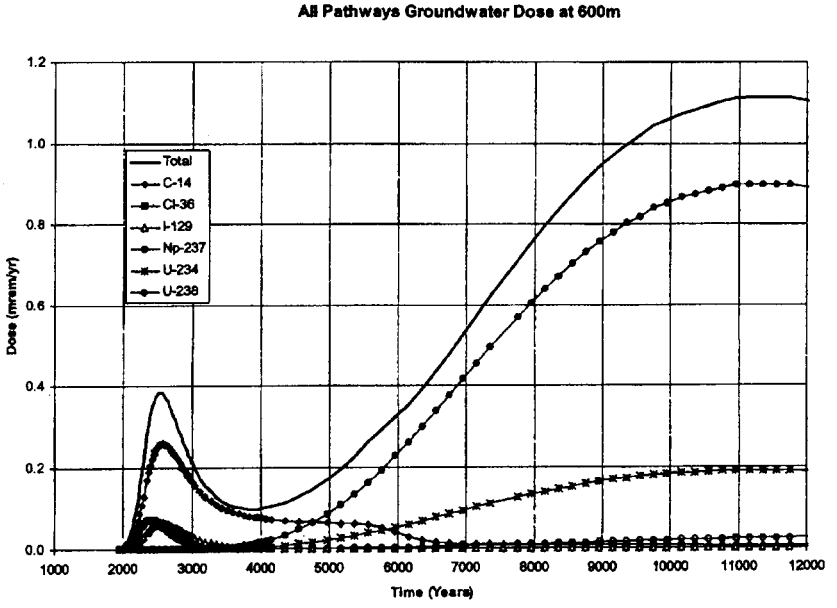

Figure 4-6. Simulated PA contaminant all-pathways groundwater dose at the 600-m receptor fence during the 10,000-yr. simulation period.

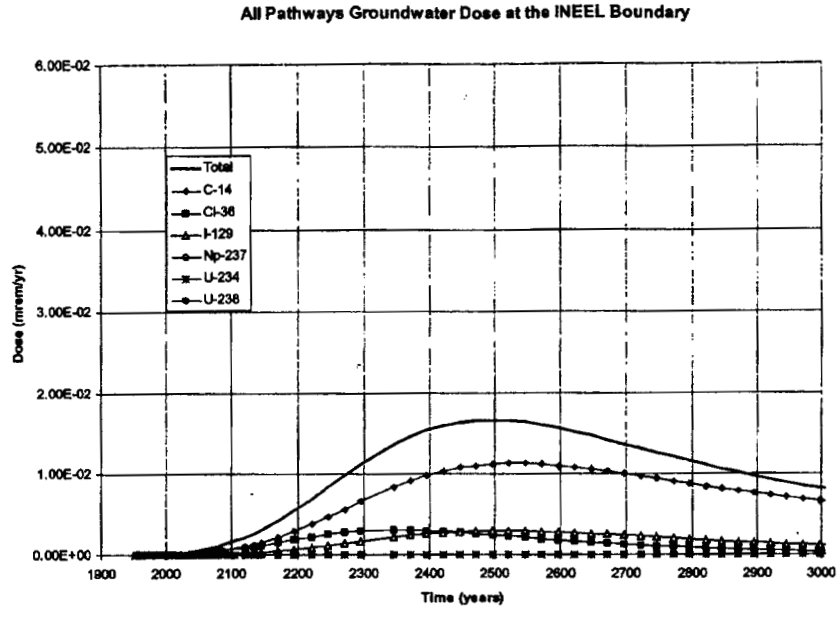

Figure 4-7. Simulated PA contaminant all-pathways groundwater dose at the INEEL boundary during the 1,000-yr-compliance period.

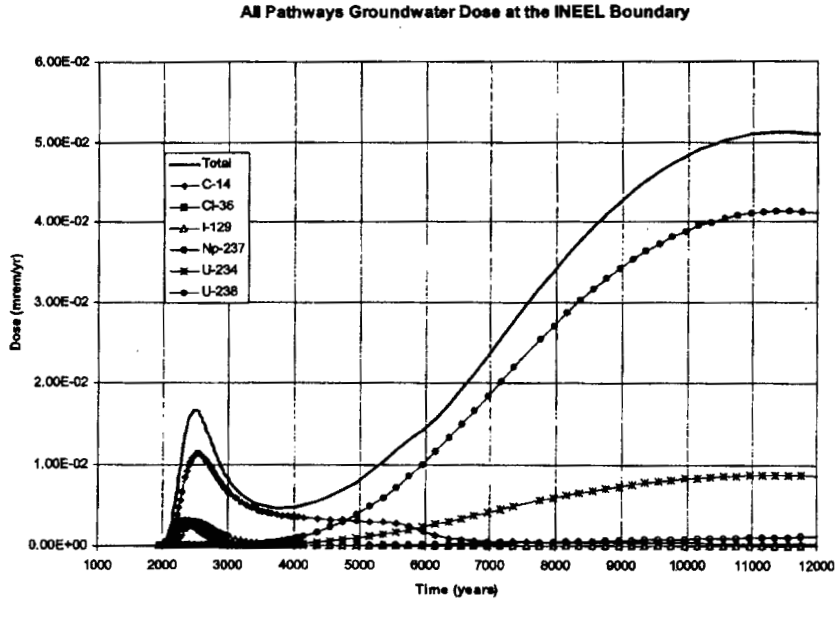

Figure 4-8. Simulated PA contaminant all-pathways groundwater dose at the INEEL boundary during the 10,000-yr. simulation period.

4.1.3 Intruders

This section presents the doses to inadvertent intruders for acute and chronic scenarios, based on a maximum time of compliance of 1000 years. Acute and chronic intruder analyses for the 1000-year compliance period are based on drilling a well through the waste in the soil vaults and pits, biointrusion into waste, and radon emanation from contaminated soil. Calculations are provided beyond 1000 years, to 10000 years, to detect potential increasing trends in doses due to ingrowth of radioactive daughters. If an increasing trend was detected, doses at one million years were calculated to address secular equalibrium of long-lived radionuclides with radioactive progeny. Basement excavation scenarios are included in the post-1000 year calculations.

4.1.3.1 Acute Intruder Drilling Scenario. For the pits, the acute intruder drilling scenario yielded a peak dose of 5 mrem in 2120, the end of institutional control (see Table 4-5). Inhalation accounted for the majority of the dose; Pu-239 and U-238 were the dominant radionuclides. The dominant radionuclide for the external exposure pathway was Cs-137.

For the soil vaults, the acute intruder drilling scenario yielded a peak dose of 66.4 mrem in the year 2120, the end of institutional control (see Table 4-5). Inhalation and external exposure accounted for approximately equal portions of the dose. Nickel-63 was the dominant radionuclide for inhalation, and Cs-137 was the dominant radionuclide for external exposures.

For both pits and soil vaults, the doses were below the DOE Order 435.1 acute exposure standard of 500 mrem. If the maximum time of compliance were extended past 1000 years, the peak doses from the acute drilling scenario would be unaffected because the peak doses occurred at 100 years.

4.1.3.2 Chronic Intruder Drilling Scenario. The maximum chronic intruder drilling dose for pits was 0.35 mrem/yr (see Table 4-5) and occurred in the year 2120 (100 years after closure of the RWMC). Inhalation was the predominant exposure pathways for both pits and soil vaults. Strontium-90 was the major contributor to the dose predicted for the pits. Nickel-63 dominated the dose calculated for the soil vaults.

The doses were well below the DOE Order 435.1 chronic exposure standard of 100 mrem/yr. If the maximum time of compliance were extended past 1000 years, the peak doses from the chronic drilling scenario would be unaffected because the peak doses occurred at 100 years after institutional control ceased.

Table 4-5. Acute and chronic intruder doses.

Scenario	Dose 100 years	500 years	1000 years	3000 years	5000 years
SVR acute drilling	86.7 mrem	2.3 mrem	2.2 mrem	2.2 mrem	2.1 mrem
BGP acute drilling	5.0 mrem	0.009 mrem	0.004 mrem	9.9E-04 mrem	2.7E-05 mrem
Acute construction	na	na	Na	2.0 mrem	0.9 mrem
SVR chronic drilling	22.0 mrem/yr	0.8 mrem/yr	0.08 mrem/yr	0.04 mrem/yr	0.003 mrem/yr
BGP chronic drilling	0.35 mrem/yr	0.01 mrem/yr	0.007 mrem/yr	0.004 mrem/yr	0.003 mrem/yr
Basement excavation	na	na	na	1.9 mrem/yr	2.1 mrem/yr

Scenario	Dose 10,000 years	Maximum dose 100 to 1000 years	Maximum dose 100 to 1E4 years	DOE 435.1 Standard
SVR acute drilling	1.9 mrem	86.7 mrem	86.7 mrem	500 mrem
BGP acute drilling	1.7E-06 mrem	5.0 mrem	5.0 mrem	500 mrem
Acute construction	0.7 mrem	na	2.1 mrem	500 mrem
SVR chronic drilling	0.02 mrem/yr	22.0 mrem/yr	22.0 mrem/yr	100 mrem/yr
BGP chronic drilling (a)	0.002 mrem/yr	0.35 mrem/yr	0.35 mrem/yr	100 mrem/yr
Basement excavation	3.8 mrem/yr	na	3.8 mrem/yr	100 mrem/yr

4.1.3.3 Acute Intruder Construction Scenario. The impacts from the acute construction scenario do not occur until the year 5020, 3000 years after closure of the RWMC (see Table 4-5). Therefore, this scenario was not used to demonstrate compliance with DOE Order 435.1. However, the peak impacts from the acute construction scenario were 1.75 mrem at 3,000 years after closure of the RWMC. Inhalation accounted for 30% of the dose, and external exposure accounted for 70% of the dose. Uranium-238, U-234, and Th-230 were the dominant radionuclides. The 1.75 mrem dose was well below the DOE Order 435.1 acute exposure standard of 500 mrem. The dose at one million years was also

estimated, because of the presence of long-lived radionuclides. The dose at that time was estimated to be 2.96 mrem, well below the standard of 500 mrem.

4.1.3.4 Chronic Intruder Basement Excavation Scenario. The impacts from the chronic basement excavation scenario do not occur until the year 5020, 3000 years after closure of the RWMC (see Table 4-5). Therefore, this scenario was not used to demonstrate compliance with DOE Order 435.1. However, the peak impacts from the chronic basement excavation scenario was 3.8 mrem/yr at 10,000 years after closure of the RWMC. Actinides (such as U-238) and their progeny dominated the doses. Because the calculated doses increased in value from 3000 to 10,000 years, the dose at one million years after closure was also estimated. The dose at this time was 38 mrem. These doses were well below the DOE Order 5820.2A chronic exposure standard of 100 mrem/yr.

4.1.3.5 Chronic Intruder Radon Scenario. Based on a maximum time of compliance of 1000 years, the peak radon doses were 52.1 mrem/yr for pits and 0.001 mrem/yr for soil vaults. These doses occurred in the year 2120, for the pits, and 3020 for the soil vaults. For pits, almost all of the dose was due to disposed Ra-226; for soil vaults, almost all of the dose was due to ingrowth of Ra-226 from disposed U-234. These doses were well below the DOE Order 435.1 chronic exposure standard of 100 mrem/yr. If the maximum time of compliance was extended past 1000 years, the maximum dose for soil vaults would increase to 0.09 mrem/yr at 10,000 years after closure.

4.1.3.6 Chronic Biointrusion Scenario. The chronic biointrusion doses were 0.01 mrem/yr for pits and 0.11 mrem/yr for soil vaults. These doses occurred in the year 2120 and included the doses from upward migration of gaseous H-3 and C-14. These doses were well below the DOE Order 435.1 chronic exposure standard of 100 mrem/yr. If the maximum time of compliance was extended past 1000 years, the peak doses from the chronic biointrusion scenario would be unaffected because the peak doses occurred before 1000 years.

4.1.3.7 Summary of Intruder Scenarios. Table 4-5 summarizes the doses from the acute drilling, acute construction, chronic drilling, and basement excavation scenarios. For both pits and soil vaults, the doses were well below the DOE Order 435.1 exposure standards, even if the maximum time of compliance were extended past 1000 years.

Table 4-6 summarizes the total doses from the chronic intruder scenarios based on an intruder being exposed to the peak impacts from all the chronic scenarios concurrently. This is an extremely conservative method of summing intruder doses because many of the scenarios do not yield peak doses at the same time.

Based on a maximum time of compliance of 1000 years, the total dose through the chronic drilling, radon, and biointrusion scenarios resulted was 52.5 mrem/yr for pits and were dominated by radon doses. If radon were excluded, the dose would be 0.36 mrem/yr. In either case, the doses were well below the DOE Order 435.1 chronic exposure standard of 100 mrem/yr. If the time of compliance were extended past 1000 years, the doses for pits would be 41.8 mrem/yr and would still be dominated by the radon dose. The dose would still be below the DOE Order 435.1 chronic exposure standard of 100 mrem/yr.

For soil vaults, the total doses based on a maximum time of compliance of 1000 years was 22.1 mrem/yr and were dominated by the chronic intruder drilling scenario. Radon contributes an extremely small fraction of the dose. As with the pits, the doses were well below the DOE Order 435.1 chronic exposure standard of 100 mrem/yr. If the time of compliance were extended past 1000 years, the doses for soil vaults would be 22.2 mrem/yr and would be dominated by the chronic drilling dose. The doses would still be below the DOE Order 435.1 chronic exposure standard of 100 mrem/yr.

Table 4-6. Summary of chronic intruder doses.

Case	1000 year time of compliance EDE (mrem/yr)	Year	Unlimited time of compliance EDE (mrem/yr)	Year
Pits				
Peak chronic scenario	0.35[a]	2120	3.8[b]	12020
Biointrusion	0.01	2120	0.01	2120
Radon	52.1	2020	52.1	2120
Total	52.5		55.9	
Soil vaults				
Peak chronic scenario	22.0[a]	2120	22.0[a]	2120
Biointrusion	0.1	2120	0.1	2120
Radon	0.001	2120	0.09	12020
Total	22.1		22.2	

a. Chronic drilling scenario.

b. Basement excavation scenario.

4.1.4 Groundwater Protection

The performance objectives for groundwater protection are defined by the six objectives listed below. This technical update did not address all of the objectives, but rather focused on the identified contaminants of concern. Therefore, the values presented in this section are a combination of results from new simulations performed for the PA and scaled values from the associated Composite Analysis (McCarthy et. al. 2000). The following bullets summarize the analysis approach used to calculate the values for each of the groundwater protection (ingestion) performance objectives.

- 4-mrem/yr man-made beta-gamma EDE - calculated based on the predicted C-14, Cl-36, and I-129 direct ingestion dose. Other beta-gamma contributors were evaluated in the CA and shown to be insignificant contributors to the beta-gamma effective dose equivalent.

- 20,000-pCi/L H-3 concentration – because H-3 was not identified as a contaminant of concern, the value was calculated based on scaled values from the Composite Analysis.

- 8-pCi/L Sr-90 concentration - because Sr-90 was not identified as a contaminant of concern, the value was calculated based on scaled values from the Composite Analysis.

- 5-pCi/L Ra-226 and Ra-228 concentration - because Ra-226 and Ra-228 were not identified as contaminants of concern, the values were calculated based on scaled values from the Composite Analysis. The value is scaled based on the ratio of the Ra-226 PA inventory (1.6

Ci) to the CA inventory (60.6 Ci). It is conservative, as it assumes no cover at the SDA. Progeny ingrowth is a significant portion of this prediction.

- 15-pCi/L adjusted gross alpha concentration – As defined in the Federal Register, Vol. 56, No. 138, Thursday, July 18, 1991, Part 141-National Primary Drinking Water Regulations, the "Adjusted gross alpha is defined as the result of a gross alpha measurement, less radium-226 and less uranium. Radon is not included in adjusted gross alpha." The nuclides contributing to the adjusted gross alpha concentration are Am-241, Np-237, Pu-238, Pu-239, Pu-240, and Pu-242. For this technical update, the only significant contributor to the adjusted gross alpha concentration is the Np-237.

- 20-ug/L total uranium concentration – calculated based on the sum of the U-234 and U-238 simulated for this technical update. Other uranium isotopes are insignificant contributors to the total uranium concentration.

A comparison of the results with the groundwater direct ingestion related performance objectives are summarized in Table 4-7. The results are discussed below.

Table 4-7. Comparison of predicted groundwater concentrations with performance objectives for groundwater protection.

Performance Objective	Operational and Institutional Control Period	Post-Institutional Control Period until the year 3000	Long-Term Post-Institutional Control Period, until the year 12000
4-mrem/yr man-made beta-gamma EDE	3.8E-04	1.4E+00	1.4E+00
20,000-pCi/L H-3 concentration	2.9E-01	2.3E+01	2.3E+01
8-pCi/L Sr-90 concentration	9.1E-08	3.2E-06	3.2E-06
5-pCi/L Ra-226 and Ra-228 concentration	9.3E-10	8.5E-06	9.2E-05
15-pCi/L adjusted gross alpha concentration	8.1E-11	4.8E-05	3.1E-01
20-ug/L uranium concentration	9.5E-08	8.6E-02	2.0E+02

4.1.4.1 Operational and Institutional Control Periods

During the operational and institutional control periods (1984 – 2120), the point of compliance was located at the INEEL site boundary, 5500-m south of the RWMC. The predicted groundwater concentrations during this time period are:

- 3.8E-4-mrem/yr man-made beta-gamma EDE. This is 0.01% of the groundwater protection standard of 4-mrem/yr.

- 0.29-pCi/L H-3. This is 0.001% of the groundwater protection standard of 20,000-pCi/L. The value is scaled from the Composite Analysis (McCarthy et. al. 2000) based on the ratio of the H-3 PA inventory (3.23E5 Ci) to the H-3 CA inventory (1.53E6 Ci). It is conservative, as it assumes no cover at the SDA.

- 9.1E-8-pCi/L Sr-90. This is 1E-6% of the groundwater protection standard of 8-pCi/L. The value is scaled from the Composite Analysis (McCarthy et. al. 2000) based on the ratio of the Sr-90 PA inventory (842 Ci) to the Sr-90 CA inventory (4.5E5 Ci). It is conservative, as it assumes no cover at the SDA.

- 9.3E-10-pCi/L Ra-226 and Ra-228. This is 2E-8% of the groundwater protection standard of 5-pCi/L. The value is scaled from the Composite Analysis (McCarthy et. al. 2000) based on the ratio of the Ra-226 PA inventory (1.6 Ci) to the CA inventory (60.6 Ci). It is conservative, as it assumes no cover at the SDA. Progeny ingrowth is a significant portion of this prediction. However, this was ignored in the scaling. The concentrations are insignificant relative to the standard.

- 8.1E-11-pCi/L adjusted gross alpha. This is 5E-10% of the groundwater protection standard of 15-pCi/L.

- 9.5E-8-ug/L total uranium. This is 5E-7% of the groundwater protection standard of 20-ug/L.

C-14, Cl-36, and I-129 dominate the groundwater ingestion dose during the operational and institutional control periods. For the primary radionuclides of concern, during the operational and institutional control period's (1984 – 2120), the maximum predicted groundwater direct ingestion doses are summarized in Table 4-8.

Table 4-8. Predicted maximum SDA radionuclide groundwater direct ingestion dose (mrem/yr) for the 100-yr institutional control period.

Radionuclide	Peak Time and Magnitude of Maximum Groundwater Direct Ingestion Dose at the INEEL Boundary	
	Date	Dose
	Year	mrem/year
C-14	2120	2.69E-04
Cl-36	2120	2.05E-05
I-129	2120	8.57E-05
Np-237	2120	8.13E-11
U-234	2120	2.60E-09
U-238	2120	5.47E-09
Total Dose	2120	3.75E-04

4.1.4.2 One Thousand Year Post Institutional Control Period (2120-3000)

During the compliance time of the post institutional control period (2120 - 3000), the point of compliance was located 100-m downgradient of the SDA. The predicted groundwater concentrations during this time period are:

- 1.4-mrem/yr man-made beta-gamma EDE. This is 35% of the groundwater protection standard of 4-mrem/yr.
- 23-pCi/L H-3. This is 0.1% of the groundwater protection standard of 20,000-pCi/L. The value is scaled from the Composite Analysis (McCarthy et. al. 2000) based on the ratio of the H-3 PA inventory (3.23E5 Ci) to the H-3 CA inventory (1.53E6 Ci). It is conservative, as it assumes no cover at the SDA.
- 3E-6-pCi/L Sr-90. This is 4E-5% of the groundwater protection standard of 20,000-pCi/L. The value is scaled from the Composite Analysis (McCarthy et. al. 2000) based on the ratio of the Sr-90 PA inventory (842 Ci) to the Sr-90 CA inventory (4.5E5 Ci). It is conservative, as it assumes no cover at the SDA.
- 8.5E-6-pCi/L Ra-226 and Ra-228. This is 2E-4% of the groundwater protection standard of 5-pCi/L. The value is scaled from the Composite Analysis (McCarthy et. al. 2000) based on the ratio of the PA inventory (1.6 Ci) to the CA inventory (60.6 Ci). It is conservative, as it assumes no cover at the SDA.
- 4.8E-5-pCi/L adjusted gross alpha. This is 3E-4% of the groundwater protection standard of 15-pCi/L.
- 0.09-ug/L total uranium. This is 0.4% of the groundwater protection standard of 20-ug/L.

During the compliance time of post institutional control (-2120 - 3000), C-14, Cl-36, and I-129 dominate the groundwater-ingestion-dose. For the primary radionuclides of concern, during the

compliance time of the post institutional control period (2120 - 3000), the maximum predicted groundwater direct ingestion doses are summarized in Table 4-9.

Table 4-9. Predicted maximum SDA radionuclide groundwater direct ingestion dose (mrem/yr) for the 1,000-yr-compliance period (from year 2120 – 3000).

Nuclide	Peak Time and Magnitude of Maximum Groundwater Direct Ingestion Dose Down-gradient from SDA							
	Receptor at 100-m		Receptor at 300-m		Receptor at 600-m		Receptor at INEEL Boundary	
	Date	Dose	Date	Dose	Date	Dose	Date	Dose
	Year	mrem/year	Year	mrem/year	Year	mrem/year	Year	mrem/year
C-14	2546	9.30E-01	2696	1.44E-01	2570	6.45E-02	2521	2.82E-03
Cl-36	2371	2.48E-02	2446	4.05E-03	2396	1.71E-03	2346	7.26E-05
I-129	2546	4.14E-01	2570	6.24E-02	2570	2.84E-02	2521	1.27E-03
Np-237	2999	4.84E-05	2999	2.10E-05	2999	8.43E-06	2999	6.15E-07
U-234	2999	1.59E-03	2999	6.04E-04	2999	1.86E-04	2999	1.49E-05
U-238	2999	4.96E-03	2999	1.96E-03	2999	6.58E-04	2999	5.10E-05
Total Dose	2521	1.36E+00	2570	2.10E-01	2521	9.44E-02	2496	4.15E-03

4.1.4.3 Ten Thousand Year Post Institutional Control Period (2120-12,000)

During the ~10,000 year post institutional control simulation period (2120 – 12,000), the point of compliance was also located 100-m downgradient of the SDA. The predicted groundwater concentrations during this time period are:

- 1.4-mrem/yr man-made beta-gamma EDE. This is 35% of the groundwater protection standard of 4-mrem/yr.

- 23-pCi/L H-3. This is 0.1% of the groundwater protection standard of 20,000-pCi/L. The value is scaled from the Composite Analysis (McCarthy et. al. 2000) based on the ratio of the H-3 PA inventory (3.23E5 Ci) to the H-3 CA inventory (1.53E6 Ci). It is conservative, as it assumes no cover at the SDA.

- 3E-6-pCi/L Sr-90. This is 4E-5% of the groundwater protection standard of 20,000-pCi/L. The value is scaled from the Composite Analysis (McCarthy et. al. 2000) based on the ratio of the Sr-90 PA inventory (842 Ci) to the Sr-90 CA inventory (4.5E5 Ci). It is conservative, as it assumes no cover at the SDA.

- 9.2E-5-pCi/L Ra-226 and Ra-228. This is 2E-3% of the groundwater protection standard of 5-pCi/L. The value is scaled from the Composite Analysis (McCarthy et. al. 2000) based on the ratio of the PA inventory (1.6 Ci) to the CA inventory (60.6 Ci). It is conservative, as it assumes no cover at the SDA.

- 0.3-pCi/L adjusted gross alpha. This is 2% of the groundwater protection standard of 15-pCi/L.

- 200-ug/L total uranium. This is ten times the groundwater protection standard of 20-ug/L.

The groundwater ingestion dose during the ~10,000 year post institutional control simulation period (2120 – 12,000), is dominated by U-238. For the primary radionuclides of concern, during the ~10,000 year post institutional control simulation period (2120 – 12,000), the maximum predicted groundwater direct ingestion doses are summarized in Table 4-10.

Table 4-10. Predicted maximum SDA radionuclide groundwater direct ingestion dose (mrem/yr) for the 10,000-yr-simulation period (from year 2120 – 12,000).

Nuclide	Peak Time and Magnitude of Maximum Groundwater Direct Ingestion Dose Down-gradient from SDA							
	Receptor at 100-m		Receptor at 300-m		Receptor at 600-m		Receptor at INEEL Boundary	
	Date	Dose	Date	Dose	Date	Dose	Date	Dose
	Year	mrem/year	Year	mrem/year	Year	mrem/year	Year	mrem/year
C-14	2546	9.30E-01	2696	1.44E-01	2570	6.45E-02	2521	2.82E-03
Cl-36	2371	2.48E-02	2446	4.05E-03	2396	1.71E-03	2346	7.26E-05
I-129	2546	4.14E-01	2570	6.24E-02	2570	2.84E-02	2521	1.27E-03
Np-237	12010	3.08E-01	12010	4.52E-02	12010	2.32E-02	12010	1.05E-03
U-234	12010	2.43E+00	12010	3.57E-01	11360	1.71E-01	11360	7.82E-03
U-238	12010	1.15E+01	12010	1.70E+00	11360	8.06E-01	11360	3.71E-02
Total Dose	12010	1.43E+01	12010	2.10E+00	11360	1.00E+00	11360	4.60E-02

The predicted groundwater direct-ingestion dose declines with distance from the SDA. The predicted groundwater direct ingestion doses are shown in Figures 4-9 through 4-16. A comparison of the groundwater all-pathways and direct ingestion doses are shown in Figure 4-17 and 4-18. The predicted chemical concentrations for total uranium are shown in Figures 4-19 and 4-20.

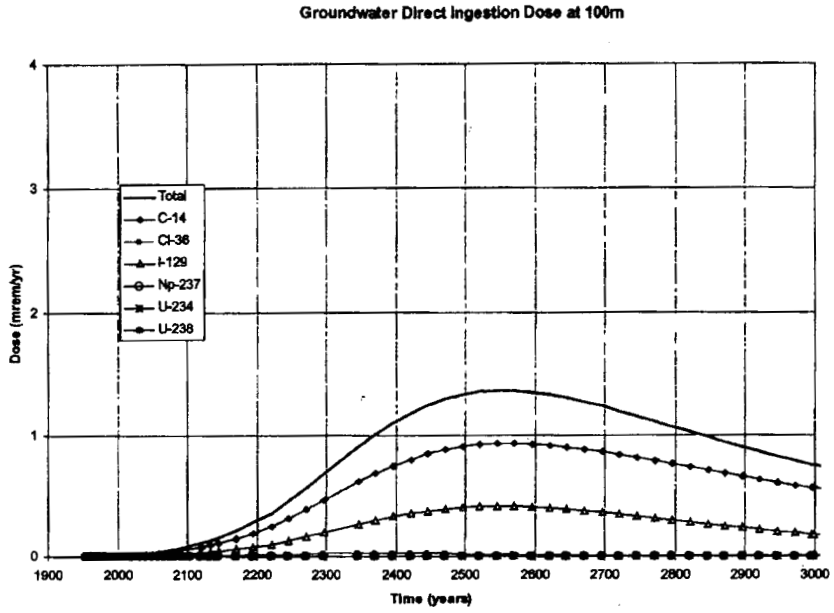

Figure 4-9. Simulated PA contaminant groundwater direct ingestion dose at the 100-m receptor fence during the 1,000-yr compliance period.

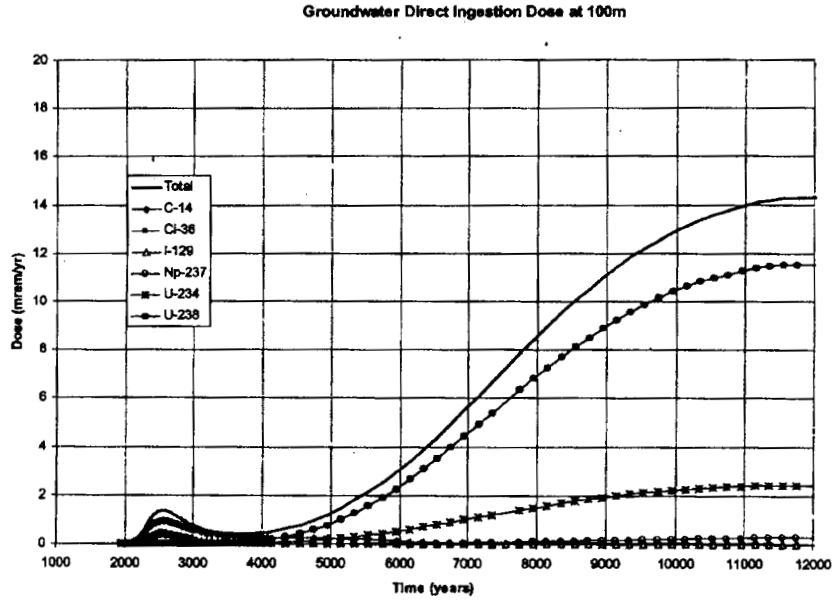

Figure 4-10. Simulated PA contaminant groundwater direct ingestion dose at the 100-m receptor fence during the 10,000-yr. simulation period.

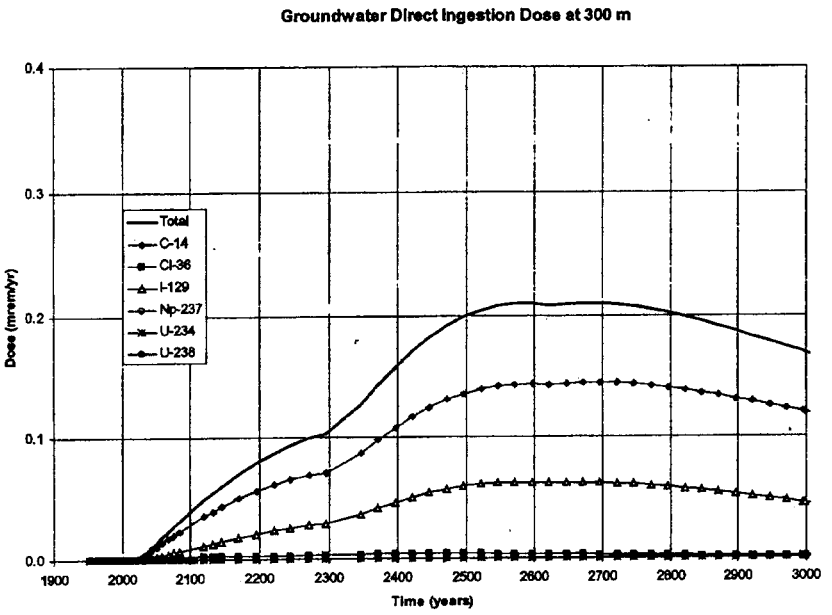

Figure 4-11. Simulated PA contaminant groundwater direct ingestion dose at the 300-m receptor fence during the 1,000-yr compliance period.

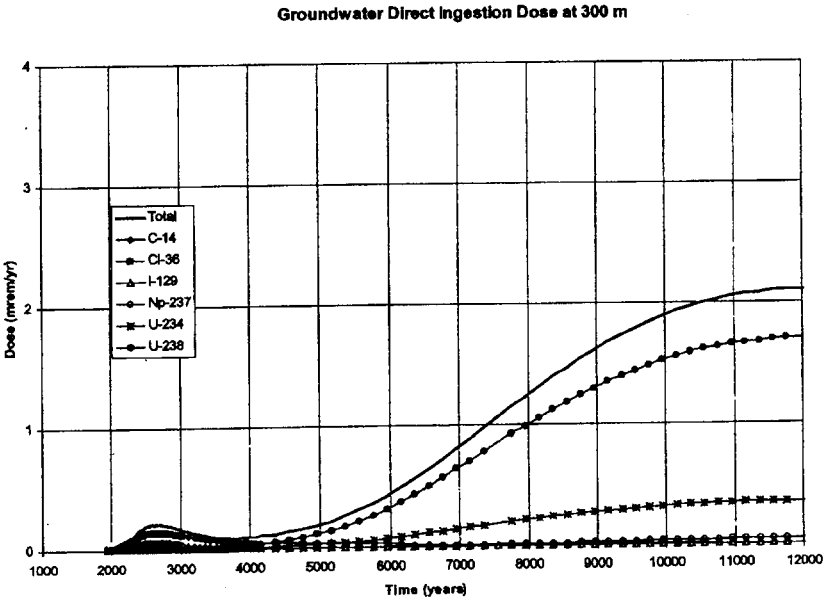

Figure 4-12. Simulated PA contaminant groundwater direct ingestion dose at the 300-m receptor fence during the 10,000-yr. simulation period.

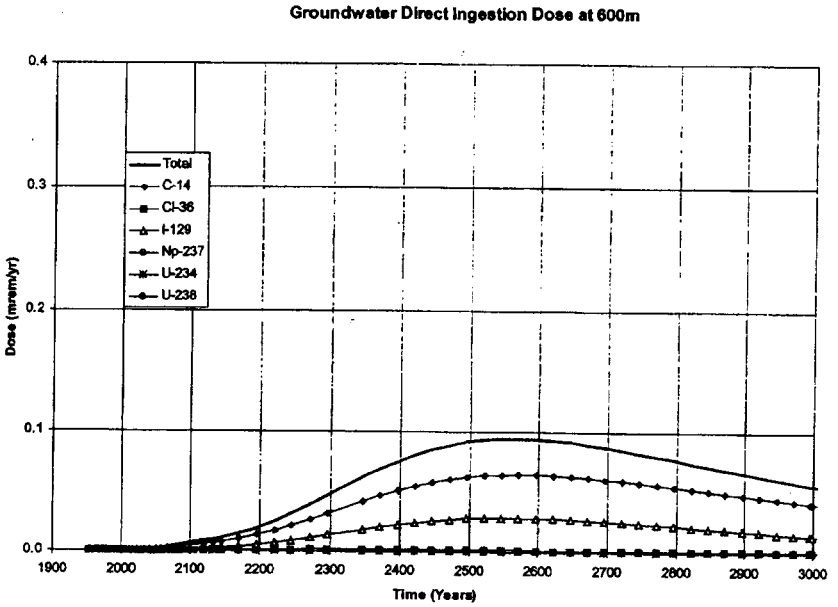

Figure 4-13. Simulated PA contaminant groundwater direct ingestion dose at the 600-m receptor fence during the 1,000-yr compliance period.

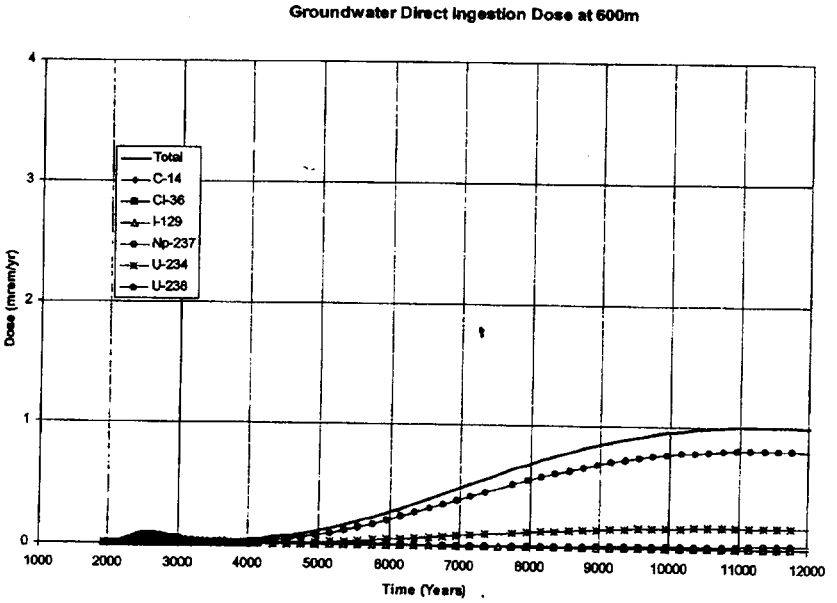

Figure 4-14. Simulated PA contaminant groundwater direct ingestion dose at the 600-m receptor fence during the 10,000-yr. simulation period.

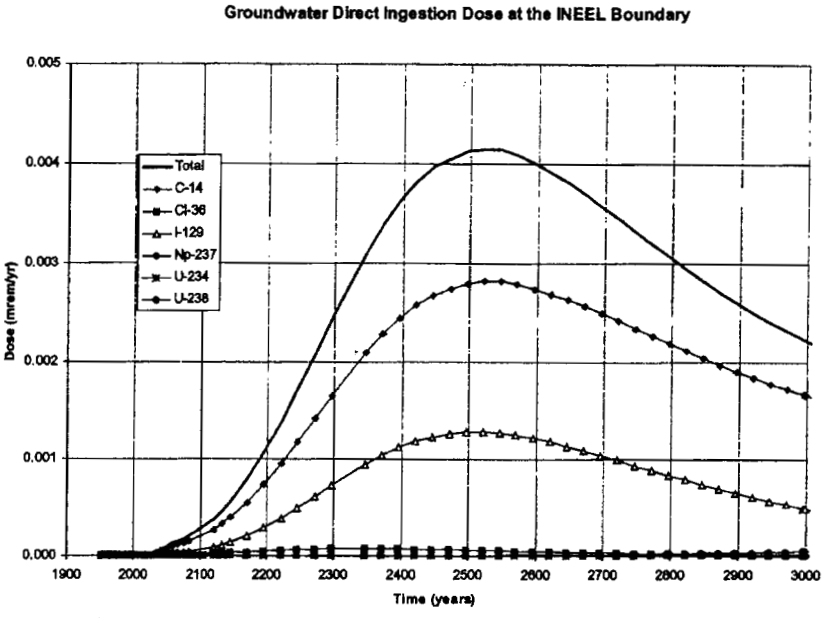

Figure 4-15. Simulated PA contaminant groundwater direct ingestion dose at the INEEL boundary during the 1,000-yr compliance period.

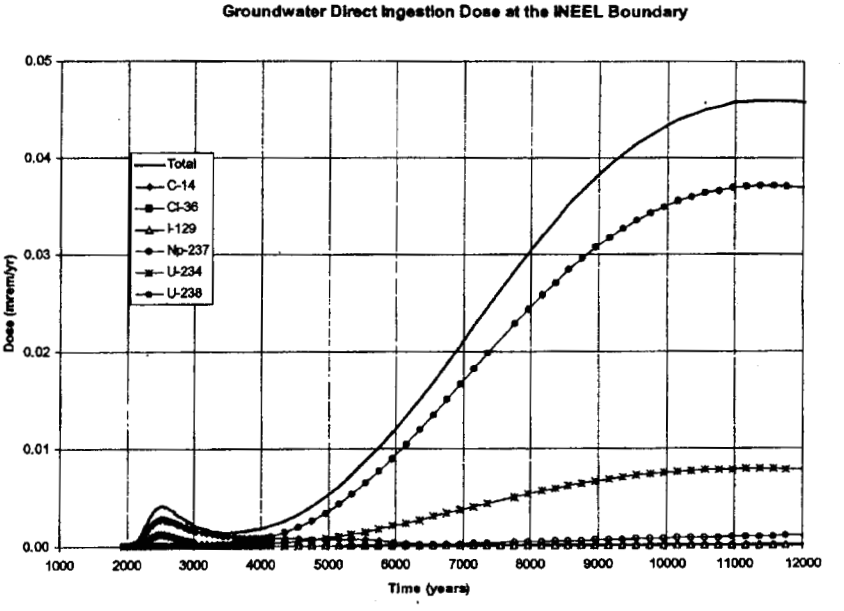

Figure 4-16. Simulated PA contaminant groundwater direct ingestion dose at the INEEL boundary during the 10,000-yr. simulation period.

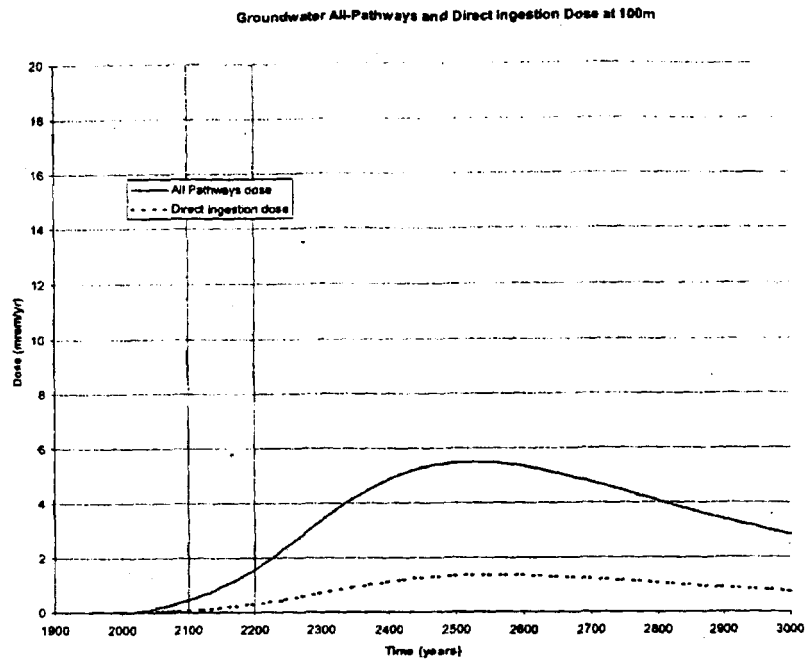

Figure 4-17. Total all-pathways and groundwater ingestion dose at 100m downgradient from the SDA boundary for the 1,000-yr-compliance period.

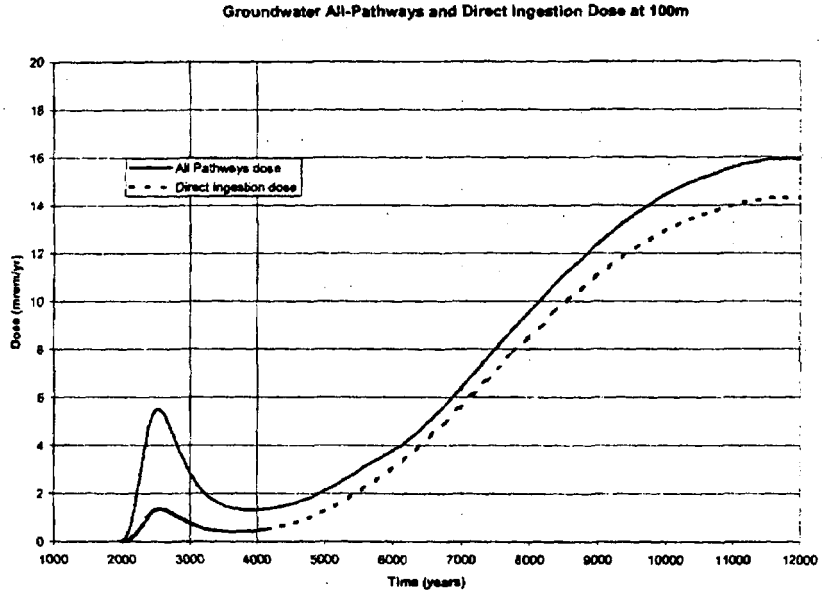

Figure 4-18. Total all-pathways and groundwater ingestion dose at 100m downgradient from the SDA boundary for the 10,000-yr-compliance period.

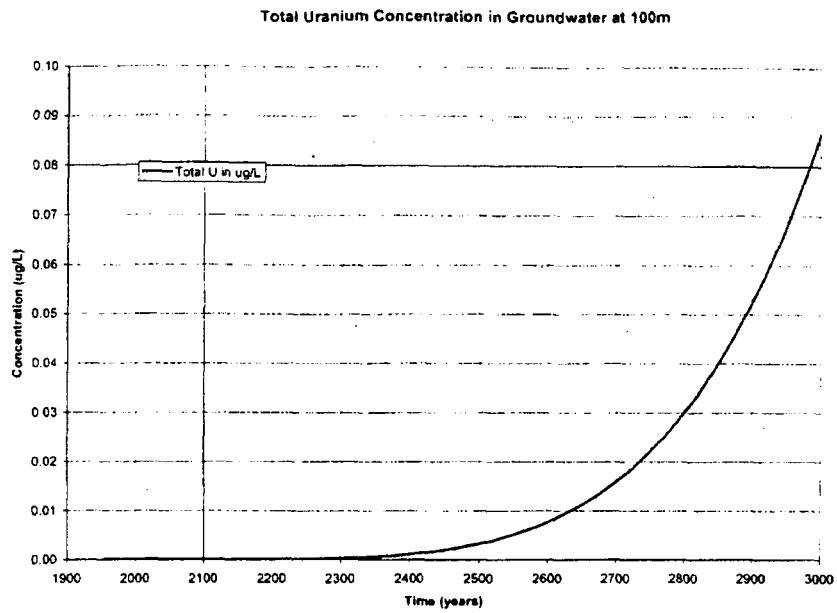

Figure 4-19. Total uranium concentration in groundwater at 100-m downgradient from the SDA boundary for the 1,000-yr-compliance period.

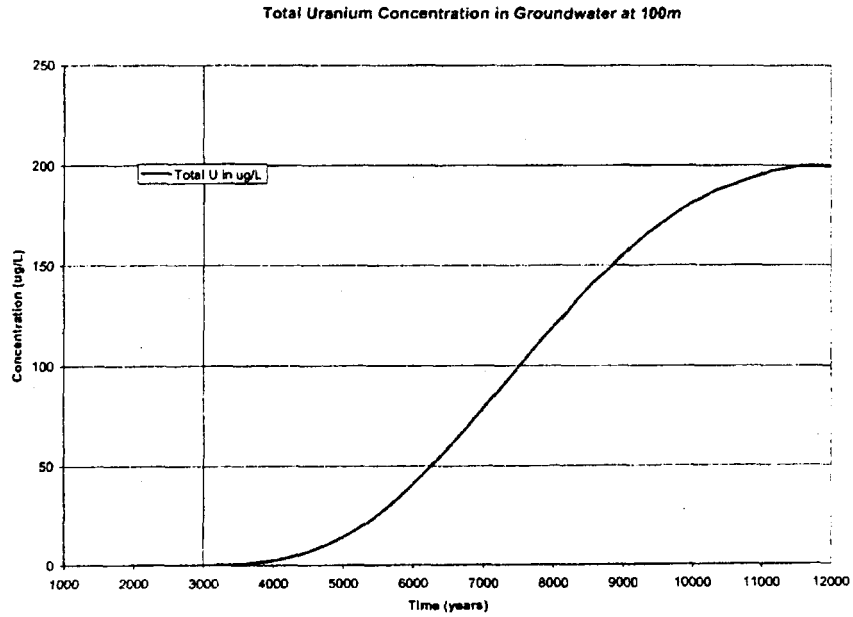

Figure 4-20. Total uranium concentration in groundwater at 100-m downgradient from the SDA boundary for the 10,000-yr-compliance period

5. UNCERTAINTY AND SENSITIVITY ANALYSIS

. This section presents the methodology and results of the uncertainty and sensitivity analysis performed for the Performance Assessment. An uncertainty analysis evaluates the precision and accuracy of the model. Sensitivity analysis evaluates the sensitivity of model output to variability in model input. Uncertainty in models arises because a) errors in model formulation and b) errors (or uncertainty) in model input parameters (parametric uncertainty). Model formulation errors are inherent in mathematical modeling because environmental models are only simplified representations of complex environmental systems. Errors in model parameterization occur because lack of knowledge about a parameter's true, but unknown value. Ideally, site-specific parameter values should be derived and used in the simulation. In practice, parameter values are often inferred from limited measured data or derived from the literature. Additionally, model parameter may represent time and space scales that differ greatly from what can be measured in the field or laboratory. Natural variability also contributes to parameter uncertainty.

Uncertainty in model formulation can only be evaluated through model validation. Model validations answers the question "Does the model accurately simulate the behavior of the system?". To demonstrate a model is valid, an independent data set is required. Often times, adequate independent data sets are not available and the analyst resorts to model calibration. In model calibration, parameter values are adjusted (within reason) so that model predictions match the field observations as close as possible.

Because performance assessment addresses impacts that occur far into the future, it is impossible to validate the model application because measurements are unavailable. Therefore, model uncertainty is addressed using whatever historical or contemporary field data that is available. Model uncertainty for the performance assessment was evaluated by comparing predicted carbon tetrachloride and nitrate groundwater concentrations to their corresponding measured values. Comparisons such as these provide a quantitative measure of what the model can accurately predict in the environment for the current time frame. Nevertheless, the use of the model for forecasting the release and transport of radionuclides far into the future can never really be truly validated.

A parametric uncertainty analysis quantifies the uncertainty in model output resulting from uncertainty in the model parameters. It is a measure of the precision of the model and cannot address the overall accuracy of the predictions. Parametric uncertainty for the performance assessment was evaluated using Monte Carlo simulation combined with simple random sampling techniques. Uncertainty is expressed in terms of a probability density function of the output variable (total dose). Information provided by the uncertainty analysis was also used to in the sensitivity analysis. Model sensitivity was evaluated by calculating the rank correlation between the output variable and each of the input parameters

5.1 Model Uncertainty Analysis

Evaluation of model uncertainty requires an independent set of field measurements by which to compare model predicted values too. Because performance assessment addresses impacts far into the future, it is impossible to obtain such data. This does not preclude model comparisons with contemporary field data, validation of the model in other environments where data exists, or model calibration with existing field data. Model calibration forces model predictions to match measured values within some predefined accuracy limit. A calibrated model is then used to extrapolate out to time and space domains where no measurement data exists. While the model may perform reasonably well for the current time frame, the use of the model for forecasting the release and transport of radionuclides far into the future can never really be truly validated.

Model calibration was performed for the TETRAD model using nitrate (Magnuson and Sondrup 1998) and carbon tetrachloride (Sondrup 1998) measurements in the Snake River Plain Aquifer. The results of these calibrations are shown in Figures 5-3 and 5-7 for carbon tetrachloride and nitrate respectively. These figures plot predicted concentration in the Snake River Plain Aquifer against the corresponding measured value observed in water wells surrounding the SDA. Points that lie within the area bounded by the two solid lines on the figures represent model predictions that were within a factor of 2 of the observations. The dotted line represents the perfect correlation line. Points above this line indicate model over prediction and points below the line represent model under prediction.

The nitrate plot shows most of the model predictions were within a factor of 2 of the observations, but the correlation between predictions and observations was poor. Predicted concentrations were limited to a minimum background concentrations of 700 $\mu g\ L^{-1}$ that was assumed to be from upgradient sources. This restriction results in the large number of predicted points that are at the 700 $\mu g\ L^{-1}$ level.

The carbon tetrachloride plot shows good correlation between predictions and observations for concentrations greater that the minimum detectable concentration of 0.21 $\mu g\ L^{-1}$. Correlation coefficients (r^2) are shown in parenthesis next the groundwater monitoring well number. Note that the correlation coefficient for well USGS 90 of 0.92 suggests strong correlation between predicted and measured values, but the model underpredicts concentrations by more than a factor of 2 in most cases. Well USGS 87 and the RWMC production well showed predicted concentrations that were all within a factor of 2 of the observations and strong correlation between predicted and measured values. Predicted concentrations in the other wells were not well correlated with measurements and mostly fell outside of the $\pm$ factor of 2 error bars.

Based on these results, we may expect the model to predict concentrations mostly within a factor of 2, but in some cases, a factor of 5 or 10 of the observations. While these results really only apply to carbon tetrachloride and nitrate, the extension to other contaminants ultimately is made. Nitrate represents a relatively good water tracer because it sorbs little and does not decay. The calibration with nitrate then provides some validation of the water flow portion of the model. Specific validation of radionuclide release and transport will have to wait till site specific measurements become available.

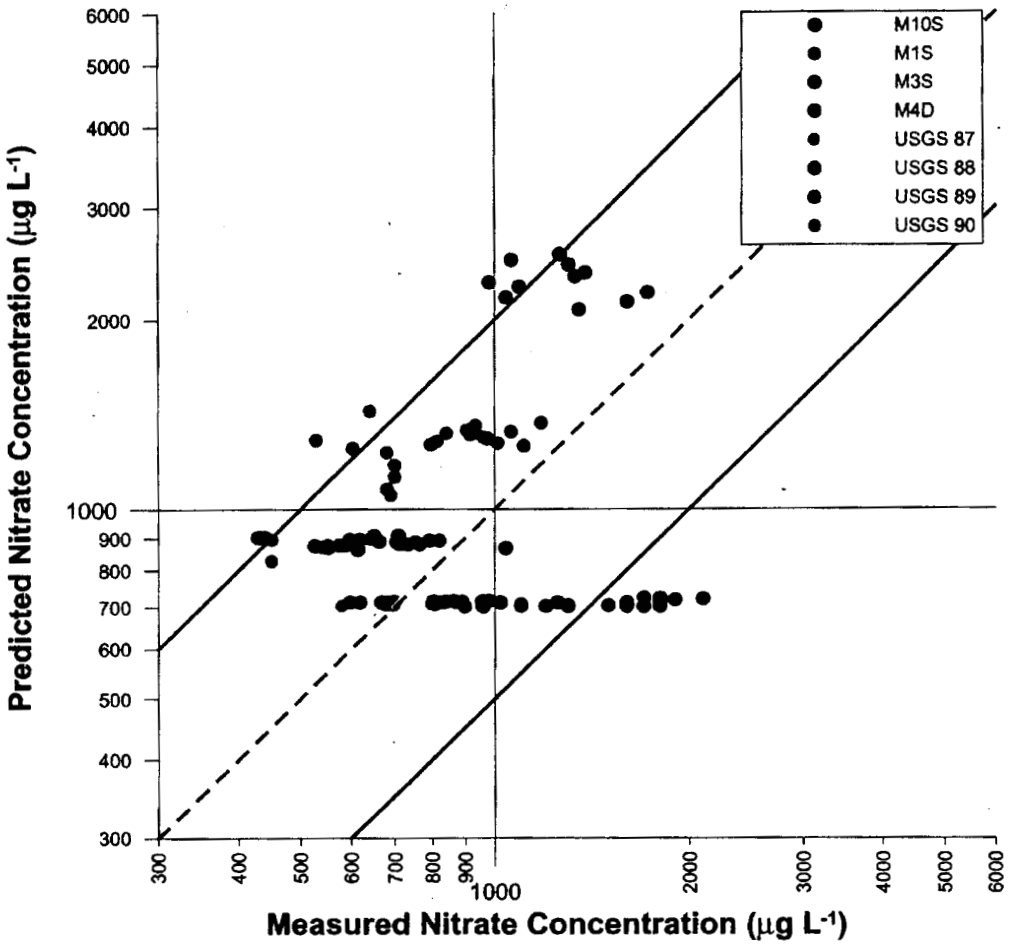

Figure 5-1. Predicted verses measured nitrate concentrations at water wells in the Snake River Plain Aquifer near the SDA. Points that lie within the area bounded by the two solid lines on the figures represent model predictions that were within a factor of 2 of the observations. The dotted line represents the perfect correlation line. Points above this line indicate model over prediction and points below the line represent model under prediction.

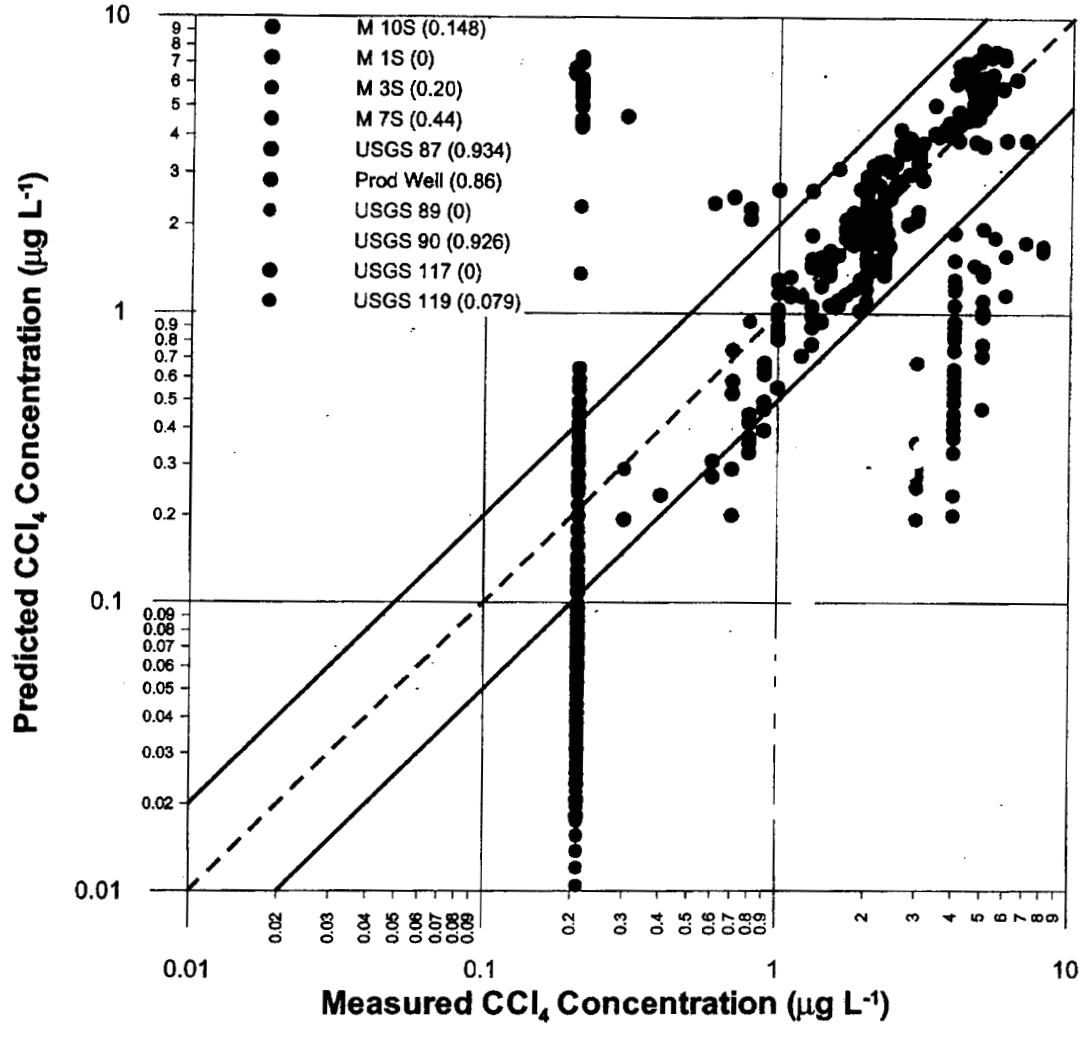

Figure 5-2. Predicted verses measured carbon tetrachloride concentrations at water wells in the Snake River Plain Aquifer near the SDA. Points that lie within the area bounded by the two solid lines on the figures represent model predictions that were within a factor of 2 of the observations. The dotted line represents the perfect correlation line. Points above this line indicate model over prediction and points below the line represent model under prediction. Correlation coefficients between measured and predicted value for each well are shown in parenthesis.

5.2 Parametric Uncertainty Analysis

5.2.1 Calibration to TETRAD

Run times for the transport model used in the updated Performance Assessment (TETRAD) were sufficiently long (1–3 weeks) such as to render Monte Carlo simulation impractical. To overcome this problem, a simpler transport model was implemented which was calibrated to the TETRAD results. The simpler model took as input, the radionuclide flux from the waste containers calculated with DUST. These radionuclide fluxes were the same as used in the TETRAD simulations. Radionuclide fluxes from DUST were fed into a one-compartment aqueous-phase transport mixing cell model that represented backfilled soil and surface sediments between the waste and the top of the fractured basalt. Fluxes from the one-compartment model were then used as an external source for the GWSCREEN Version 2.5 (Rood 1999) model. The conceptual model of the system is illustrated in Figure 5-3. Parameter values were taken from the TETRAD simulations or used as a calibration parameter (Table 5-1).

The radionuclide inventory in the soil mixing cell illustrated in Figure 5-3 is described by the equation

$$\frac{dQ}{dt} = F(t) - (k+\lambda)Q \tag{5-1}$$

where

Q = radionuclide soil inventory (Ci)

$F(t)$ = flux of radionuclides from the waste to soil calculated with DUST (Ci y^{-1})

k = first order leach rate constant (y^{-1})

λ = decay rate constant (y^{-1}).

The leach rate constant is given by

$$k = \frac{P}{\theta T\left(1+\frac{K_d \rho}{\theta}\right)} \tag{5-2}$$

where

θ = soil moisture content (m^3 m^{-3})

ρ = soil bulk density (g m^{-3})

P = percolation rate (m y^{-1})

K_d = sorption coefficient (mL g^{-1})

T = soil compartment thickness (m)

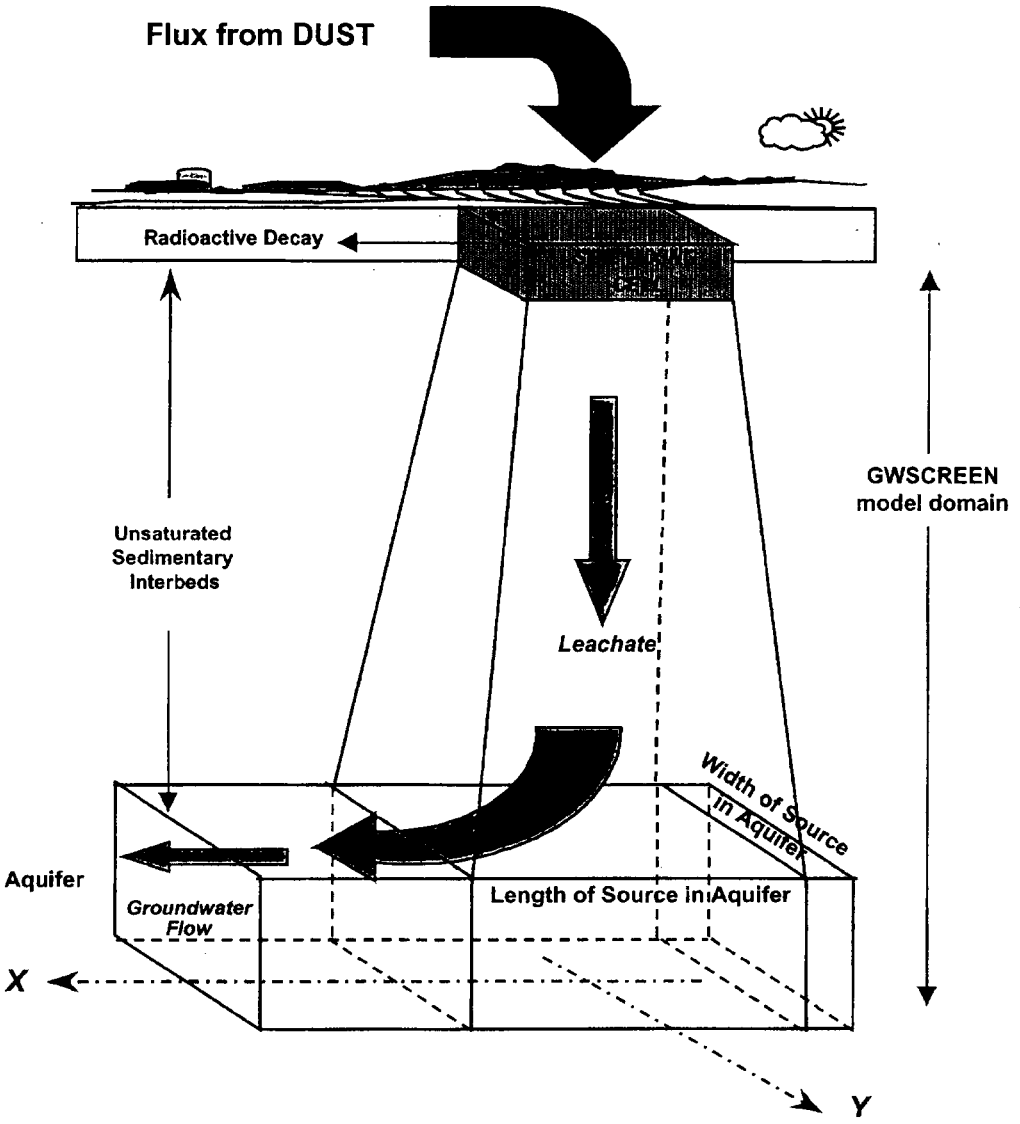

Figure 5-3. Conceptual model of RWMC and underlying aquifer used to calibrate the GWSCREEN model to prediction concentrations in the aquifer made by TETRAD.

Table 5-1. Calibrated and fixed GWSCREEN transport parameters that were used in the TETRAD calibration.

Calibrated parameter name	Calibrated values	Fixed parameter name	Value
Depth in aquifer concentrations are evaluated (m)	7	Percolation, before 2020 (m y^{-1})[a]	0.085
		Percolation, after 2020 (m y^{-1})	0.01
Unsaturated Thickness	12.5	Aquifer porosity	0.06
Dispersivity in vadose zone, α_v (m)	2.25	Bulk density, aquifer g cm^{-3}	1.9
Longitudinal dispersivity in aquifer α_L (m)	20	Well location perpendicular to groundwater flow (m)	0
Transverse dispersivity in aquifer α_T (m)	5	Source length perpendicular to groundwater flow (m)[c]	481
Vertical dispersivity in aquifer α_V (m)	1.7	Source length parallel groundwater flow (m)[c]	481
Darcy velocity in aquifer, u (m y^{-1})	0.75	Bulk density, unsaturated zone [from TETRAD](g cm^{-3})	1.26
Surface sediment and backfilled soil thickness, U (m)[b]	4.1	Sorption coefficient, C (mL g^{-1})[e]	0.1
Surface sediment/ backfilled soil thickness, C, I (m)[b]	6.1	Sorption coefficient, I (mL g^{-1})[e]	0.1
Surface sediment/ backfilled soil thickness, Np (m)[b]	3.8	Sorption coefficient, U (mL g^{-1})[e]	6.0
Well location parallel to groundwater flow from center of source (m)[d]	340	Sorption coefficient, Np (mL g^{-1})[e]	8.0

a. The percolation rate used in the TETRAD simulations across the SDA model domain before cap emplacement ranged from 0.06 to 0.24 m y^{-1} with a mean of about 0.085 m y^{-1}. After cap emplacement, infiltration was fixed at 0.01 m y^{-1}. The change in infiltration (from 0.085 to 0.01 m y^{-1}) was accounted for in the one compartment model. The GWSCREEN simulation assumed a constant 0.01 m y^{-1} infiltration for the entire simulation.

b. This is the thickness of the backfilled soil and surficial sediments where the radionuclides released from the DUST model entered the system.

c. This area represents the area of the source at the surface of the aquifer as inferred from unsaturated TETRAD fluxes to the aquifer.

d. This distance is 100 m from the center of the source as projected to the aquifer. The actual compliance point is 100 m from the downgradient edge of the source or 228 m from the center of pits 17–20.

e. Sorption coefficients for sediment and sedimentary interbeds. Sorption coefficient values for the aquifer (basalt) were zero for all nuclides.

The moisture content was calculated using the van Genuchten equations (van Genuchten 1978) for unsaturated flow.

$$K(\theta) = K_{sat}\left(\frac{\theta - \theta_r}{\theta_s - \theta_r}\right)^{1/2}\left\{1-\left[1-\left(\frac{\theta-\theta_r}{\theta_s-\theta_r}\right)^{\frac{1}{m}}\right]^m\right\}^2 \quad (5\text{-}3)$$

and

$$\left(\frac{\theta - \theta}{\theta_s - }\right) = \left(\frac{1}{1+\alpha n}\right)^m \quad (5\text{-}4)$$

where

θ = moisture content,

θ_r = residual moisture content (0.142),

θ_S = saturated moisture content (0.484),

K_{sat} = saturated hydraulic conductivity (23.9 m y^{-1}),

α = fitting parameter (1.066 m^{-1}),

n = fitting parameter (1.523),

m = 1 - 1/n.

The fitting parameters, α and n, and the other parameters were obtained from Bishop (1991), McElroy and Hubbell (1990), and Baca (1992). Equation (1) was solved using a 4th-order Runga Kutta solver described in Press et al. (1992). These fluxes were then read into GWSCREEN as an external source.

Calibration was performed for 5 radionuclides where TETRAD results were readily available. These nuclides (C-14, I-129, U-234, U-238, Np-237) were the primary dose contributors in the PA. An additional nuclide was also included in the uncertainty analysis (Cl-36) however calibration could not be performed because TETRAD results were not available at the time calibration was performed. (TETRAD results became available in time for publication of this report). Results of the calibration are shown in Figures 5-4 – 5-8. Qualitatively, there was reasonably good agreement between the two models. GWSCREEN tended to over predict C-14 concentrations after the peak in year 600. Otherwise, GWSCREEN peak concentrations and time of peaks were within about 4% of their corresponding TETRAD values. Quantitative results of the calibration are presented in Table 5-2. A copy of a GWSCREEN input file for C-14 is given in Figure 5-9.

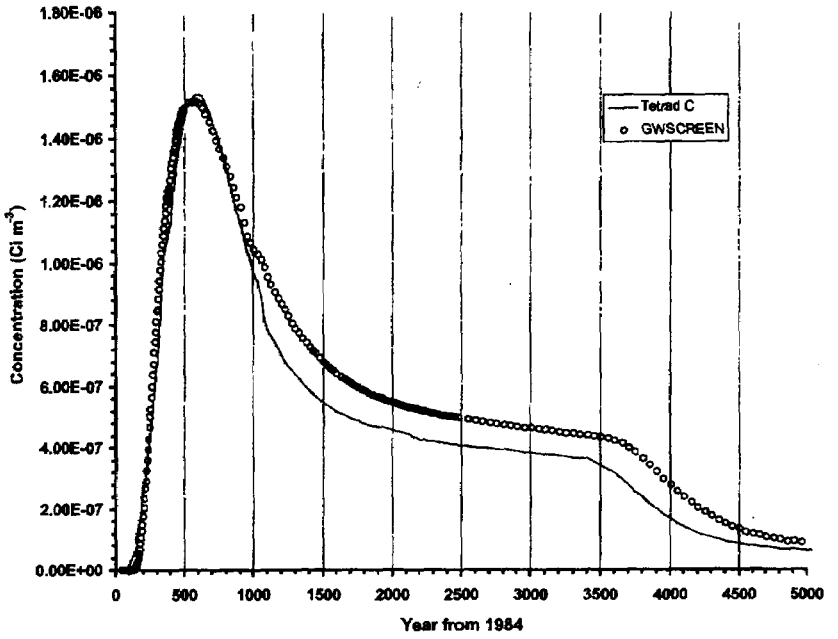

Figure 5-4. GWSCREEN calibration of C-14 with TETRAD.

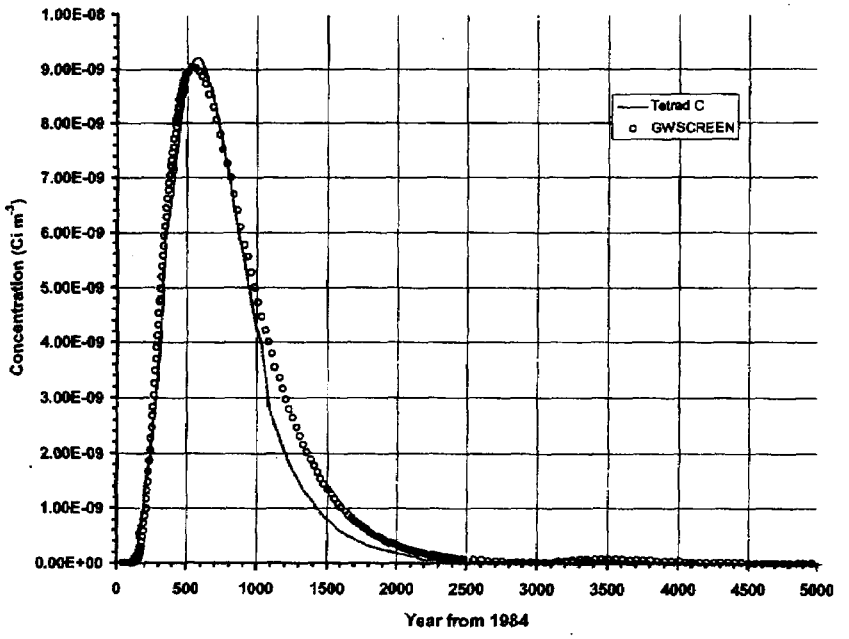

Figure 5-5. GWSCREEN calibration of I-129 with TETRAD.

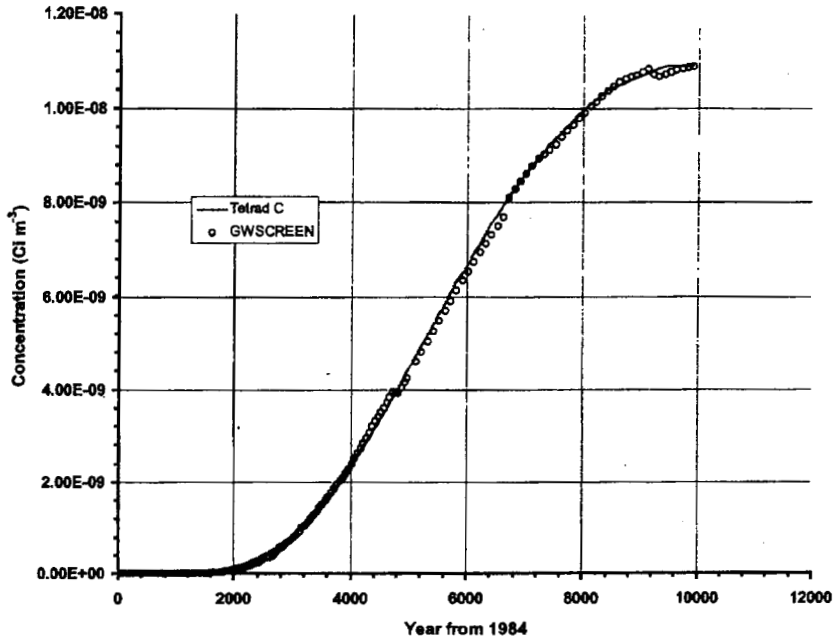

Figure 5-6. GWSCREEN calibration of U-234 with TETRAD

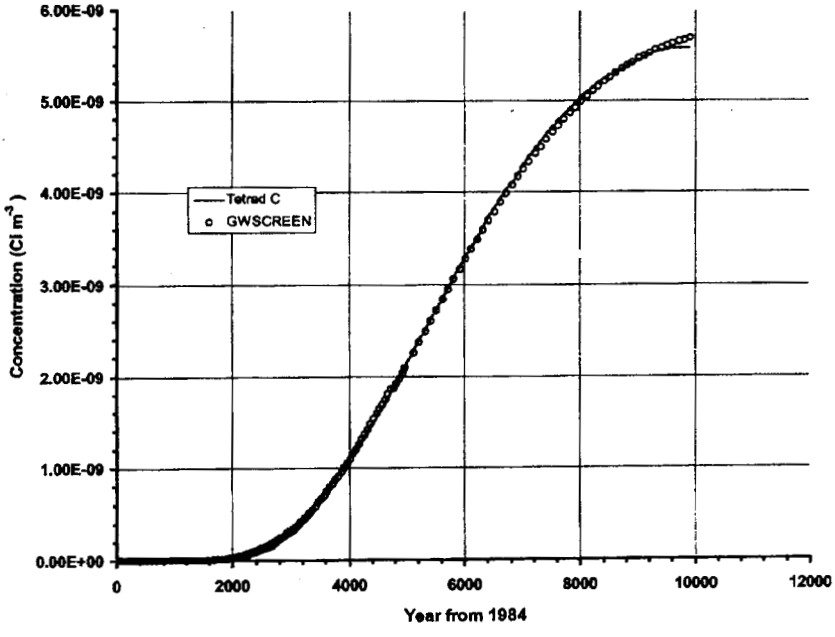

Figure 5-7. GWSCREEN calibration of U-238 with TETRAD.

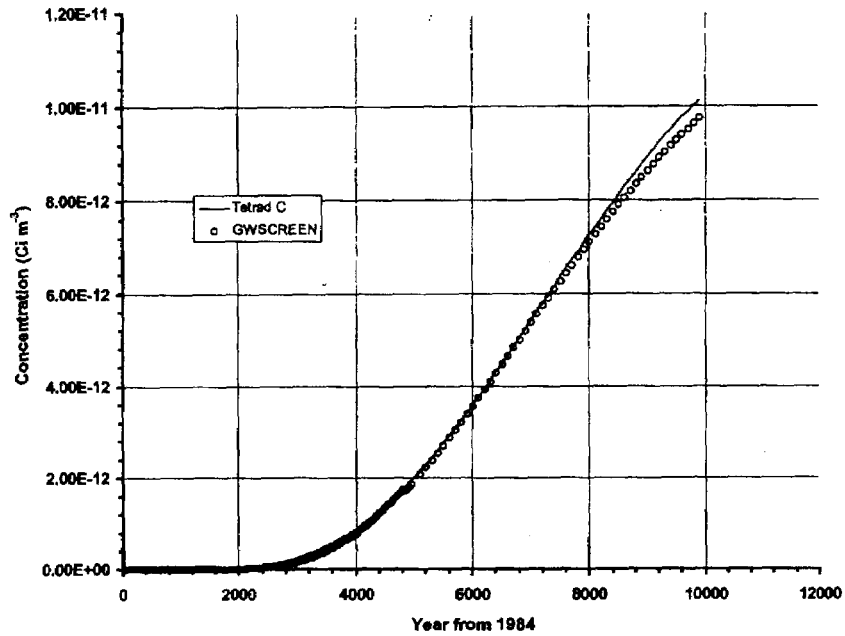

Figure 5-8. GWSCREEN calibration of Np-237 with TETRAD.

Table 5-2. Quantitative results of GWSCREEN calibration with TETRAD

Nuclide	Maximum Concentration, TETRAD (pCi L^{-1})	Maximum Concentration, GWSCREEN (pCi L^{-1})	Geometric mean P/O ratio[a]	Regression coefficient, r^2
C-14	1540	1520	1.14	0.983
I-129	9.21	9.04	1.09	0.987
U-234	10.9	10.9	0.971	1.0
U-238	5.58	5.68	0.971	1.0
Np-237	0.0101	0.00975	0.966	1.0

[a] Predicted to Observed ratio. Only values within a factor of 100 of the peak TETRAD concentration were included in the calculation.

```
C-14 - Calibration Kd=0.1  7/9/98      (Card 1)
1 2 0 2  2                             (Card 2) imode,itype,idisp,kflag idil
3 1 2 1  2                             (Card 3) imodel,isolve,isolveu,imoist,imoistu
6 12 0.01                              (Card 4) jstart jmax eps
70. 2.555E+04 2.0  350.  1.  4.0E-3    (Card 5) bw,at,wi,ef,ed,dlim
0.  0.                                 (Card 6) x0,y0
481. 481. 0.01                         (Card 7) l,w,perc
12.5  1.26 2.25                        (Card 9) depth,rhou,axu
0.3195 2.534 0.7  0.48 0.0384          (Card 9b) alphau nu ksatu porsu thetaru
20.0    5.0    1.706  76.  7.         (Card 10) ax,ay,az,b,z
0.75  0.06  1.9                        (Card 11) u,phi,rhoa
1                                      (Card 12a) nrecept
340.  0.                               (Card 12b) xrec(i) yrec(i)
$ output time data
4                                      (Card 13a) ntimes
40    500     5                        (Card 13b) t1(i) t2(i) tp(i)
525  2500    25
2550 5000    50
5100 10000  100
$ Contaminant data
1                                      (Card 14) ncontam
0  0.1 0.1  14.  1. 1.0 1.0E6 0.0      (Card 14a) nprog kds kdu zmw q0 rmi sl other
C-14   5.73E3 7.6E-06 0.99999          (Card 14b) cname(i),thalf(i),kda(i),dcf(i)
d:\fy2000\rwmc-pa\srcterm\c14\c14src.out        (Card 14c)
```

Figure 5-9. GWSCREEN version 2.5 input file for C-14. The nuclide flux is read from the file c14src.out (last line) and was generated by the one-compartment source term model described in Equations 1 and 2.

5.2.2 Parametric Uncertainty Analysis

The simplified model that was calibrated to TETRAD output and described in Section 5.1.1 was used as the computational engine for the Monte Carlo analysis. A Perl[g] script was used as the Monte Carlo driver for the simulation and performed the following functions for each Monte Carlo trial:

- sample parameter values from assigned distributions
- write input files for the source term model and generate release files for each of the nuclides
- write GWSCREEN input files and execute GWSCREEN
- extract and store output from the GWSCREEN model run.

One of the major limitations of this uncertainty analysis is that it did not consider uncertainty in the release mechanisms modeled in DUST. Time constraints and the preliminary nature of this analysis did not warrant inclusion of DUST in the analysis. However, the Perl script written for the uncertainty analysis is certainly amenable to inclusion of DUST in the future. This deficiency in the uncertainty analysis was partially accounted for by assigning rather large uncertainty to the radionuclide inventory scaling factor. However, adjusting the inventory scaling factor only affects the total quantity of radionuclides available for release and does not affect the rate at which radionuclides are released. For future uncertainty analyses, the DUST model should be explicitly included in the simulation. A copy of the Perl script is found in Appendix D.

---

g Perl (Practical Extraction Reporting Language) is a scripting language available on most Unix workstations and recently made available for Windows-based machines

Uncertainty was also not evaluated for the food chain pathway or the exposure scenario. The food chain pathway includes exposure to radionuclides derived from the groundwater other than direct ingestion. Food chain exposure pathways include transfer of radioactivity to crops via irrigation with contaminated water and transfer of radioactivity to livestock via ingestion of contaminated water and animal feed.. Equations and parameter values are described in Maheras et al (1994). Food chain doses were incorporated into the total dose (including direct ingestion) by calculating an all pathway dose conversion factor. The all pathway dose conversion factor is the all pathway dose (mrem/y) divided by the groundwater concentration (pCi/L) and has units of mrem-L pCi^{-1} y^{-1} (Table 5-3). Uncertainty in the food chain pathway model could be performed external to these calculations because the parameters that describe food chain transport (concentration factors, animal transfer factors and animal ingestion rates) are generally independent from those used to calculate fate and transport. There is however, correlation between soil depletion rates and contaminant leaching. Due to time constraints and the preliminary nature of this analysis, food chain transport was not considered stochastically. However, the Perl script that was written is certainly amenable to inclusion this pathway in the future.

Table 5-3 All pathway dose conversion factors for the principle radionuclides in the performance assessment.

Nuclide	All pathway dose conversion factor (mrem-L pCi^{-1} y^{-1})	Nuclide	All pathway dose conversion factor (mrem-y pCi^{-1} L^{-1})
C-14	5.90E-03	U-238	1.91E-01
I-129	4.51E-01	U-234	2.02E-01
Cl-36	8.86E-02	Th-230[b]	3.90E-01
Np-237	2.89E+00	Ra-226[b]	8.49E-01
U-233[a]	2.10E-01	Pb-210[b]	3.83E+00
Th-229[a]	2.88E+00		

a. Daughter products of Np-237

b. Daughter products of U-238 and U-234

Uncertainty in the exposure scenario parameters, (which mostly consist of human ingestion rates of water and food products) were also ignored. The reason for this is that the exposure scenario represents a hypothetical future resident who's behavior is neither predictable or measurable. In contrast, the transport of radionuclides represents real physical processes that can be measured (albeit with difficulty) and predicted with mathematical models. The same cannot be said of the hypothetical resident. The resident exposure scenario is only a means to translate concentrations of radionuclide in the environment to relevant health impacts that can be compared with regulatory standards. For these reasons, all exposure scenario parameters were considered fixed.

Output from the Monte Carlo simulation consists of an empirical distribution containing *n* values. These values are arranged in ascending order and reported in terms of their ordered-statistics[h] or percentiles. For example, the 5th percentile represents the 5th highest value of 100 values. In this way, statements about model precision can be made. For example, suppose the output distribution contained

[h] The ordered statistics is the ordered ranking of all *n* values comprising an empirical distribution.

100 values. The 5th highest value (out of the 100 values) was 2 and the 95th highest value 45. We could then state that 90% of the model predictions fell between 2 and 45 or that 95% of the model predictions were less than 45.

Five-hundred model realizations were run for the Monte Carlo simulation. This was a convenient number to choose because run times were relatively short (several hours) and confidence intervals around the percentiles on the tails could be reasonably well defined. Using the non-parametric ordered statistics described in Hahn and Meeker (1998), confidence intervals for an empirical distribution containing 500 values were determined. Given a distribution of 500 values, the 95% confidence interval around the 95th percentile value (475th highest value) is ~92nd percentile and 98th percentile. These values can easily be extracted from model output and were used to report percentile values in the results section.

Parameter distributions are summarized in Table 5-4. In many cases, distributions were assumed based on current knowledge of the parameter. In general, all parameter distributions developed for environmental systems tend to have some degree of subjectivity within them because there is typically not enough data to develop a purely quantitative distribution (Till and Meyer 1983). The distribution is a statement of belief about the parameter's true but unknown value. In general, triangular or log-triangular distributions were assigned to the parameters. These distributions are useful when there are only estimates of a central (mean or mode), minimum, and maximum value of a parameter. A discussion and justification for each parameter follows.

5.2.2.1 Percolation Rate. Percolation rate is the amount of water that passes through the waste and into the vadose zone every year. The best-estimate percolation rate was estimated to be 8.5 cm y^{-1} before emplacement of the cap. After emplacement of the cap, the infiltration rate was reduced to 1 cm y^{-1} and was assumed to remain constant forever. Cap infiltration estimates were based on engineering studies of various cap designs (Magnuson 1993) and the estimated background percolation rate that ranged between 0.4 and 1.2 cm y^{-1} (Cecil et al. 1992). Quantitative uncertainty analysis of these caps were not performed, therefore a distribution was assumed based on a reasonable expectation of expected uncertainties. For this analysis, a factor of 2 uncertainty was assumed for the post-cap percolation rate. A triangular distribution was assigned having a minimum value of 0.5 cm y^{-1}, a mode value of 1 cm y^{-1}, and a maximum value of 2 cm y^{-1}.

5.2.2.2 Dispersivity in Aquifer. Dispersivity is parameter that describes the spreading that occurs while a contaminant is advected in a fluid medium. This parameter was used as a means of calibrating the GWSCREEN model to TETRAD output and values of 20 m, 5 m, and 1.7 m for the longitudinal, transverse, and vertical dispersivity were obtained from the calibration. Although equations and generic values exist for estimating dispersivity (Xu and Eckstien 1995), dispersivity tends to be a site-specific parameter. Because little information was available from which to develop a distribution, the distribution assigned was based on a reasonable expectation of expected uncertainties. For this analysis, a factor of 2 uncertainty was assumed for the longitudinal dispersivity. In order to keep the relative proportions of transverse to longitudinal dispersion and vertical to longitudinal dispersion constant, the ratios of these values for the base-case condition ($\alpha_T/\alpha_L = 0.25$, $\alpha_V/\alpha_L = 0.085$), were computed and used to calculate α_T and α_V for a newly sampled α_L. A triangular distribution was assigned to α_L having a minimum of value of 10 m, a mode value of 20 m, and a maximum value of 40 m.

5.2.2.3 Dispersivity in Unsaturated Zone. Like dispersivity in the aquifer, dispersivity in the unsaturated zone was treated as a calibration parameter. Therefore, dispersivity in the unsaturated zone was similarly treated. A triangular distribution was defined having a minimum of 1.125 m, a mode of 2.25 (the calibrated value), and maximum of 4.5 m.

5.2.2.4 Sorption Coefficients. Sorption coefficients (K_d) describe the partitioning between the liquid aqueous and solid sorbed phases and are known to vary over several orders of magnitude in some cases. Dicke (1998) reviewed sorption studies performed at the INEEL and reported in the open literature and provided best-estimate K_d values in sediment with an uncertainty range. Sediment K_d values were scaled to fractured basalt by accounting for the surface area in the fractured basalt that was lined with either fine-grained sediments or chemical alteration products. In general, this scaling resulted in aquifer K_d values near zero for sediment K_d values less than 1000 mL g^{-1}. For this analysis, the range of values was applied to triangular distribution having a mode value equal to the best estimate value. In the case of carbon, iodine, and neptunium, a log-transformed distribution was applied because the range of possible values varied over an order of magnitude. In the case of carbon, the minimum Kd value was set at 0.01 because the best estimate K_d value reported in Dicke (1998) of 0.1 mL g^{-1} was also reported as the minimum value. For chlorine, a K_d value of zero was reported in all cases. Therefore, this parameter was not treated stochastically.

5.2.2.5 Inventory Scaling Factors. There were two inventory scaling factors used in the simulation. The first was a stochastic factor that represents the uncertainty in the inventory estimate. The second was a deterministic value that represents the difference between in the inventory used in the TETRAD model runs that GWSCREEN was calibrated to and the most recent best estimate of the inventory from 1984 to 1999 and projected out to 2020 (Table 5-5). The stochastic values were developed from best-estimate and upper bound inventories reported in Table 5-5 of the RWMC Composite Analysis [CA] (McCarthy et al. 2000). The ratio of the upper-bound CA inventory (I_{UB}) and the best-estimate CA inventory (I_{BE}) was the basis for the factor.

$$F = \frac{I_{UB}}{I_{BE}} \tag{5-5}$$

This factor was then assumed to be symmetrical around the best estimate inventory. A log-triangular distribution was assigned having a minimum equal to $1/F$, a mode equal to 1.0, and a maximum equal to F. Table 5-5 in McCarthy et al. (2000) does not contain data for C-14. For this analysis, an F value of 3 was assumed for C-14 and was based on the average value of F (2.2) computed from data in Table 5-5 in McCarthy et al. (2000) with additional allowance made for lack of knowledge.

Table 5-4. Parameter distributions used uncertainty sensitivity analysis.

Parameter	Distribution Type	Units	Distribution parameters
Percolation rate	Triangle	m y^{-1}	minimum 0.005; mode 0.01; maximum 0.02
Longitudinal dispersivity (aquifer)	Triangle	m	minimum: 10; mode: 20; maximum 40
Unsaturated dispersivity	Triangle	m	minimum 1.25; mode 2.25; maximum 4.5
Darcy velocity in aquifer	Triangle	m y^{-1}	minimum 0.37; mode 0.75; maximum 1.5
Carbon K_d	Log triangle	mL g^{-1}	minimum 0.01; mode 0.1; maximum 1.5
Iodine K_d	Log-triangle	mL g^{-1}	minimum 0.02; mode 0.1; maximum 5.0
Uranium K_d	Triangle	mL g^{-1}	minimum 3.4; mode 6.0; maximum 9.0
Neptunium K_d	Log-triangle	mL g^{-1}	minimum 1.0; mode 8.0; maximum 80
C-14 inventory scaling factors	Log-triangle	n/a	minimum 0.33; mode 1.0; maximum 3
I-129 inventory scaling factors	Log-triangle	n/a	minimum 0.286; mode 1.0; maximum 3.5
Cl-36 inventory scaling factors	Log-triangle	n/a	minimum 0.189; mode 1.0; maximum 5.3
U-234 inventory scaling factors	Log-triangle	n/a	minimum 0.421; mode 1.0; maximum 2.3
U-238 inventory scaling factors	Log-triangle	n/a	minimum 0.302; mode 1.0; maximum 3.3
Np-237 inventory scaling factors	Log-triangle	n/a	minimum 0.39; mode 1.0; maximum 2.56

Table 5-5. Deterministic inventory scaling factors.

Nuclide	Deterministic Inventory Scaling Factor
C-14	0.411
I-129	0.229
Cl-36	1.0
U-234	1.22
U-238	12
Np-237	11

5.2.3 Uncertainty Results

Results for the uncertainty analysis are expressed in terms of percentiles of the distribution of the output variable. The output variable is the total dose. Figure 5-10 shows the distribution of all pathway doses as a function of time for the compliance time period (0 to 1000 years). Ninety-fifth percentile doses (with 95% confidence) are highest at year 300 and reach a maximum of 13 mrem. The breakdown of dose by nuclide at year 300 (Table 5-6) shows that at the 5th and 50th percentiles, dose is dominated by Cl-36 while at the 95th percentile, the dose is dominated by C-14. The importance of a nuclide depends on the time window and percentile of the output distribution.

The time-dependence of individual nuclide doses affects the maximum dose calculated. For example, the 95th percentile individual nuclide doses at year 300 for C-14, I-129, and Cl-36 were 10, 2.2, and 4 mrem respectively. Note that the sum of these (16.2 mrem) is different from the 95th percentile *total* dose of 13 mrem. This difference is because individual nuclide doses occurred in different model realizations and therefore cannot be summed together.

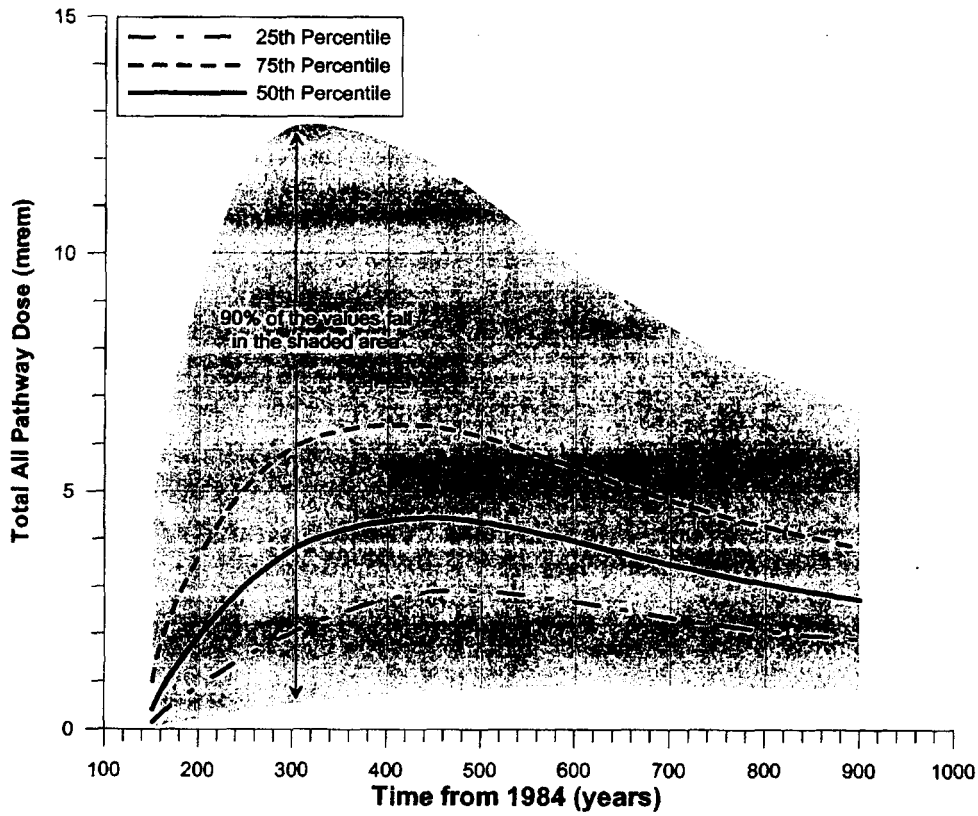

Figure 5-10. Uncertainty in the all pathway dose as a function of time from 0 to 1000 years. The gray area of the curve represents model parameter uncertainty where 90% of the model output resides (with 95% confidence). The solid red line represents the 50th percentile. The red dashed red line represents the 75th percentile and the dashed-dotted blue line is the 25th percentile

Table 5-6. Fraction of total all pathway dose at year 300 attributed to each nuclide for the 5th, 50th, and 95th percentile.

Nuclide	5th percentile (0.52 mrem)	50th percentile (3.8 mrem)	95th percentile (13 mrem)
C-14	0	0.0193	0.892
I-129	0.055	0.0033	0.0296
Cl-36	0.945	0.977	0.0786
U-234	0	0	0
U-238	0	0	0
Np-237	0	0	0

Figure 5-11 shows the uncertainty in the all pathway dose as a function of time for the 0 to 10,000 time period. Ninety-fifth percentile doses (with 95% confidence) reach a maximum around the year 7000 and remain near 45 mrem. The breakdown of dose by nuclide at year 7000 (Table 5-7) shows that the dose is dominated by U-238 for all percentiles followed by U-234. Carbon-14 makes up about 11 percent of the dose at the 5th percentile, ~1% at the 50th percentile, and <1% at the 95th percentile. Doses at the 75th percentile only slightly exceed the 25 mrem dose limit after year 7000.

Table 5-7. Fraction of total all pathway dose at year 7000 attributed to each nuclide for the 5th, 50th, and 95th percentile.

Nuclide	5th percentile (2.4 mrem)	50th percentile (15 mrem)	95th percentile (48 mrem)
C-14	0.1092	0.0129	0.0044
I-129	0.0	0.0	0.0
Cl-36	0.0	0.0	0.0
U-234	0.1253	0.289	0.231
U-238	0.765	0.645	0.765
Np-237	0.0	0.0537	0.0002

The results presented here indicate the precision of the model is roughly an order of magnitude. However, distributions are not symmetrical and the tails in some cases are quite long. The fact that doses at the 95th percentile are all below 25 mrem for the 1000 year time frame of compliance provides some confidence that the predicted dose limit will not be exceeded in future modeling endeavors.

The uncertainty analysis presented here is in no way comprehensive, and many deficiencies remain. However, a template has been laid out for uncertainty analysis in the future. Ideally, the same model used to predict concentrations and doses for the base case should be used in the uncertainty analysis. As it currently stands, the TETRAD model is not practical to use in Monte Carlo simulation because its run-times are too long. Decoupling of the unsaturated zone with the aquifer and other modifications to the TETRAD simulation may improve run-time performance and enable the use of this model in future uncertainty analysis.

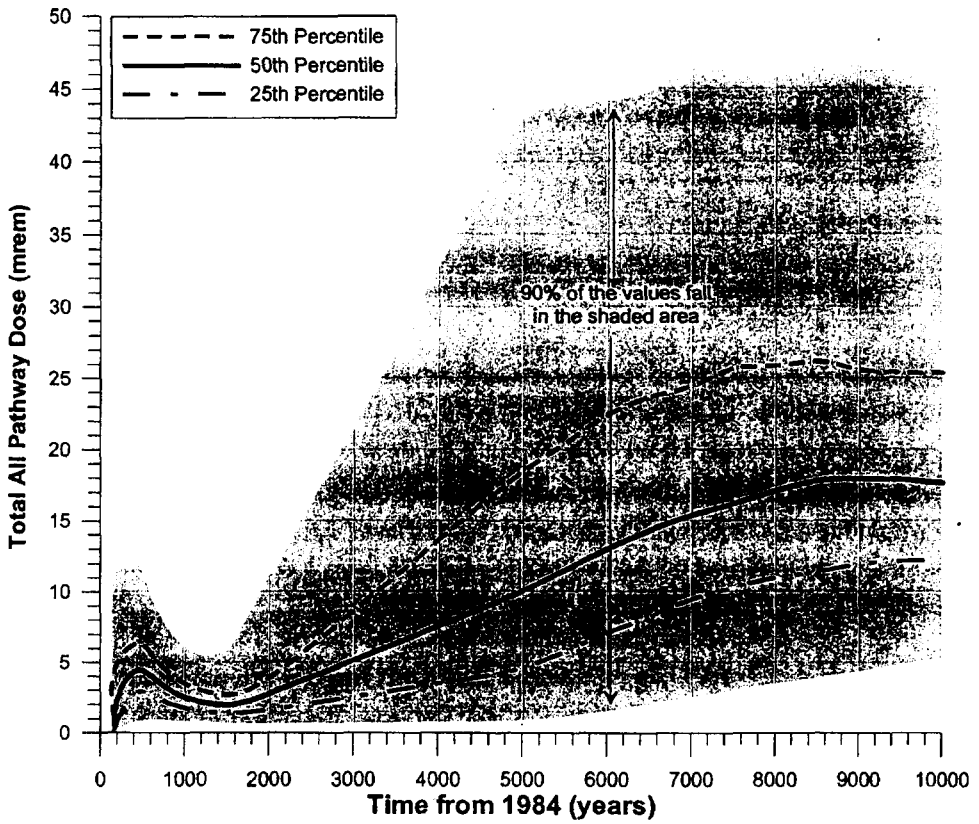

Figure 5-11. Uncertainty in the all pathway dose as a function of time from 0 to 10,000 years. The gray area of the curve represents model parameter uncertainty where 90% of the model output resides (with 95% confidence). The solid red line represents the 50th percentile. The red dashed red line represents the 75th percentile and the dashed-dotted blue line is the 25th percentile

5.3 Sensitivity Analysis

A quantitative sensitivity analysis was performed using the data generated during the uncertainty analysis. Previous attempts at addressing model sensitivity (McCarthy et al. 1998; Becker and Magnuson 1998) have been semi-quantitative in nature, typically employing a one-factor-at-a-time approach to evaluate the sensitivity of groundwater concentrations or ingestion dose to several model parameters. In the approach presented here, the Monte Carlo sampling techniques described earlier were used to propagate input parameter uncertainty into the predicted dose estimates. Then, using regression techniques, rank correlation coefficients were calculated between each parameter and the corresponding predicted dose. Parameter sensitivities are then established by the degree of correlation between the parameter and the output variable (predicted dose).

5.3.1 Methodology

The methods used to evaluate parameter sensitivity are described in Crystal Ball software package (Decisioneering Inc. 1993). The rank correlation coefficients provide a quantitative measure of the sensitivity of the predicted dose to variations in the input parameters. Rank correlation replaces each input parameter and endpoint value pair, with its ranking within the distribution. Linear correlation of the rankings is then performed. Consider a simulation of n Monte Carlo trials where the parameters, a, b, and

c are defined stochastically. The output variable defined as y, is calculated n times during the simulation. The results may be tabulated as follows:

a_1	b_1	c_1	$\Rightarrow$	y_1
a_2	b_2	c_2	$\Rightarrow$	y_2
a_3	b_3	c_3	$\Rightarrow$	y_3
.				
.				
.				
a_n	b_n	c_n	$\Rightarrow$	y_n

The subscript 1, 2, 3, ...n refer to the Monte Carlo trial number. To calculate the rank correlation coefficient, the values of a_i, b_i, c_i, and y_i are replaced by their ranking within the distribution of values. For example, suppose for the third Monte Carlo Trial, the values a_3, b_3, c_3, are selected yielding an output value of y_3. Suppose 500 trials are performed and the value of a_3 was ranked at 23 –that is, it is the 23rd highest value within the distribution 500 values of a. The value of a_3 is replaced by 23. Likewise, the values of b_3, c_3, and y_3 are replaced by their respective ranks. Linear correlation is then performed between the ranks of each of the parameters and output variable, y.

The advantage of rank correlation over simple liner correlation is that it nonparameteric. That is, it is not dependent on the underlying distribution of either the input or output variables. The rank correlation coefficient is given by (Press et al. 1992)

$$r_s = \frac{\sum_i \left(R_i - \overline{R}\right)\left(S_i - \overline{S}\right)}{\sqrt{\sum_i \left(R_i - \overline{R}\right)^2}\sqrt{\sum_i \left(S_i - \overline{S}\right)^2}} \tag{5-6}$$

where

r_S = the rank correlation coefficient

R_i = the rank of the input parameter value

S_i = the rank of the corresponding output value.

The advantage of using Monte Carlo techniques over that of a one-factor-at-a-time approach is that interaction between parameters are included in the analysis. For example, the sensitivity of the dose due to parameter Y may depend on the value chosen for parameter X. Rank correlation coefficients provides a meaningful measure of the degree to which parameters and the endpoint (all pathway dose) *change together*. The rank correlation coefficient takes on a value between –1 and +1. Perfect correlation is achieved when the absolute value of the correlation coefficient equals 1. Degree of correlation (and thereby degree of sensitivity), decreases with a decrease in the absolute value of the correlation coefficient. A positive correlation coefficient indicates that an increase in the value of the parameter results in an increase in the computational endpoint. A negative correlation coefficient indicates that a increase in the value of the parameter results in a decrease in the computational endpoint.

Another way to visualize the sensitivity analysis results is to compute the percent contribution each parameter has to the to the total variance. The contribution to the total variance was *approximated* using a simple technique described in the Crystal Ball software (Decisioneering Inc. 1993) where the rank correlation coefficient for each parameter is squared and normalized to 100%. The output variable for this analysis is total (all nuclides) all pathway dose at a specific time. Based on the results of the uncertainty analysis, two time-periods were chosen; year 450 year and year 9500. These time periods correspond roughly to the time of maximum dose in the 0–1000 year time frame and 0–10,000 year time frame.

5.3.2 Sensitivity Analysis Results

Results of the sensitivity analysis at 450 years (Table 5-8) indicates that the total dose is most sensitive to the carbon K_d, the C-14 inventory scaling factor, and the aquifer Darcy velocity. The sign of the rank correlation coefficient indicates total dose is inversely related to the carbon K_d and Darcy velocity and is directly related to the C-14 scaling factor. Note that the longitudinal, transverse and vertical dispersivity have the same rank correlation coefficient. This is because the transverse and vertical dispersivity are correlated to the longitudinal dispersivity as described in section 4.1.2.2. None of the actinides (U-234, U-238, and Np-237) exhibited high sensitivities because doses from these nuclides at 450 years were minimal.

Table 5-8. Rank correlation coefficients and percent contribution to variance for the total (all nuclides) all pathway dose at 450 years.

Parameter	Rank correlation coefficient	Percent contribution to total variance
Percolation	0.247	6.38
Longitudinal dispersivity	–0.199	4.16
Transverse dispersivity	–0.199	4.16
Vertical dispersivity	–0.199	4.16
Unsaturated dispersivity	–0.087	0.806
Aquifer Darcy velocity	–0.359	13.5
Carbon K_d	–0.575	34.7
Iodine K_d	–0.189	3.72
Uranium K_d	0.058	0.353
Neptunium K_d	–0.0169	0.030
C-14 scaling factor	0.439	20.23
I-129 scaling factor	0.0787	0.649
Cl-36 scaling factor	0.236	5.82
U-234 scaling factor	0.0665	0.463
U-238 scaling factor	0.0756	0.599
Np-237 scaling factor	0.0493	0.255

Sensitivity analysis results at 9500 years (Table 5-9) indicates that the total dose is most sensitive to the U-238 scaling factor followed by the Darcy velocity in the aquifer and the uranium K_d. Typically, the K_d value tends to be one of the more sensitive parameters. However the distribution assigned to the uranium K_d was somewhat narrow (3.4 to 9 mL g^{-1}) compared to the K_d values of the other nuclides. Consequently, its value changed relatively little compared the other parameters and translates to a low sensitivity. The sign of the rank correlation coefficient indicates total dose is inversely related to the uranium K_d and Darcy velocity, and is directly related to the uranium scaling factor. The longitudinal, transverse, and vertical dispersivity have the same rank correlation coefficient. This is because the transverse and vertical dispersivity are correlated to the longitudinal dispersivity as described in section 5.1.2.2. None of the fission and activation products (C-14, I-129, and Cl-36) exhibited high sensitivities because doses from these nuclides at 9500 years were minimal.

Table 5-9. Rank correlation coefficients and percent contribution to variance for the total (all nuclides) all pathway dose at 9500 years.

Parameter	Rank Correlation Coefficient	Percent Contribution to Variance
Percolation	0.337	11.0
Longitudinal dispersivity	–0.283	7.7
Transverse dispersivity	–0.283	7.7
Vertical dispersivity	–0.283	7.7
Unsaturated dispersivity	–0.097	0.915
Aquifer Darcy velocity	–0.439	18.6
Carbon K_d	–0.010	0.01
Iodine K_d	–0.037	0.13
Uranium K_d	–0.232	5.18
Neptunium K_d	–0.024	0.053
C-14 scaling factor	0.005	0.002
I-129 scaling factor	–0.004	0.002
Cl-36 scaling factor	0.0007	0.006
U-234 scaling factor	0.195	3.66
U-238 scaling factor	0.621	37.2
Np-237 scaling factor	0.158	0.024

The results of the sensitivity analysis indicate future studies should focus on C-14 and U-238. Specifically, C-14 mobility as suggested by its sorption coefficient, and the U-238 inventory scaling factor. Addressing these two parameters would have the greatest impact on reducing the uncertainty in the dose calculation.

6. WASTE CONCENTRATION LIMITS

Maheras et al (1997) presented waste concentration limits for pits and soil vaults based on the results of the inadvertant intruder analyses in the RWMC performance assessment. Recalculation of these limits, based on current methodology, will be completed in the next revision.

7. REFERENCES

Abbott, M. L., 1997a, *Revised Report on NRF Expended Resin Waste Activity Inventories*, MLA-9-97, LMITCO Interdepartmental Communication.

Abbott, M. L., 1997b, *Revised Report on NRF Core Structural Waste Activity Inventories*, MLA-8-97, LMITCO Interdepartmental Communication.

Abbott, M. L., 1998, LMITCO Interdepartmental Communication from to J. A. Logan, *Estimated C-14 Inventory in TRA Resin Shipments to the RWMC*, April 14, 1998, MLA-03-98.

Anderson, J. E. and R. Inouye, 1988, *Long-term Dynamics of Vegetation on a Sagebrush Steppe of Southeastern Idaho*, Department of Biological Services, Idaho State University.

Arthur, W. J., 1982, "Radionuclide Concentrations in Vegetation at a Solid Radioactive Waste Disposal Area in Southeastern Idaho," *Journal of Environmental Quality*, 11, 3, pp. 394-399.

Baca, R.G., S.O. Magnuson, H.D. Nguyen, and P. Martin, 1992. *A Modeling Study of Waterflow in the Vadose Zone Beneath the Radioactive Waste Management Complex, Idaho National Engineering Laboratory*, EGG-GEO-10068, Idaho National Engineering and Environmental Laboratory, Idaho Falls, ID, January.

Baes, C. F. et al., 1984, *A Review and Analysis of Parameters for Assessing Transport of Environmentally Released Radionuclides through Agriculture*, ORNL-5786.

Baes, C. F. III and T. H. Orton, 1979, "Productivity of Agricultural Crops and Forage, Y_v" in *A 'Statistical Analysis of Selected Parameters for Predicting Food Chain Transport and Internal Dose of Radionuclides*, NUREG/CR-1004, November.

Banaee, J. and P. K. Nagata, 1996, Interdepartmental Communication to D. J. Jorgensen, Underground Corrosion of Austentic Stainless Steel and Nickel-based Alloys at the Radioactive Waste Management Complex, PKN-02-96, EG&G Idaho, Inc.Becker, B. H., 1997, Selection and Development of Models Used in the Waste Area Group 7 Baseline Risk Assessment, INEL/EXT-97-00391, Lockheed Martin Idaho Technologies Company, May.

Becker B.H. and S.O. Magnuson 1998, *Sensitivity Simulation Results for Models used to support both the WAG7 IRA and LLW CA*. Engineering Design File EDF-ER-032, Idaho National Engineering and Environmental Laboratory, Idaho Falls, ID.

Becker, B. H., J. D. Burgess, K. J. Holdren, D. K. Jorgensen, S. O. Magnuson, and A. J. Sondrup, 1998, *Interim Risk Assessment and Contaminant Screening for the Waste Area Group 7 Remedial Investigation*, DOE/ID-10569, Lockheed Martin Idaho Technologies Company, Draft Rev. 2, March.

Becker, B. H., T. A. Bensen, C. S. Blackmore, D. E. Burns, B.N. Burton, N. L. Hampton, R. M. Huntley, R. W. Jones, D. Jorgensen, S. O. Magnuson, C. Shapiro, R. L. VanHorn, 1996, *Work Plan for Operable Unit 7-13/14 Waste Area Group 7 Comprehensive Remedial Investigation/Feasibility Study*, INEL-95/0343, Lockheed Martin Idaho Technologies Company, May.Bishop, C.W., 1991. *Hydrologic Properties of Vesicular Basalt.* MS Thesis, University of Arizona, Tucson, AZ.

Bishop, C.W., 1991. *Hydrologic Properties of Vesicular Basalt.* MS Thesis, University of Arizona, Tucson, AZ.

Blom, P. E., W. H. Clark, J. B. Johnson, 1991, "Colony Densities of the Seed Harvesting Ant *Pogonomyrmex salinus* in Seven Plant Communities on the Idaho National Engineering Laboratory," *Journal of the Idaho Academy of Science*, 27, 1, pp. 28-36.

Bradley, T. M., 1998, Letter from Bradley, Manager Naval Reactors Idaho Branch Office, to J. T. Case, Manager Waste Management Programs, *Additional Information on Past and Projected Future Radioisotope Inventory from Naval Reactors Facility and Comments on the Assumptions Used in the Radioactive Waste Management Complex Performance Assessment*, February 27, 1998, NR:IBO-98/034.

Burgess, J. D., 1996, *Tritium and Nitrate Concentrations at the RWMC*, Engineering Design File EDF-ER-024, INEL-96/204, Lockheed Martin Idaho Technologies Company.

Burns, D. E., B. H. Becker, R. M. Huntley, C. A. Loehr, S. M. Rood, P. Sinton, and T. H. Smith, 1994, *Revised Preliminary Scoping Risk Assessment for Waste Pits, Trenches, and Soil Vaults at the Subsurface Disposal Area, Idaho National Engineering Laboratory*, EG&G-ER-11395, EG&G Idaho, Inc., June.

Carboneau, M. L., 1998 Interdepartmental Communication to J. A. Logan, *Reassessment of Neutron-Activation-Product Curies Sent from EBR-II to Disposal at the RWMC*, February 27, 1998, MLC-01-98.

Cecil, L. D., J. R. Pittman, T. M. Beasley, R. L. Michel, P. W. Kubik, P. Sharma, U. Fehn, and H. Gove, 1992, "Water Infiltration Rates in the Unsaturated Zone at the Idaho National Engineering Laboratory Estimated from Chlorine-36 and Tritium Profiles, and Neutron Logging," in Proceedings of the 7th International Symposium on Water-Rock Interaction - WRI-7, Y. K. Kharaka and A. S. Meest (eds.), Park City, UT.

Decisioneering Inc. 1993. *Crystal Ball Version 3.0; Forecasting and Risk Analysis for Spreadsheet Users.* Decisioneering Inc., Denver Colorado.

Dicke, C. A., 1997a, *Distribution Coefficients and Contaminant Solubilities for the Waste Area Group 7 Baseline Risk Assessment*, INEL/EXT-97-00201, Lockheed Martin Idaho Technologies Company, May.

Dicke, C. A., 1997b, *Carbon-14 Distribution Coefficients Measured from Batch Experiments on SDA Sediments*, INEEL/INT-98-00068, EDF-RWMC-1011, Lockheed Martin Idaho Technologies Company, May.

Dodge, R. L. et al., 1991, *Performance Assessment Review Guide for DOE Low-Level Radioactive Waste Disposal Facilities*, Idaho National Engineering Laboratory, EG&G Idaho, DOE/LLW-93, October.

DOE (U.S. Department of Energy), 1996, *Idaho National Engineering Laboratory Comprehensive Facility and Land Use Plan*, DOE/ID- 10514.

DOE, 1987, Environmental Assessment: *Fuel Processing and Restoration at the Idaho National Engineering Laboratory*, DOE/EA-0306.

DOE, 1988a, "Radioactive Waste Management," Order 5820.2A, September 26.

DOE, 1988b, *Internal Dose Conversion Factors for Calculation of Dose to the Public*, DOE/EH-0071.

DOE, 1988c, *External Dose-Rate Conversion Factors for Calculation of Dose to the Public*, DOE/EH-0070.

DOE, 1993, 1992 *INEL National Emission Standard for Hazardous Air Pollutants Annual Report*, DOE/ID-10342(92), June.

DOE, 1999, *Radioactive Waste Management*, DOE Order 435.1, July 9.

DOE, 2000, 1999 Idaho National Engineering and Environmental Laboratory (INEEL) National Emission Strandards for Hazardous Air Pollutants (NESHAPS) – Radionuclides Annual Report, DOE/ID-10342(00), June.

Eckerman, K. F. et al., 1988, *Limiting Values of Radionuclide Intake and Air Concentration and Dose Conversion Factors for Inhalation, Submersion, and Ingestion*, Federal Guidance Report No. 11, EPA-520/1-88-020.

EPA (U.S. Environmental Protection Agency), 1991a, *Sole Source Designation of the Eastern Snake River Plain Aquifer, Southern Idaho*, 58 FR 50634-50638, October 7.

EPA, 1986, National Primary Drinking Water Regulations; Radionuclides; Advance Notice of Proposed Rulemaking, 51 FR 34836-34862, September 30.

EPA, 1988, *CERCLA Compliance with Other Laws Manual*, EPA/540/G-89/006.

EPA, 1989, *Risk Assessments Methodology, Environmental Impact Statement, NESHAPs for Radionuclides, Background Information Document - Volume 1*, EPA/520/1-89-005.

EPA, 1991, National Primary Drinking Water Regulations; Radionuclides; Proposed Rule, 56 FR 33050-33127, July 18.

EPA, 1995, *User's Guide for the Industrial Source Complex (ISC3) Dispersion Models*. EPA-454/B-95-003a, September.

Farris, W. T., 1988, *Probabilistically Derived Concentration Limits for Near-Surface Disposal of Radioactive Waste*, M.S. thesis, University of Washington, Seattle, Washington.

Federal Register, 1991, *Part 141-National Primary Drinking Water Regulations*, Vol. 56, No. 138, Thursday, July 18, 1991.

Forman, S. L., 1991, *The Quaternary Stratigraphy and Geochronology at the REWMC and Spreading Area Sites, INEL, Idaho*, report prepared for EG&G Idaho, Inc, by Ohio State University.

Fraley, L., Jr., 1978, "Revegetation Following a 1974 Fire at the Idaho National Engineering Laboratory," in *Ecological Studies on the Idaho National Engineering Laboratory Site 1978 Progress Report*, O. D. Markham (ed.), IDO-12087, pp. 194-199.

Gadd, M, S., 1993, *The Origins and Pathways of ^{222}Rn Entering into Basement Structures*, Ph.D. Dissertation, Colorado State University, Fort Collins, Colorado.

Gilbert, T. L. et al., 1989, *A Manual for Implementing Residual Radioactive Material Guidelines*, ANL/ES-160, DOE/CH/8901, June.

Groves, C. R. and B. L. Keller, 1983, "Ecological Characteristics of Small Mammals on a Radioactive Waste Disposal Area in Southeastern Idaho," *The American Midland Naturalist, 109*, 2, pp. 253-265.Honeycutt, T. K., 1998, LMITCO Interdepartmental Communication, Summary of Radionuclide Source Term Refinement for ANL-W, NRF, TRA, and SMC Waste Streams, May 5, 1998.

Hahn and Meeker 1998. Statistical Intervals.

ICRP (International Commission on Radiological Protection), 1975, *International Commission on Radiological Protection, Task Group Report on Reference Man*, ICRP Publication 23, Pergamon Press, NY.

Kennedy, W. E., Jr. and R. A. Peloquin, 1988, Intruder Scenarios for Site-Specific Low-Level Radioactive Waste Classification, DOE/LLW-71T.

Kennedy, W. E., Jr., L. L. Cadwell, D. W. McKenzie, 1985, "Biotic Transport of Radionuclides from a Low-Level Radioactive Waste Site," *Health Physics*, 49, 1, pp. 11-24.

Knobel, L. L., B. R. Orr, L. D. Cecil, 1992, "Summary of Background Concentrations of Selected Radiochemical and Chemical Constituents in Groundwater from the Snake River Plain Aquifer, Idaho: Estimated from an Analysis of Previously Published Data," *Journal of the Idaho Academy of Science, 28*, 1, pp. 48-60.

Konz, J. J. et al., 1989, *Exposure Factors Handbook*, EPA/600/8-89/043.

Koslow, K. N. and D. H. Van Haaften, 1986, *Flood Routing Analysis for a Failure of Mackay*

Leonard, P. R., 1992, "Radon Doses to Inadvertent Intruders into the Pits and Trenches and the Soil Vaults 100 years and 3,000 Years After Closure," Engineering Design File RWMC-589.

LMITCO (Lockheed Martin Idaho Technologies Company), 1995a, *A Comprehensive Inventory of Radiological and Nonradiological Contaminants in Waste Buried in the Subsurface Disposal Area of the INEL RWMC During the Years 1952-1983*, INEL-95/0310 (formerly EGG-WM-10903), Lockheed Martin Idaho Technologies Company, Rev. 1, August.

LMITCO, 1995b, *A Comprehensive Inventory of Radiological and Nonradiological Contaminants in Waste Buried or Projected to Be Buried in the Subsurface Disposal Area of the INEL RWMC During the Years 1984-2003*, INEL-95/0135, Lockheed Martin Idaho Technologies Company, Rev. 1, August.

Magnuson, S. O., 1996, LITCO Interdepartmental Communication to D. K. Jorgensen, *Transmittal of TETRAD Benchmarking Report*, SOM-01-96, Lockheed Martin Idaho Technologies Company, Idaho Falls, ID.

Magnuson, S. O., 1995, *Inverse Modeling for Field-Scale Hydrologic and Transport Parameters of Fractured Basalt*, INEL-95/0637, Lockheed Martin Idaho Technologies Company, Idaho Falls, ID.

Magnuson, S.O., 1993. *A Simulation Study of Moisture Movement in Proposaed Barriers for the Subsurface Disposal Area, INEL*. EGG-WM-10947. Idaho National Engineering and Environmental Laboratory, Idaho Falls ID.

Magnuson, S. O., and A. J. Sondrup, 1998, *Development, Calibration, and Predictive Results of a Simulator for Subsurface Pathway Fate and Transport of Aqueous and Gaseous Phase Contaminants in the Subsurface Disposal Area at the Idaho National Engineering and Environmental Laboratory*, INEL-97/00609, Lockheed Martin Idaho Technologies Company, Draft Rev. 1, March.

Maheras, S. J., 1993, *Revised Doses to Inadvertent Intruders for the RWMC Performance Assessment*, Engineering Design File RWMC-622, Revision 1.

Maheras, S. J., 1995a, *RWMC LLW Performance Assessment Biointrusion Scenarios for Inadvertent Intruders*, Engineering Design File RWMC-809.

Maheras, S. J., 1995b, *Radon Doses to Inadvertent Intruders*, Engineering Design File RWMC-589, Revision 4.

Maheras, S. J., 1997a, *Radon Doses to Inadvertent Intruders Based on a Maximum Time of Compliance of 1000 Years*, Engineering Design File RWMC-936.

Maheras, S. J., 1997b, *Site-Specific Low-Level Waste Concentration Limits Based On Acute and Chronic Inadvertent Intruder Scenarios*, Engineering Design File RWMC-78 1.

Maheras, S. J., A. S. Rood, S. O. Magnuson, M. E. Sussman, and R. N. Bhatt, 1994, *Radioactive Waste Management Complex Low-Level Waste Radiological Performance Assessment*, EGG-WM-8773, EG&G Idaho, Inc., May.

Maheras, S. J., A. S. Rood, S. O. Magnuson, M. E. Sussman, and R. N. Bhatt, 1997, *Addendum to Radioactive Waste Management Complex Low-Level Waste Radiological Performance Assessment* (EGG-WM-8773), INEEL/EXT-97-00462, LMITCO, April.

Martian, P., 1995, *UNSAT-H Infiltration Model Calibration at the Subsurface Disposal Area, Idaho National Engineering Laboratory*, INEL-95/0596, Lockheed Martin Idaho Technologies Company.

McCarthy, J. M., B. H. Becker, S. O. Magnuson, K. N. Keck, and T. K. Honeycutt, 2000, *Radioactive Waste Management Complex Low-Level Waste Radiological Composite Analysis*, INEEL/EXT-97-01113, September 26.

McElroy, D.L. and J.M. Hubbell, 1990. *Hydrologic and Physical Properties of Sediments at the Radioactive Waste Management Complex*, EGG-BG-9147, Idaho National Engineering and Environmental Laboratory, Idaho Falls, ID.

McKenzie, D. H., L. L. Caldwell, K. A. Gano, W. E. Kennedy, Jr., B. A. Napier, R. A. Peloquin, L. A. Prohammer, and M. A. Simmons. 1985, *Relevance of Biotic Pathways to the Long-Term Regulation of Nuclear Waste Disposal, Topical Report on Reference Western Arid Low-Level Sites*, NUREG/CR-2675, Volume 2.

Nagata, P. K., 1997, LMITCO Interdepartmental Communication to J. A. Logan, *Literature Search on Underground Corrosion Rates of Austenitic Steels*, September 22, PKN-15-97.

Nagata, P. K., 1993, Interdepartmental Communication to T. H. Smith, *Letter Report on Tritium Release from Buried Beryllium Reflectors*, EG&G Idaho, Inc., December 22.

Napier, B. A. et al., 1988, *GENII - The Hanford Environmental Radiation Dosimetry Software System*, Volumes 1-3, PNL-6584, December.

NCRP (National Council on Radiation Protection and Measurements), 1984, *Radiological Assessment: Predicting the Transport, Bioaccumulation, and Uptake by Man of Radionuclides Released to the Environment*, NCRP Report No. 76, March.

Ng, Y. C. et al., 1978, *Methodology for Assessing Dose Commitment to Individuals and to the Population from Ingestion of Terrestrial Foods Contaminated by Emissions from a Nuclear Fuel Reprocessing Plant at the Savannah River Plant*, UCID-17743, Lawrence Livermore Laboratory, March.

NRC (U.S. Nuclear Regulatory Commission), 1982, *Final Environmental Impact Statement on 10 CFR Part 61 "Licensing Requirements for Land Disposal of Radioactive Waste*, NUREG-0945, Volumes 1-3.

NRC, 1977, *Regulatory Guide 1.109 Calculation of annual Doses to Man From Routine Releases of Reactor Effluents for the Purpose of Evaluating Compliance With 10 CFR Part 50 Appendix I*, Revision 1.

NRC, 1981, *Draft Environmental Impact Statement on 10 CFR Part 61 "Licensing Requirements for Land Disposal of Radioactive Waste*," NUREG-0782, Volumes 1-4.

Orr, B. R., and L. D. Cecil, 1991, *Hydrologic Conditions and Distribution of Selected Chemical Constituents in Water, Snake River Plain Aquifer, Idaho National Engineering Laboratory, Idaho, 1986 to 1988*, DOE/ID-22096, U.S. Geological Survey Water Resource Investigations Report 91-4047, Idaho Falls, ID.

Oztunali, O. I. and G. W. Roles, 1986, *Update of Part 61 Impacts Analysis Methodology*, NUREG/CR-4370, Volumes I and 2.

Peterson, H. T. Jr., 1983, "Terrestrial and Aquatic Food Chain Pathways," in *Radiological Assessment - A Textbook on Environmental Dose Analysis*, J.E. Till and H.R. Meyer (eds.), NUREG/CR-3332.

Press, W.H., B.P. Flannery, S.A. Teukolsky, and W.T. Vetterling, 1992. *Numerical Recipes: The Art of Scientific Computing.* Cambridge: Cambridge University Press.

Price, K. R., 1972, *Uptake of Np-237, Pu-239, Am-241, and Cm-244 from Soil by Tumbleweed and Cheatgrass*, BNWL-1688.

Reynolds, T. D. and J. W. Laundre, 1988, "Vertical Distribution of Soil Removed by Four Species of Burrowing Rodents in Disturbed and Undisturbed Soils," *Health Physics*, 54, 4.

Reynolds, T. D. and L. Fraley, Jr., 1989, "Root Profiles of Some Native and Exotic Plant Species in Southeastern Idaho," *Environmental and Experimental Botany, 29*, pp. 241-248.

Reynolds, T. M. and W. L. Wakkinen, 1987, "Characteristics of the Burrows of Four Species of Rodents in Undisturbed Soils in Southeastern Idaho," *The American Midland Naturalist, 118*, 2, pp. 245-250.

Robertson, J. B., 1974, *Digital Modeling of Radioactive and Chemical Waste Transport in the Snake River Plain Aquifer at the National Reactor Testing Station, Idaho*, IDO-22054, U.S. Geological Survey Open File Report, U.S. Geological Survey.

Rogers, V. C. and C. Hung, 1987, *PATHRAE-EPA: A Low-Level Radioactive Waste Environmental Transport and Risk Assessment Code, Methodology and Users Manual*, EPA 520/1-87-028.

Rogers, V. C., M. W. Grant, A. A. Sutherland, 1982, *Low-Level Waste Disposal Site Performance Assessment With the RQ/PQ Methodology*, EPRI-NP-2665.

Rood, A. S., 1994, *Groundwater Pathway Dose Calculations for the RWMC Performance Assessment,- Release From Disposal Pits and Soil Vaults, and All Pathway and Drinking Water Scenarios Results*, Engineering Design File RWMC-760, September.

Rood, A. S., 1997, *Total Inventory Limits for the Radioactive Waste Management Complex*

Rood, A.S., 1999. *GWSCREEN: A Semi-Analytical Model for Assessment of the Groundwater Pathway from Surface or Buried Contamination, Theory and User's Manual Version 2.5*, INEEL/EXT-98-00750. Idaho National Engineering and Environmental Laboratory, June.

Rupp, E. M., 1980, "*Age-Dependent Values of Dietary Intake for Assessing Human Exposures to Environmental Pollutants*," *Health Physics, 39*, pp. 151-163.

Schnitzler, B. G., 1995, LMITCO Interdepartmental Communication to M. M. Garland, *Radionuclide Inventories of Advanced Test Reactor Outer Shim Control Cylinder and Reflector Block Components*, August 21, 1995, BGS-12-95.

Seitz, R. R. et al., 199 1, *Sample Application of Sensitivity/Uncertainty Analysis Techniques to a Groundwater Transport Problem*, DOE/LLW-108.

Shook, G. M., 1995, *Development of an Environmental Simulator from Existing Petroleum Technology*, INEL-94/0283, Lockheed Martin Idaho Technologies Company, Idaho Falls, ID.Sterbentz, J. W., 1998, LMITCO Interdepartmental Communication to J. A. Logan, *Radionuclide Inventories for Advanced Test Reactor Core Components (DRAFT)*, April 1, 1998, JWS-04-98.

Sondrup, A. J., 1998, *Preliminary Modeling of VOC Transport for Operable Unit 7-08, Evaluation of Increased Carbon Tetrachloride Inventory*, INEEL/EXT-98-00849, Lockheed Martin Idaho Technologies Company, Idaho Falls, ID.

Sullivan, T. M., 1993, *DUST Data Input Guide*, NUREG/CR-6041, April 1993.

Sussman, M. E., 1993, "Parameters for Basement Construction for Intruder Scenarios at RWMC," Engineering Design File RWMC-603, March 23.

Till, J.E. and H.R. Meyer (eds), 1983. *Radiological Assessment: A Textbook on Environmental Dose Analysis*. NUREG/CR-3332. U.S. Nuclear Regulatory Commission, Washington, D.C.

USDC (U.S. Department of Commerce), 1963, *Maximum Permissible Body Burdens and Maximum Permissible Concentrations of Radionuclides in Air and in Water for Occupational Exposure*, National Bureau of Standards Handbook 69, August.

van Genuchten, M. Th., 1978, *Calculating the Unsaturated Hydraulic Conductivity with a New Closed-Form Analytical Model*, 78-WR-08, Water Resources Program, Department of Civil Engineering, Princeton University, Princeton, NJ.

Vinsome, P. K. W., and G. M. Shook, 1993, "Multi-Purpose Simulation," *Journal of Petroleum Science and Engineering*, Vol. 9, pp. 29-38.

Vigil, M. J., 1988, *Estimate of Water in Pits During Flooding Events*, Engineering Design File BWP-12, EG&G Idaho, Inc., Idaho Falls, ID.

Ward, D. C., T. B. Borak, M. S. Gadd, 1993, "Characterization of ^{222}Rn Entry into a Basement Structure Surrounded by Low-Permeability Soil," *Health Physics, 65*, 1, July.

Wood, T. R., and G. T. Norrell, 1996, Integrated Large-Scale Aquifer Pumping and Infiltration Tests, Groundwater Pathways OU 7-06, Summary Report, INEL-96/0256, Lockheed Martin Idaho Technologies Company, Rev. 0.

Xu, M. and Y. Eckstien, 1995. Use of Weighted Lest-Squares Method in Evaluation of the Relationship Between Dispersivity and Field Scale.

Yang, Y. Y. and C. B. Nelson, 1984, *An Estimation of the Daily Average Food Intake by Age and Sex for Use in Assessing the Radionuclide Intake of Individuals in the General Population*, EPA 520/1-84-021.

Yang, Y. Y. and C. B. Nelson, 1986, "An Estimation of Daily Food Usage factors for Assessing Radionuclide Intakes in the U.S. Population," *Health Physics, 50*, 2, pp. 245-257.

APPENDIX A

GUIDE TO RESOLUTION OF LFRG REVIEW TEAM AND DAS COMMENTS ON THE DRAFT CA

APPENDIX A: GUIDE TO RESOLUTION OF LFRG REVIEW TEAM AND DAS COMMENTS ON THE DRAFT CA

This appendix presents Table A-1 as a roadmap to the resolution of identified Composite Analysis related issues from the first draft of the Composite Analysis (McCarthy et al. 1998) and the associated Information Supplement (Honeycutt et al. 1999). The issues were identified in comments from the Review Team for the Low-Level Waste Disposal Facility Federal Review Group (DOE 2000a) and the disposal authorization letter for the INEEL Subsurface Disposal Area, Low-Level Radioactive Waste Disposal Facility at the Radioactive Waste Management Complex (DOE 2000b). The Low-Level Waste Disposal Facility Federal Review Group is referred to as LFRG in this appendix.

The issues identified in DOE 2000a are referenced as either "Key" or "Secondary" issues in Table A-1. The issues identified in DOE 2000b are referenced as "DAS CA Conditions" in Table A-1. The table lists the document and section in which the issue resolution is presented and a brief comment regarding the resolution of the issue. The issues are resolved in one of the following three documents.

CA –Composite Analysis report (McCarthy et al., 2000)

PA –Performance Assessment report (Case et al., 2000)

PA and CA Maintenance –PA and CA Maintenance report (Shuman, 2000)

Table A-1. Roadmap to the resolution of Composite Analysis comments from the LFRG.

Issue #	Type Issue	Issue Title	Document	Section	How the issue was resolved
1	Key	Upgradient sources and CERCLA Cleanup Activities, DOE 2000a, page 11	CA	3.3	1. The revised CA has been updated by incorporation of the Information Supplement writeup regarding upgradient sources. This satisfies the LFRG review team concerns expressed in DOE 2000a based on the following comments. • The DOE 2000a report says that the "Information Supplement contained in Appendix F mitigates this key issue." • The DOE 2000a report also says that "While significant uncertainties remain that could have significant effect on the Composite Analysis results, justification is presented for screening other sites from the contributing source terms for the Composite Analysis".
			PA and CA Maintenance	3.1	2. In the PA and CA Maintenance Report, is presented a description of future regular monitoring of the upgradient sources and a plan to incorporate future findings into the CA.
				2	3. In the PA and CA Maintenance Report, is discussed the plan to monitor the evolution of the final disposition of the co-located facilities.
2	Key	Consistency of the composite analysis and performance assessment, DOE 2000a, page 12	CA	4	1. Consistent conceptual and numerical models are used in revised PA and CA.
			PA	3.2 And 4	• Use the IBRA RWMC conceptual and numerical model for the critical radionuclides for the determination of dose • Used a consistent set of contaminants of potential concern • vadose zone travel times of contaminants are consistent • vadose zone dispersivities are consistent • Kd values are consistent. 2. Consistent source term • Source inventory • Source release assumptions, in particular the corrosion rate.
3	Key	Land use planning relative to the RWMC,	PA and CA	3.2.3.4	• The PA and CA Maintenance report addresses this issue. No policy or guidelines have

Issue #	Type Issue	Issue Title	Document	Section	How the issue was resolved
		DOE 2000a, page 13.	Maintenance		been established for action beyond the 100 year institutional control timeframe. However, the INEEL has taken actions to support DOE Headquarters efforts in the Long-Term Stewardship initiative.
4	Key	Documentation of assumptions and justifications, DOE 2000a, page 14.	CA	3 and 4	1. The CA was updated with Information Supplement additions. This will address the flow and transport documentation of assumptions issue. This is the primary set of information for which the CA relied too heavily on the references.
					2. The revised CA addresses the omission of dose contributions from upgradient sources and CERCLA cleanup sites by adding a 1 mrem/year dose to the CA dose.
			PA and CA Maintenance	2, 3.1, 3.2.3.4, 5.1, and 5.2	3. The Maintenance Plan addresses the lack of land use planning documents, the monitoring and tracking planned for upgradient sources, and the long term reconciliation of the inconsistencies between the PA, CA, and CERCLA documents by coordinating all future PA, CA, and CERCLA studies and modeling efforts.
5	Key	Consideration of alternatives and the Options Analysis, DOE 2000a, page 14.	CA	7	1. The revised CA used TETRAD rather than PATHRAE for the simulations.
				3.3	2. The revised CA incorporates the writeup from the Information Supplement. As stated in DOE 2000a, "The Information Supplement ... provides additional justification for screening out potential sources up-gradient of the RWMC. In addition, a cap was considered for the RWMC ... These two items of additional analysis reduce the significance of this key issue. However, administrative controls identified in the CA have not been formally adopted in the Comprehensive Facility and Land Use Plan."
			PA and CA Maintenance	3.2.1	3. The reviewers were concerned that the "(CIDRA) best estimate values are 'considered analogous to 95% confidence limit values with reasonable certainty'". There was some misunderstanding on this issue. The CIDRA upper bound estimates are considered to be the 95% confidence limit values. For the CA the best estimates were used. Inventory refinement continues at this time.
				4, 5.1, and 5.2	4. A detailed options analysis and sensitivity analysis is planned upon completion of the refinements. The CA lab studies, field studies, and modeling efforts will be coordinated with the RWMC CERCLA efforts.
6	Key	Uncertainty and sensitivity analysis, DOE 2000a, page 15.	PA and CA Maintenance	3 and 4	▪ The uncertainty analysis and sensitivity analysis will be expanded upon in the future. Currently, as listed in the PA and CA Maintenance report, monitoring and research and development activities are ongoing in order to quantify the uncertainty associated with the

Issue #	Type Issue	Issue Title	Document	Section	How the issue was resolved
					composite analysis.
7	Secondary	Radiological monitoring in the Snake River Plain Aquifer, DOE 2000a, page 16	PA and CA Maintenance	3.1	▪ Discussed in the PA and CA Maintenance report.
8	Secondary	Comprehensive and integrated data quality objectives, data validation, and database management, DOE 2000a, page 17	PA and CA Maintenance	3.1	▪ The monitoring plan will contain data quality objectives and procedures that are integrated with the RWMC CERCLA work.
9	Secondary	Uncertainty analysis for better aquifer parameterization, DOE 2000a, page 17	PA and CA Maintenance	4	• The PA and CA Maintenance report explains the quantitative uncertainty analysis conducted for the recent revision to the performance assessment, and discusses work planned for the future.
10	Secondary	Low permeability zone down gradient of the RWMC, DOE 2000a, page 17	PA and CA Maintenance	3.2.2.4	▪ The PA and CA Maintenance report explains that there are multiple studies ongoing in order to better understand the flow speed and direction in the aquifer.
11	Secondary	Corrosion, DOE 2000a, page 17	PA and CA Maintenance	3.2.2.3	▪ The PA and CA Maintenance report describes the ongoing and planned corrosion experiments.
12	DAS CA Conditions	Additional source term info regarding screening of upgradient facilities, DOE 2000b, page 6	CA	3.3	▪ This was addressed as Key Issue #1.
13	DAS CA Conditions	Uncertainty and sensitivity analysis performed on the revised base case analysis of the RWMC LLRWDF performance with assumptions of a permanent surface barrier and land restrictions , DOE 2000b, page 6	PA and CA Maintenance	3 4	1. This was primarily addressed as Key Issue #6 2. The PA and CA Maintenance report discusses recently completed efforts that address some of the key and secondary issues, and discusses plans to further this work. The report also states that plans for future work include addressing the uncertainty and sensitivity of parameters that have not yet been evaluated.
14	DAS CA Conditions	Information to clearly define the subsurface pathway flow and transport modeling assumptions along with justification of the assumptions, DOE 2000b, page 6	CA	3 and 4	▪ This was addressed as part of Key Issue #4.
15.	DAS CA Conditions	The Performance Assessment is to be revised to be consistent with the conceptual model, inventory, source term model, transport model, and site characteristics presented in the Composite Analysis, DOE 2000b, page 6	CA PA	4 3.2 And 4	▪ This was addressed as Key Issue #2.

Issue #	Type Issue	Issue Title	Document	Section	How the issue was resolved
16	DAS CA Conditions	ID will ensure maintenance of 600 meter buffer zone downgradient of the SDA. Also, integration with ER Program relative to compliance concerns, DOE 2000b, page 6	PA and CA Maintenance CA	3.2.3.4 7	1. This was primarily addressed in key issue #3 and key issue #5. 2. The CA was written assuming a 100 m buffer zone. However, the Options Analysis presents the results at 300 m and 600 m.

References

Case, M. J., A. S. Rood, J. M. McCarthy, S. O. Magnuson, B. H. Becker, 2000, *Technical Revision of the Radioactive Waste Management Complex Low-Level Waste Radiological Performance Assessment for Calendar Year 2000*, INEEL/EXT-2000-01089, Bechtel BWXT Idaho, LLC.

DOE, 2000a, *Final Report for the Idaho National Engineering and Environmental Laboratory Radioactive Waste Management Complex Low-Level Waste Radiological Composite Analysis*, prepared by the DOE INEEL RWMC Low-Level Radiological Composite Analysis Review Team, Feb. 4, 2000.

DOE, 2000b, *Disposal Authorization for the Idaho National Engineering and Environmental Laboratory Subsurface Disposal Area Low-Level Waste Disposal Facility within the Radioactive Waste Management Complex Radiological Composite Analysis*, Letter from Mark W. Frei, Deputy Assistant Secretary for Project Completion, April 28, 2000.

Honeycutt, T.K., et al., 1999, "Information Supplement for the Draft Final Radioactive Waste management Complex Low-Level Waste Radiological Composite Analysis," Idaho National Engineering and Environmental Laboratory report INEEL/EXT-97-01113, December 15, 1999.

Maheras, S. J., A. S. Rood, S. O. Magnuson, M. E. Sussman, and R. N. Bhatt, 1994, *Radioactive Waste Management Complex Low-Level Waste Radiological Performance Assessment*, EGG-WM-8773, EG&G Idaho, Inc., May.

Maheras, S. J., A. S. Rood, S. O. Magnuson, M. E. Sussman, and R. N. Bhatt, 1997, *Addendum to Radioactive Waste Management Complex Low-Level Waste Radiological Performance Assessment* (EGG-WM-8773), INEEL/EXT-97-00462, LMITCO, April.

McCarthy, J. M., B. H. Becker, S. O. Magnuson, K. N. Keck, and T. K. Honeycutt, 1998, *Radioactive Waste Management Complex Low-Level Waste Radiological Composite Analysis*, INEEL/EXT-97-01113, May.

McCarthy, J. M., B. H. Becker, S. O. Magnuson, K. N. Keck, and T. K. Honeycutt, 2000, *Radioactive Waste Management Complex Low-Level Waste Radiological Composite Analysis*, INEEL/EXT-97-01113, September 26, 2000, , Bechtel BWXT Idaho, LLC.

Shuman, R., 2000, *Maintenance for the Radioactive Waste Management Complex Performance Assessment and Composite Analysis*, INEEL/EXT-2000-01262, Bechtel BWXT Idaho, LLC.

Appendix B

Waste Inventory

Appendix B

Waste Inventory

The RWMC radiological performance assessment evaluates LLW disposed of in the SDA from 1984 through 1999. In addition, it evaluates projected LLW that will be disposed of in the SDA from 1999 through 2020. The LLW disposed of in the SDA from 1984 through 1993 through 199 is buried in Pits 17 through 20 and Soil Vault Rows 14 through 20. No trench burial occurred during this time period; the last opened trench, Trench 55, closed in 1982. The inventory data in the radiological performance assessment was generated from the Contaminant Inventory Database for Risk Assessment (CIDRA). The CIDRA was developed in support of Environmental Restoration (ER) activities (LIMITCO 1995a and 1995b). It was developed using waste generation process knowledge and various supporting information from reports, shipping, databases, and nuclear physics calculations. The CIDRA effort has resulted in a best estimate quantity for each known disposed contaminant including lower and upper bounding estimates.

For the composite analysis (CA), refinements to radionuclide inventory estimates were performed to rectify identified data gaps associated with CIDRA. These refinements are discussed in McCarthy et al (2000). The data developed for the CA was adapted for the performance assessment, per direction of the Low-Level Waste Disposal Facility Federal Review Group (LFRG), because of the high confidence associated with them. Defensible uncertainty estimates for CIDRA best estimate values relied on professional judgement, reasonable assumptions, and standard statistical techniques, and are considered analogous to 95% confidence limit values with reasonable certainty (McCarthy et al 2000).

Table B-1 presents the source term data used in the performance assessment developed using the CIDRA and subsequent modifications of CIDRA data for specific radionuclides. The CIDRA does not distinguish between waste disposed in soil vaults and waste disposed in pits. However, previous performance assessment calculations (Maheras et al 1994, 1997) show that it is important to separate the waste into that disposed in soil vaults versus that disposed in pits because of the significantly different doses associated with each area. For this reason, data from Appendix A in Maheras (1994) were used to develop radionuclide fractions to apportion radionuclide inventories into soil vaults and pits (see footnotes in Table A-1).

Table B-2 presents the source term data for the year 2020 and include radioactive decay and daughter ingrowth. The inventory in Table A-1 was decayed and ingrown using the MicroShield Version 5 code (Grove Engineering 1996). For this application it was assumed that the inventory for 1984 through 1993 was disposed in 1993; the inventory for 1994 through 1999 was disposed in 1999; and the inventory projected for 2000 through 2020 was disposed in 2020. The RESRAD code was used for decay and ingrowth of radionuclides after 2020.

Table B-1. Radioactivity (Ci) disposed of in pits (1984 to 1999) and projected to be disposed (2000-2020).

Nuclide	Actual (1984-1993)		Actual (1994-1999)		Projected (2000-2020)		Totals (1984-2020)	
	Pits[a]	SVR[a]	Pits[a]	SVR[a]	Pits[b]	SVR[b]	Pits	SVR
AM-241	3.7067E+00	3.4903E-03	1.2133E-01	1.1424E-04	6.3697E-01	5.9977E-04	4.4650E+00	4.2043E-03
AM-243	0.0000E+00	0.0000E+00	6.7520E-06	0.0000E+00	3.5448E-05	0.0000E+00	4.2200E-05	0.0000E+00
C-14	2.5974E-01	4.0215E+01	6.6163E-02	1.0244E+01	3.4736E-01	5.3781E+01	6.7326E-01	1.0424E+02
CL-36	0.0000E+00	0.0000E+00	1.9792E-02	0.0000E+00	1.0391E-01	0.0000E+00	1.2370E-01	0.0000E+00
CM-244	7.5961E-02	1.6939E-04	1.0772E-02	2.4023E-05	5.6555E-02	1.2612E-04	1.4329E-01	3.1953E-04
CO-60	1.4033E+04	1.3923E+06	2.7784E+02	2.7565E+04	1.4587E+03	1.4472E+05	1.5770E+04	1.5645E+06
CS-137	7.8345E+02	2.3075E+03	1.6763E+01	4.9374E+01	8.8008E+01	2.5921E+02	8.8822E+02	2.6161E+03
EU-152	2.6037E+00	1.5346E+00	1.5404E+01	9.0787E+00	8.0869E+01	4.7663E+01	9.8877E+01	5.8276E+01
EU-154	3.0159E+00	3.2868E-01	6.7566E+01	7.3635E+00	3.5472E+02	3.8658E+01	4.2530E+02	4.6351E+01
H-3	2.9735E+03	2.9321E+05	4.2798E+01	4.2201E+03	2.2469E+02	2.2156E+04	3.2410E+03	3.1958E+05
I-129	5.5108E-07	2.1069E-03	1.2276E-06	4.6937E-03	6.4451E-06	2.4642E-02	8.2238E-06	3.1442E-02
NA-22	5.3520E-01	0.0000E+00	1.9476E-02	0.0000E+00	1.0225E-01	0.0000E+00	6.5693E-01	0.0000E+00
NB-94	3.5445E-05	2.0396E-01	9.4189E-05	5.4200E-01	4.9449E-04	2.8455E+00	6.2413E-04	3.5914E+00
NI-59	0.0000E+00	1.3873E+03	0.0000E+00	4.1680E+02	0.0000E+00	2.1882E+03	0.0000E+00	3.9923E+03
NI-63	1.7986E+04	4.5846E+05	1.9387E+03	4.9417E+04	1.0178E+04	2.5944E+05	3.0103E+04	7.6732E+05
NP-237	3.6982E-03	0.0000E+00	7.8783E-03	0.0000E+00	4.1361E-02	0.0000E+00	5.2938E-02	0.0000E+00
PU-238	3.4953E-01	7.8048E-03	5.5264E-02	1.2340E-03	2.9014E-01	6.4787E-03	6.9493E-01	1.5518E-02
PU-239	2.2344E+00	1.6630E-01	1.3973E-01	1.0400E-02	7.3358E-01	5.4598E-02	3.1077E+00	2.3129E-01
PU-240	5.4396E-02	2.8183E-03	4.4558E-02	2.3086E-03	2.3393E-01	1.2120E-02	3.3288E-01	1.7247E-02
PU-241	1.4771E+01	2.1945E+00	2.0110E+00	2.9876E-01	1.0558E+01	1.5685E+00	2.7340E+01	4.0618E+00
PU-242	1.2249E-08	8.8874E-13	4.1010E-08	2.9755E-12	2.1530E-07	1.5621E-11	2.6856E-07	1.9486E-11
RA-226	1.1000E+00	0.0000E+00	8.0636E-02	0.0000E+00	4.2334E-01	0.0000E+00	1.6040E+00	0.0000E+00
RA-228	0.0000E+00	0.0000E+00	1.0709E-05	0.0000E+00	5.6222E-05	0.0000E+00	6.6931E-05	0.0000E+00
SR-90	2.9281E+02	2.8470E+02	2.1462E+01	2.0868E+01	1.1268E+02	1.0956E+02	4.2695E+02	4.1513E+02
TC-99	1.9622E-02	4.7841E-01	2.5916E-02	6.3187E-01	1.3606E-01	3.3173E+00	1.8160E-01	4.4276E+00
TH-228	1.0200E+01	0.0000E+00	4.6538E-04	0.0000E+00	2.4432E-03	0.0000E+00	1.0203E+01	0.0000E+00
TH-230	0.0000E+00	0.0000E+00	1.1075E-02	0.0000E+00	5.8145E-02	0.0000E+00	6.9221E-02	0.0000E+00
TH-232	0.0000E+00	0.0000E+00	1.1625E-02	0.0000E+00	6.1034E-02	0.0000E+00	7.2659E-02	0.0000E+00
U-232	2.2100E+00	0.0000E+00	6.5078E-04	0.0000E+00	3.4166E-03	0.0000E+00	2.2141E+00	0.0000E+00
U-233	0.0000E+00	0.0000E+00	7.0520E-03	0.0000E+00	3.7023E-02	0.0000E+00	4.4075E-02	0.0000E+00
U-234	3.5251E+00	5.4149E-03	1.4049E-01	2.1581E-04	7.3760E-01	1.1330E-03	4.4032E+00	6.7637E-03
U-235	1.5549E-01	1.0666E-03	1.4430E-02	9.8983E-05	7.5760E-02	5.1966E-04	2.4568E-01	1.6852E-03
U-236	2.2688E-03	1.2377E-05	7.3697E-03	4.0205E-05	3.8691E-02	2.1108E-04	4.8330E-02	2.6366E-04
U-238	1.4325E+00	8.1670E-02	2.9401E+00	1.6762E-01	1.5436E+01	8.7999E-01	1.9808E+01	1.1293E+00

[a]Apportioned according to fractions determined from totals in Table A-1 and A-2 of EGG-WM-8773.

[b]Apportioned according to fractions determined from totals in Table A-3 of EGG-WM-8773.

Table B-2. Decayed and ingrown inventory (Ci) at the end of institutional control (2020).

Nuclide	Waste disposed from 1984 to 1993		Waste disposed from 1994 to 1999		Total projected (2000-2020)		Total decayed & ingrown (1984-2020)[c]		
	Inventory at year 2020[a]		Inventory at year 2020[a]		Inventory at year 2020				
	Pits[b]	SVR[b]	Pits[b]	SVR[b]	Pits[b]	SVR[b]	Pits	SVR	TOTAL
AM-241	3.8986E+00	5.5130E-02	1.5901E-01	6.3193E-03	6.3697E-01	5.9977E-04	4.6946E+00	6.2049E-02	4.7566E+00
AM-243			6.7387E-06	0.0000E+00	3.5449E-05	0.0000E+00	4.2187E-05	0.0000E+00	4.2187E-05
C-14	2.5885E-01	4.0084E+01	6.5992E-02	1.0218E+01	3.4736E-01	5.3781E+01	6.7220E-01	1.0408E+02	1.0476E+02
CL-36	0.0000E+00	0.0000E+00	1.9792E-02	0.0000E+00	1.0391E-01	0.0000E+00	1.2370E-01	0.0000E+00	1.2370E-01
CM-244	2.7026E-02	6.0268E-05	4.8211E-03	1.0754E-05	5.6555E-02	1.2612E-04	8.8403E-02	1.9714E-04	8.8600E-02
CO-60	4.0278E+02	3.9971E+04	1.7558E+01	1.7419E+03	1.4587E+03	1.4472E+05	1.8790E+03	1.8643E+05	1.8831E+05
CS-137	4.1987E+02	1.2366E+03	1.0317E+01	3.0393E+01	8.8008E+01	2.5921E+02	5.1819E+02	1.5262E+03	2.0444E+03
Ba-137m	3.9719E+02	1.1698E+03	0.0000E+00	2.8752E+01			3.9719E+02	1.1986E+03	1.5957E+03
EU-152	6.3959E-01	3.7693E-01	5.1888E+00	3.0464E+00	8.0869E+01	4.7663E+01	8.6678E+01	5.1086E+01	1.3776E+02
EU-154	3.5960E-01	3.9188E-02	1.2924E+01	1.4084E+00	3.5472E+02	3.8658E+01	3.6801E+02	4.0106E+01	4.0811E+02
H-3	6.5335E+02	6.4425E+04	1.3169E+01	1.2985E+03	2.2469E+02	2.2156E+04	8.9121E+02	8.7879E+04	8.8770E+04
I-129	5.5110E-07	2.1069E-03	1.2280E-06	4.6937E-03	6.4451E-06	2.4642E-02	8.2242E-06	3.1442E-02	3.1451E-02
NA-22	4.0257E-04		7.2454E-05	0.0000E+00	1.0225E-01	0.0000E+00	1.0273E-01	0.0000E+00	1.0273E-01
NB-94	3.5417E-05	2.0377E-01	9.4122E-05	5.4160E-01	4.9449E-04	2.8455E+00	6.2403E-04	3.5909E+00	3.5915E+00
NI-59		1.3870E+03	0.0000E+00	4.1672E+02	0.0000E+00	2.1882E+03	0.0000E+00	3.9919E+03	3.9919E+03
NI-63	1.4904E+04	3.7726E+05	1.6659E+03	4.2465E+04	1.0178E+04	2.5944E+05	2.6648E+04	6.7916E+05	7.0581E+05
NP-237	3.7316E-03	3.0728E-07	7.8789E-03	2.5595E-08	4.1361E-02	0.0000E+00	5.2972E-02	3.3288E-07	5.2972E-02
PU-238	2.8237E-01	6.3056E-03	4.6812E-02	1.0454E-03	2.9014E-01	6.4787E-03	6.1932E-01	1.3830E-02	6.3315E-01
PU-239	2.2323E+00	1.6617E-01	1.3962E-01	1.0394E-02	7.3358E-01	5.4598E-02	3.1056E+00	2.3116E-01	3.3367E+00
PU-240	5.4380E-02	2.8105E-03	4.4477E-02	2.3035E-03	2.3393E-01	1.2120E-02	3.3279E-01	1.7234E-02	3.5002E-01
PU-241	4.0270E+00	5.9828E-01	7.3183E-01	1.0872E-01	1.0558E+01	1.5685E+00	1.5317E+01	2.2755E+00	1.7592E+01
PU-242	1.2249E-08	8.8870E-13	4.1008E-08	2.9754E-12	2.1530E-07	1.5821E-11	2.6856E-07	1.9485E-11	2.6858E-07
RA-226	1.0872E+00	7.8698E-09	8.0010E-02	1.8783E-10	4.2334E-01	0.0000E+00	1.5905E+00	7.8574E-09	1.5905E+00
RA-228	2.1296E-12	1.1617E-14	1.0701E-02	2.6508E-14	5.6222E-05	0.0000E+00	1.0757E-02	3.8125E-14	1.0757E-02
SR-90	1.5398E+02	1.4972E+02	1.3019E+01	1.2659E+01	1.1268E+02	1.0956E+02	2.7968E+02	2.7194E+02	5.5161E+02
Y-90	1.5402E+02	1.4976E+02	1.3022E+01	1.2662E+01			1.6704E+02	1.6242E+02	3.2946E+02
TC-99	1.9618E-02	4.7837E-01	2.5918E-02	6.3183E-01	1.3606E-01	3.3173E+00	1.8159E-01	4.4275E+00	4.6091E+00
TH-228	1.7511E+00	1.0029E-14	1.0789E-02	2.1683E-14	2.4432E-03	0.0000E+00	1.7643E+00	3.1712E-14	1.7643E+00
TH-230	8.5664E-04	1.3167E-06	1.1099E-02	4.1733E-08	5.8145E-02	0.0000E+00	7.0101E-02	1.3584E-06	7.0102E-02
TH-232	3.0224E-12	1.6488E-14	1.1600E-02	4.1654E-14	6.1034E-02	0.0000E+00	7.2634E-02	5.8142E-14	7.2634E-02
U-232	1.7041E+00		5.3166E-04	0.0000E+00	3.4166E-03	0.0000E+00	1.7080E+00	0.0000E+00	1.7080E+00
U-233	4.3684E-07	1.3684E-11	7.0520E-03	8.4634E-13	3.7023E-02	0.0000E+00	4.4076E-02	1.4530E-11	4.4076E-02
U-234	3.5249E+00	5.4213E-03	1.4066E-01	2.2580E-04	7.3760E-01	1.1330E-03	4.4032E+00	6.7801E-03	4.4099E+00
U-235	1.5550E-01	1.0666E-03	1.4430E-02	9.8983E-05	7.5760E-02	5.1966E-04	2.4569E-01	1.6852E-03	2.4737E-01
U-236	2.2690E-03	1.2379E-05	7.3697E-03	4.0206E-05	3.8691E-02	2.1108E-04	4.8030E-02	2.5966E-04	4.8293E-02
U-238	1.4325E+00	8.1670E-02	2.9401E+00	1.6762E-01	1.5436E+01	8.7999E-01	1.9808E+01	1.1293E+00	2.0938E+01

a. Decayed and ingrown using MICROSHIELD (run by Henry Peterson on July b. Microshield output for (1984-1993 to 2020) + (1994-1999 to 2020) + (projections for 1999-2020)

c. Apportioned according to fractions determined from totals in Tables A-1 & A-d. Apportioned according to fractions determined from totals in Table A-3 of PA.

Appendix C

A Comparison of GENII and RESRAD Calculations

Appendix C

A Comparison of GENII and RESRAD Calculations

This Appendix presents a discussion of a benchmarking exercise conducted to compare RESRAD and GENII calculations. The calculations were conducted in an attempt to provide the means to compare estimates made for this revision of the Performance Assessment, using the RESRAD code, with previous calculations (Maheras et al 1994, 1997), using the GENII code. The GENII and RESRAD codes were used primarily to assess inhalation and ingestion doses. The MICROSHIELD code was used to estimate external doses in the previous performance assessment and the current performance assessment.

In order to compare the two codes, previous GENII runs were recreated using the RESRAD code. The GENII runs are contained in an engineering design file entitled "Revised Doses to Inadvertent Intruders for the RWMC Radiological Performance Assessment", EDF Serial Number RWMC-622, Rev. 1, dated 10/31/93. Source term, occupancy and shielding, and dietary parameter values identical to those used in the GENII runs were used in the RESRAD runs. The RESRAD default dose conversion factor and food-chain transport libraries were used, as they are similar to those used in GENII. GENII runs were not available for the gaseous tritium and C-14 releases, so the information provided in Maheras et al (1993) was used.

The RESRAD code has some parameters that are not used in the GENII code. In these instances, the default values were used or values were estimated that closely simulated the GENII code bounds. For example, the RESRAD code estimates a dilution length, based on wind speed, mixing height, resuspension rate, and thickness of resuspendable dust layer. If the dilution length is increased, the fraction of airborne dust at the receptor location will be decreased. In other words, the particulate concentrations are diluted due to mixing with uncontaminated air. To minimize the dilution length, such that mass loading was localized and particulate concentrations were maximized, a minimum wind speed was selected for acute scenarios.

A comparison of GENII and RESRAD analyses of the tritium/carbon-14 gaseous release and acute intruder scenarios, which address only inhalation, and the chronic intruder scenarios, which also address ingestion, are shown in Figure D-1. Figure D-2 presents the ratios of RESRAD results/GENII results. A ratio of one indicates perfect agreement.

The GENII and RESRAD results show good correlation for the inhalation scenarios. The ratio of RESRAD results/GENII results approach one in each inhalation scenario. However, the RESRAD ingestion doses are approximately twice the values calculated by the GENII code. This indicates that for the chronic scenarios involving ingestion of food raised at the site, the doses estimated by RESRAD for the current revision may be more conservative than if they were estimated by GENII.

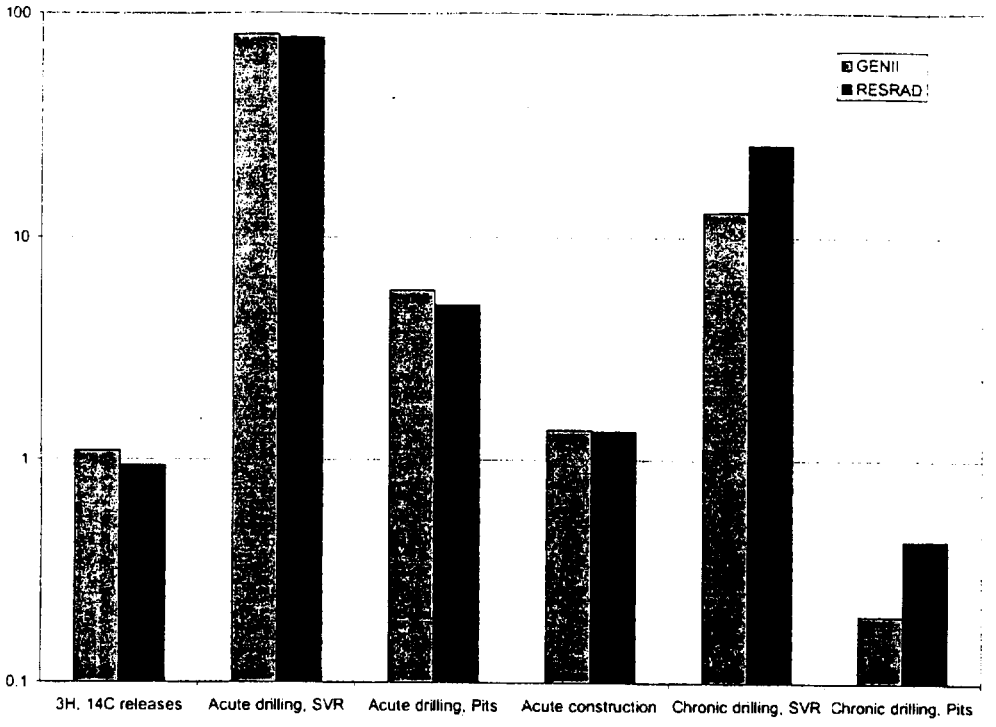

Figure C-1. Comparison of GENII and RESRAD results for select scenarios.

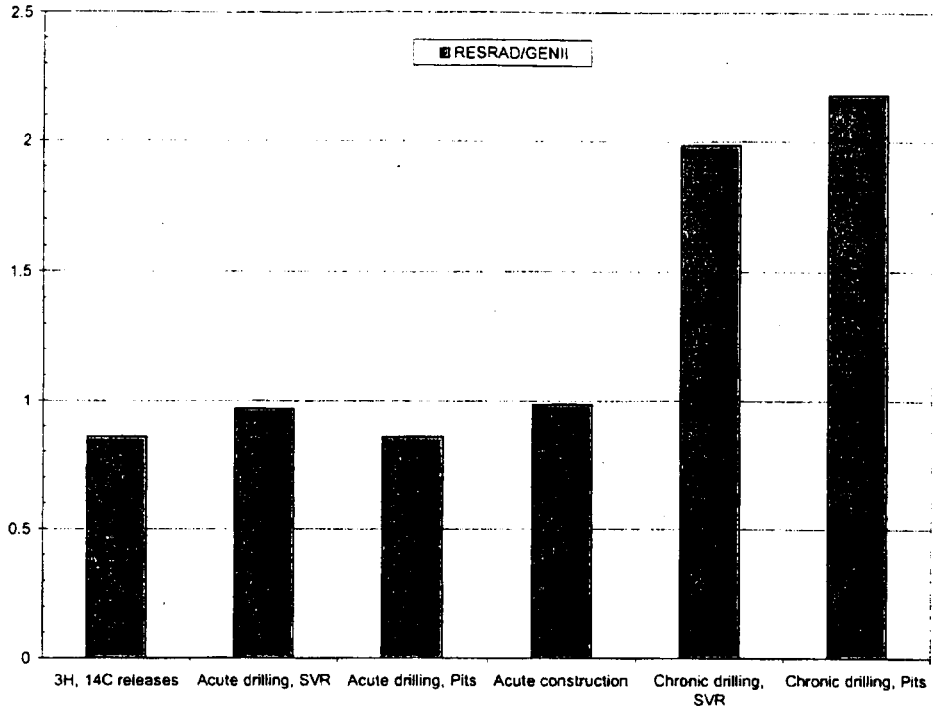

Figure C-2. Comparison of RESRAD results/GENII results. A value of 1 indicates identical results. A value greater than 1 indicates that RESRAD results are greater than GENII results. A value less than 1 indicates that GENII results are greater than RESRAD results.

Appendix D
Perl Script for Performing Monte Carlo Uncertainty/Sensitivity Analysis

Appendix H

Perl Script for Performing Monte Carlo Uncertainty/Sensitivity Analysis

```
# gwsmc.pl
# This script is a Monte Carlo Driver for GWCREEN version 2.5a used to
# calculate distributions of committed effective dose equivalent for
# radionuclides in the Radioactive Waste Management Complex. The scripts uses the
# TEMPLATE file define the conceptual model and exposure scenario and the values of the
# deterministic variables. Stochastic variables are defined and sampled within the
script.
# The user must make sure the number of output times match what is written in the script
#

# Written by: Arthur S. Rood
# July 27, 2000

# usage perl gwsmc.pl [template file] [number of Monte Carlo trials]


#Stochastic transport variables
#    0     1    2    3     4
#   PERC   AX   AY   AXU   U

# Stochastic nuclide specific parameters
#    0
#    U_kd    Np_kd   C_kd   I_kd   U238_sf   U234_sf   Np237_sf   C14_sf I129_sf C136_sf
# the _sf designation is the source term uncertainty factor


# calculational times
#   150   300   450   600   850 1000   1150   1300   1500   1800
#   5000 5500 6000 6500 7000   7500 8000 8500   9000 9500 10000

    require "d:\\fy2000\\rwmc-pa\\scripts\\sample2.pl";
    srand(314159265);            # set randon number seed

    $filetemplate=$ARGV[0];
    $nmc=$ARGV[1];  # number of mc trials

# the following output times must correspond to the number of files defined

    @times=(150, 300, 450, 600, 750, 900, 1050, 1200, 1350, 1500,
     5000,5500,6000,6500,7000, 7500,8000,8500, 9000,9500,10000);

    @fileconc = ("C0.DAT","C1.dat","C2.dat","C3.dat","C4.dat","C5.dat","C6.dat",
     "C7.dat","C8.dat","C9.dat","C10.dat","C11.dat","C12.dat","C13.dat","C14.dat"
     ,"C15.dat","C16.dat","C17.dat","C18.dat","C19.dat","C20.dat");

    @filedose = ("D0.dat","D1.dat","D2.dat","D3.dat","D4.dat","D5.dat","D6.dat",
     "D7.dat","D8.dat","D9.dat","D10.dat","D11.dat","D12.dat","D13.dat","D14.dat"
     ,"D15.dat","D16.dat","D17.dat","D18.dat","D19.dat","D20.dat");

    @filehandc = ("\*C0","\*C1","\*C2","\*C3","\*C4","\*C5","\*C6","\*C7","\*C8",

"\*C9","\*C10","\*C11","\*C12","\*C13","\*C14","\*C15","\*C16","\*C17","\*C18","\*C19","\
*C20");

    @filehandd = ("\*D0","\*D1","\*D2","\*D3","\*D4","\*D5","\*D6","\*D7","\*D8",
```

```
"\*D9","\*D10","\*D11","\*D12","\*D13","\*D14","\*D15","\*D16","\*D17","\*D18","\*D19","\
*D20");


# open files for concentration and dose output

   for $i (0..20)
   {
      $fc=$filehandc[$i];
      $fd=$filehandd[$i];
      open ($fc, ">$fileconc[$i]");
      open ($fd, ">$filedose[$i]");

      print $fc "    Time      C-14      I-129      Cl-36      Np-237     U-233     Th-
229    U-234     Th-230    Ra-226    Pb-210    U-238      U-234     Th-230    Ra-226
Pb-210  (Ci m**3) \n";
      print $fd "    Time      C-14      I-129      Cl-36      Np-237     U-233     Th-
229    U-234     Th-230    Ra-226    Pb-210    U-238      U-234     Th-230    Ra-226
Pb-210    Total (rem) \n";
   }


# ***************************************************************************
# *                          Define Distributions                           *
# ***************************************************************************


# Define the distributitions:  The procedure here is to define the variable being samples
followed by
# and underscore and the distrubution parameter name.  For example perc_min would be the
minimum value
# for the percolation rate.  The calling sequence for the sampling is as follows

# $perc = sample("TRIANGLE", $perc_min, $perc_mode, $perc_max);

# the legal distribtions are TRIANGLE, UNIFORM, NORM, LNORM, LTRIANGLE

# ---------- Transport Parameters -----------------

# PERC - Triangular distribution  min mode max value (meters/y)
# sub TRIANGLE_sample(min,mode,max,value)

  $perc_min=0.005;
  $perc_mode=0.01;
  $perc_max=0.02;

# AX - Triangle  (meters)
  $ax_min=10;
  $ax_mode=20;
  $ax_max=40;
# Note: AY and AZ area based on the value of AX; AY=0.25*AX, AZ=0.085*AX

# AXU - Triangle Distribution (meters)
  $axu_min=1.25;
  $axu_mode=2.25;
  $axu_max=4.5;

# U - Triangle Distribution (darcy velocity) (meters/y)
  $u_min=0.37;
  $u_mode=0.75;
  $u_max=1.5;

# ------------------ Kd Values  -----------------

# U_kd - triangle
  $u_kd_min=3.4;
  $u_kd_mode=6;
  $u_kd_max=9;

# Np_kd -log triangle
```

```
# In LTRIANGLE_sample: $a > 0 and $b are the min and max of the sampling range,
# NOTE THE ORDER OF THE PARAMETERS: min mode max.
  $np_kd_min=1;
  $np_kd_mode=8;
  $np_kd_max=80;

# C_kd - triangle
  $c_kd_min=0.0;
  $c_kd_mode=0.1;
  $c_kd_max=1.5;

# I_kd - log triangle
  $i_kd_min=0.02;
  $i_kd_mode=0.1;
  $i_kd_max=5.0;

# Cl_kd -triangle
  $cl_kd_min=0.0;
  $cl_kd_mode=0.001;
  $cl_kd_max=0.002;


# -------------- Inventory Uncertainty Factors ---------------

# U238_sf - lognormal
  $u238_sf_gm=1.0;
  $u238_sf_gsd=2.5;

# U234_sf - lognormal
  $u234_sf_gm=1.0;
  $u234_sf_gsd=2.5;

# Np237_sf - lognormal
  $np237_sf_gm=1.0;
  $np237_sf_gsd=2.5;

# C14_sf - lognormal
  $c14_sf_gm=1.0;
  $c14_sf_gsd=2.5;


# I129_sf
  $i129_sf_gm=1.0;
  $i129_sf_gsd=2.5;

# Cl36sf
  $cl36_sf_gm=1.0;
  $cl36_sf_gsd=2.5;


# -------------- Inventory Scaling  Factors (fixed) ---------------

  $u238_isf=1.0;
  $u234_isf=1.0;
  $np237_isf=1.0;
  $c14_isf=1.0;
  $i129_isf=1.0;
  $cl36_isf=1.0;

#  ------------- Open values file -----------------
  open (VALUES, ">values.out");

  print VALUES " perc  ax  ay  az  axu  u  c_kd  i_kd  cl_kd  u_kd  np_kd  sf_c14
sf_i129  sf_cl36  sf_u234  sf_u238
 sf_np237\n";


# ************************************************************************
# *                        Monte Carlo Simulation                        *
```

```
# ************************************************************************

   for $imc (1..$nmc)
   {

# Sample Transport parameters
      $perc = sample("TRIANGLE", $perc_min, $perc_mode, $perc_max);
      $ax = sample("TRIANGLE",$ax_min,$ax_mode,$ax_max);
      $axu = sample("TRIANGLE",$axu_min,$axu_mode,$axu_max);
      $u = sample("TRIANGLE",$u_min,$u_mode,$u_max);
      $ay=0.25*$ax;
      $az=0.085*$ax;

# Sample kd values
      $u_kd = sample("TRIANGLE", $u_kd_min, $u_kd_mode, $u_kd_max);
      $np_kd = sample("LTRIANGLE", $np_kd_min, $np_kd_mode, $np_kd_max);
      $c_kd = sample("TRIANGLE", $c_kd_min, $c_kd_mode, $c_kd_max);
      $i_kd = sample("LTRIANGLE", $i_kd_min, $i_kd_mode, $i_kd_max);
      $cl_kd = sample("TRIANGLE", $cl_kd_min, $cl_kd_mode, $cl_kd_max);

# Sample inventory uncertainty factors

      $u238_sf=sample("LNORM",$u238_sf_gm,$u238_sf_gsd);
      $u234_sf=sample("LNORM",$u234_sf_gm,$u234_sf_gsd);
      $np237_sf=sample("LNORM",$np237_sf_gm,$np237_sf_gsd);
      $c14_sf=sample("LNORM",$c14_sf_gm,$c14_sf_gsd);
      $i129_sf=sample("LNORM",$i129_sf_gm,$i129_sf_gsd);
      $cl36_sf=sample("LNORM",$cl36_sf_gm,$cl36_sf_gsd);

      print VALUES "$perc  $ax  $ay  $az  $axu  $u $c_kd $i_kd $cl_kd $u_kd $np_kd
$c14_sf $i129_sf $cl36_sf $u234_sf
      $u238_sf $np237_sf\n";


# ------------------- End of Sampling ----------------------


#  ------------------ Run Source Term Model -----------------


# ****** C-14
      $fpar="d:\\fy2000\\rwmc-pa\\srcterm\\c14\\srcterm.par";
      open (REL, "<d:\\fy2000\\rwmc-pa\\srcterm\\c14\\c14src.par");
      open (RELPAR, ">$fpar");
# read and print 5 lines
      for $j (0..4)
      {
          $line=<REL>;
          print RELPAR "$line";
      }
# read kd thalf and invf
      $line=<REL>;
      $line =~ s/^[ ]+//; # delete initial spaces
      @field = split /[ \t]+/, $line;
      printf RELPAR "%g  %g  %g   kd thalf  invf \n",$c_kd,$field[1],$c14_sf*$c14_isf;
# read and print 5 lines
      for $j (0..4)
      {
          $line=<REL>;
          print RELPAR "$line";
      }
      close REL;
      close RELPAR;
      system "d:\\fy2000\\rwmc-pa\\srcterm\\f77\\srcterm $fpar >nul";

# ****** I-129
      $fpar="d:\\fy2000\\rwmc-pa\\srcterm\\i129\\srcterm.par";
      open (REL, "<d:\\fy2000\\rwmc-pa\\srcterm\\i129\\i129src.par");
      open (RELPAR, ">$fpar");
# read and print 5 lines
      for $j (0..4)
```

```
      {
          $line=<REL>;
          print RELPAR "$line";
      }
# read kd thalf and invf
      $line=<REL>;
      $line =~ s/^[ ]+//; # delete initial spaces
      @field = split /[ \t]+/, $line;
      printf RELPAR "%g  %g  %g   kd thalf  invf \n",$i_kd,$field[1],$i129_sf*$i129_isf;
# read and print 5 lines
      for $j (0..4)
      {
          $line=<REL>;
          print RELPAR "$line";
      }
      close REL;
      close RELPAR;
      system "d:\\fy2000\\rwmc-pa\\srcterm\\f77\\srcterm $fpar >nul";

# ****** Cl-36
      $fpar="d:\\fy2000\\rwmc-pa\\srcterm\\cl36\\srcterm.par";
      open (REL, "<d:\\fy2000\\rwmc-pa\\srcterm\\cl36\\cl36src.par");
      open (RELPAR, ">$fpar");
# read and print 5 lines
      for $j (0..4)
      {
          $line=<REL>;
          print RELPAR "$line";
      }
# read kd thalf and invf
      $line=<REL>;
      $line =~ s/^[ ]+//; # delete initial spaces
      @field = split /[ \t]+/, $line;
      printf RELPAR "%g  %g  %g   kd thalf  invf \n",$cl_kd,$field[1],$cl36_sf*$cl36_isf;
# read and print 5 lines
      for $j (0..4)
      {
          $line=<REL>;
          print RELPAR "$line";
      }
      close REL;
      close RELPAR;
      system "d:\\fy2000\\rwmc-pa\\srcterm\\f77\\srcterm $fpar >nul";


# ****** Np-237
      $fpar="d:\\fy2000\\rwmc-pa\\srcterm\\np237\\srcterm.par";
      open (REL, "<d:\\fy2000\\rwmc-pa\\srcterm\\np237\\np237src.par");
      open (RELPAR, ">$fpar");
# read and print 5 lines
      for $j (0..4)
      {
          $line=<REL>;
          print RELPAR "$line";
      }
# read kd thalf and invf
      $line=<REL>;
      $line =~ s/^[ ]+//; # delete initial spaces
      @field = split /[ \t]+/, $line;
      printf RELPAR "%g  %g  %g   kd thalf  invf
\n",$np_kd,$field[1],$np237_sf*$np237_isf;
# read and print 5 lines
      for $j (0..4)
      {
          $line=<REL>;
          print RELPAR "$line";
      }
      close REL;
      close RELPAR;
      system "d:\\fy2000\\rwmc-pa\\srcterm\\f77\\srcterm $fpar >nul";
```

```
# ****** U-234
      $fpar="d:\\fy2000\\rwmc-pa\\srcterm\\u234\\srcterm.par";
      open (REL, "<d:\\fy2000\\rwmc-pa\\srcterm\\u234\\u234src.par");
      open (RELPAR, ">$fpar");
# read and print 5 lines
      for $j (0..4)
      {
          $line=<REL>;
          print RELPAR "$line";
      }
# read kd thalf and invf
      $line=<REL>;
      $line =~ s/^[ ]+//; # delete initial spaces
      @field = split /[ \t]+/, $line;
      printf RELPAR "%g  %g  %g   kd thalf  invf \n",$u_kd,$field[1],$u234_sf*$u234_isf;
# read and print 5 lines
      for $j (0..4)
      {
          $line=<REL>;
          print RELPAR "$line";
      }
      close REL;
      close RELPAR;
      system "d:\\fy2000\\rwmc-pa\\srcterm\\f77\\srcterm $fpar >nul";

# ****** U-238
      $fpar="d:\\fy2000\\rwmc-pa\\srcterm\\u238\\srcterm.par";
      open (REL, "<d:\\fy2000\\rwmc-pa\\srcterm\\u238\\u238src.par");
      open (RELPAR, ">$fpar");
# read and print 5 lines
      for $j (0..4)
      {
          $line=<REL>;
          print RELPAR "$line";
      }
# read kd thalf and invf
      $line=<REL>;
      $line =~ s/^[ ]+//; # delete initial spaces
      @field = split /[ \t]+/, $line;
      printf RELPAR "%g  %g  %g   kd thalf  invf \n",$u_kd,$field[1],$u238_sf*$u238_isf;
# read and print 5 lines
      for $j (0..4)
      {
          $line=<REL>;
          print RELPAR "$line";
      }
      close REL;
      close RELPAR;
      system "d:\\fy2000\\rwmc-pa\\srcterm\\f77\\srcterm $fpar >nul";


# ------------------ Source Term Finished ------------------

# open GWSCRREN.PAR - use this file to execute the code
      open (GWSF, ">gwscreen.par");
# open GWSCREEN template file use this file to provide a template for GWSCREEN
      open (TEMP, "<$filetemplate");

# skip 6 lines (model parameters and exposure settings)
      for $j (1..6)
        {
        $line=<TEMP>;
        print GWSF "$line";
        } # skip 6 lines

# substitute PERC  (1 w perc)
     $line=<TEMP>;
     $line =~ s/^[ ]+//; # delete initial spaces
     @field = split /[ \t]+/, $line;
     printf GWSF "%7f  %7f  %3G             1 w perc \n", $field[0],  $field[1],  $perc;
```

```
# substitute axu (depth rhou axu)
     $line=<TEMP>;
     $line =~ s/^[ ]+//; # delete initial spaces
     @field = split /[ \t]+/, $line;
     printf GWSF "%7f  %7f  %7f       depth rho axu \n", $field[0],$field[1],  $axu;

# copy vanG parameters
     $line=<TEMP>;
     print GWSF "$line";

# substitute ax,ay,az,b and z
     $line=<TEMP>;
     $line =~ s/^[ ]+//; # delete initial spaces
     @field = split /[ \t]+/, $line;
     printf GWSF "%7f  %7f  %7f  %7f  %7f       ax ay az b z \n",$ax,$ay,
$az,$field[3],$field[4];

# substitute u,phi,rhoa
     $line=<TEMP>;
     $line =~ s/^[ ]+//; # delete initial spaces
     @field = split /[ \t]+/, $line;
     printf GWSF "%7f  %7f  %7f    u phi  rhoa \n",$u,$field[1],$field[2];

# read and write receptor data (2 lines)
     for $j (1..2)
     {
        $line=<TEMP>;
        print GWSF "$line";
     }

# read ntimes and t1,t2, and tp in template file and print
     $line=<TEMP>;
     print GWSF "$line";
     $line =~ s/^[ ]+//; # delete initial spaces
     @field = split /[ \t]+/, $line;
     for $j (1..$field[0])
     {
       $line=<TEMP>;
       print GWSF "$line";
     }


# Nuclide Data - number of nuclides is fixed at 6 as defined in template file

     $line=<TEMP>;
     print GWSF "$line";
# ------------------ C-14 -------------------------
# C-14 data  nprog kds kdu zmw q0 rmi sl other
     $line=<TEMP>;
     $line =~ s/^[ ]+//; # delete initial spaces
     @field = split /[ \t]+/, $line;
     printf GWSF "%d  %g  %g  %g  %g  %g  %g  %g\n",$field[0],
$c_kd,$c_kd,$field[3],$field[4],$field[5],$field[6],$field[7];

# C-14 data  cname(i),thalf(i),kda(i),dcf(i)
     $line=<TEMP>;
     print GWSF "$line";

# C-14 data  release file name
     $line=<TEMP>;
     print GWSF "$line";
# ------------------ I-129 -------------------------

# I-129 data  nprog kds kdu zmw q0 rmi sl other
     $line=<TEMP>;
     $line =~ s/^[ ]+//; # delete initial spaces
     @field = split /[ \t]+/, $line;
     printf GWSF "%d  %g  %g  %g  %g  %g  %g
%g\n",$field[0],$i_kd,$i_kd,$field[3],$field[4],$field[5],$field[6],$field[7];
```

```
# I-129 data  cname(i),thalf(i),kda(i),dcf(i)
     $line=<TEMP>;
     print GWSF "$line";

# I-129 data  release file name
     $line=<TEMP>;
     print GWSF "$line";
# ------------------- Cl-36 -------------------------

# Cl-36 data  nprog kds kdu zmw q0 rmi sl other
     $line=<TEMP>;
     $line =~ s/^[ ]+//; # delete initial spaces
     @field = split /[ \t]+/, $line;
     printf GWSF "%d  %g  %g  %g  %g  %g  %g
%g\n",$field[0],$cl_kd,$cl_kd,$field[3],$field[4],$field[5],$field[6],$field[7];


# Cl-36 data  cname(i),thalf(i),kda(i),dcf(i)
     $line=<TEMP>;
     print GWSF "$line";

# Cl-36 data  release file name
     $line=<TEMP>;
     print GWSF "$line";


# -------------------- Np-237 -------------------------

# Np-237 data  nprog kds kdu zmw q0 rmi sl other
     $line=<TEMP>;
     $line =~ s/^[ ]+//; # delete initial spaces
     @field = split /[ \t]+/, $line;
     printf GWSF "%d  %g  %g  %g  %g  %g  %g
%g\n",$field[0],$np_kd,$np_kd,$field[3],$field[4],$field[5],$field[6],$field[7];
     $nprog=$field[0];

# Np-237 data  cname(i),thalf(i),kda(i),dcf(i)
     $line=<TEMP>;
     print GWSF $line;

# Np-237 progeny
     for $j (1..$nprog)
     {
        $line=<TEMP>;
        print GWSF $line;
     }

# Np-237 data  release file name
     $line=<TEMP>;
     print GWSF "$line";

# ------------------ U-234 --------------------------

# U-234 data  nprog kds kdu zmw q0 rmi sl other
     $line=<TEMP>;
     $line =~ s/^[ ]+//; # delete initial spaces
     @field = split /[ \t]+/, $line;
     printf GWSF "%d  %g  %g  %g  %g  %g  %g
%g\n",$field[0],$u_kd,$u_kd,$field[3],$field[4],$field[5],$field[6],$field[7];
      $nprog=$field[0];

# U-234 data  cname(i),thalf(i),kda(i),dcf(i)
     $line=<TEMP>;
     print GWSF $line;

# U-234 progeny
     for $j (1..$nprog)
     {
        $line=<TEMP>;
        print GWSF $line;
     }
```

```
# U-234 data  release file name
     $line=<TEMP>;
     print GWSF "$line";

# ---------------- U-238 ----------------------------

# U-238 data  nprog kds kdu zmw q0 rmi sl other
     $line=<TEMP>;
     $line =~ s/^[ ]+//; # delete initial spaces
     @field = split /[ \t]+/, $line;
     printf GWSF "%d  %g  %g  %g  %g  %g  %g
%g\n",$field[0],$u_kd,$u_kd,$field[3],$field[4],$field[5],$field[6],$field[7];
      $nprog=$field[0];

# U-238 data  cname(i),thalf(i),kda(i),dcf(i)
     $line=<TEMP>;
     print GWSF $line;

# U-238 progeny
     for $j (1..$nprog)
     {
        $line=<TEMP>;
        print GWSF $line;
     }

# U-238 data  release file name
     $line=<TEMP>;
     print GWSF "$line";



# End of parameter substitution

     close TEMP;
     close GWSF;


# ----------------------- Run GWSCREEN ----------------------------

     system "c:\\gwscreen\\ver25\\fsrc\\gwscreen <run.rep >nul";

     if ($imc % 5 == 0) { print STDERR "$imc"; }
     else { print STDERR ".";}



# ---------------------- Process Output ----------------------
# Concentrations ************
# Order of Nuclides: C-14, I-129, Cl-36, Np-237, (U-233, Th-229), U-234, (Th-230,Ra-
226,Pb-210), U-238 (U-234,Th-230,Ra-226,Pb-210)
     open (GWSO, "<gwscreen.out");
     $count=0;

     while ($line = <GWSO>)
     {
       if ($line=~/Concentration vs Time Results for Receptor X/)
       {
         $count=$count+1;
         for $j (1..4) { $line=<GWSO>;} # skip 4 lines

#        loop for all times in output file
         for $k (0..20)
         {
           $fc=$filehandc[$k];
           $line=<GWSO>;
           $line =~ s/^[ ]+//; # delete initial spaces
           chop ($line); # remove carrige return
           @field = split /[ \t]+/, $line;
           if ($count == 1)                                  # C-14 concentration data
             {print $fc " $field[0] $field[2] ";}
```

```
            if ($count == 2)                                    # I-129 concentration data
              {print $fc " $field[2] ";}
            if ($count == 3)                                    # Cl-36 concentration data
              {print $fc " $field[2] ";}
            if ($count == 4)                                    # Np-237 data
              {print $fc " $field[2] $field[3] $field[4]";}
            if ($count == 5)                                    # U-234 data
              {print $fc " $field[2] $field[3] $field[4] $field[5]";}
            if ($count == 6)                                    # U-238 data
              {print $fc " $field[2] $field[3] $field[4] $field[5] $field[6]\n ";}
          }
        }
      }               # end of concentration post process loop
      close GWSO;

# Doses **************
      open (GWDO, "<dose.out");

      $count=0;

      while ($line = <GWDO>)
      {
        if ($line=~/DOSE VS. TIME RESULTS FOR RECEPTOR X/)
        {
          $count=$count+1;
          for $j (1..3) { $line=<GWDO>;}          # skip 3 lines

#         loop for all times in output file
          for $k (0..20)
          {
            $fd=$filehandd[$k];
            $line=<GWDO>;
            $line =~ s/^[ ]+//; # delete initial spaces
            chop ($line); # remove carrige return
            @field = split /[ \t]+/, $line;
            if ($count == 1)                                    # C-14 dose data
            {  $c14d[$k]=$field[2];
              print $fd " $field[0] $field[2] ";}
            if ($count == 2)                                    # I-129 concentration data
            { $i129d[$k]=$field[2];
              print $fd " $field[2] ";}
            if ($count == 3)                                   # Cl-36 concentration data
            { $c136d[$k]=$field[2];
              print $fd " $field[2] ";}
            if ($count == 4)                                    # Np-237 data
            {  $np237d[$k]=$field[4];
               print $fd " $field[1] $field[2] $field[3]";}
            if ($count == 5)                                    # U-234 data
            {  $u234d[$k]=$field[5];
               print $fd " $field[1] $field[2] $field[3] $field[4]";}
            if ($count == 6)                                    # U-238 data
            {  $u238d[$k]=$field[6];

$totald[$k]=$c14d[$k]+$i129d[$k]+$c136d[$k]+$np237d[$k]+$u234d[$k]+$u238d[$k];
               print $fd " $field[1] $field[2] $field[3] $field[4] $field[5] $totald[$k]\n
";}
          }
        }
      }               # end of dose post process loop

      close GWDO;

# ----------------------End Process Output ---------------------


   }  # end of simulation loop

      close VALUES;


#-------------------------------------------------------------
```

```
# End of main program
#-------------------------------------------------------------

   exit;


# ---------------------------------------------------
# Subroutine Sample
# ---------------------------------------------------
# Front-end subroutine for Monte Carlo sampling.

# Calling sequence: $value = sample("LNORM", $GM, $GSD);
sub sample
{
    local ($type, $p1, $p2, $p3) = @_;      # arguments: distribution and 3 parameters
    local ($u, $rv);
    # Get a uniformly distributed [0,1] random number
    do { $u = rand(1.0) } until $u>0 && $u<1;        # discard 0 and 1
    SWITCH2:
    {
      $rv = NORM_sample($p1, $p2, $u), last SWITCH2 if ($type eq "NORM");
      $rv = LNORM_sample($p1, $p2, $u), last SWITCH2 if ($type eq "LNORM");
      $rv = TRIANGLE_sample($p1, $p2, $p3, $u), last SWITCH2 if ($type eq "TRIANGLE");
      $rv = LTRIANGLE_sample($p1, $p2, $p3, $u), last SWITCH2 if ($type eq "LTRIANGLE");
      $rv = UNIFORM_sample($p1, $p2, $u),last SWITCH2 if ($type eq "UNIFORM");
      die "Distribution type not found in subroutine sample";
    }
    return ($rv);
}



# ---------------------------------------------------------------------------
# ---------------------------------------------------------------------------
sub linterp
{
    local ($N = shift);
    local ($x = shift);
    local ($pxtab, $pytab) = @_;

    local ($i, $found = 0);
    for $i (0 .. $N-2)
    {
      local ($x0 = $$pxtab[$i]);
      local ($x1 = $$pxtab[$i+1]);
      next if (!($x >= $x0 && $x < $x1));

      local ($y0 = $$pytab[$i]);
      local ($y1 = $$pytab[$i+1]);
      local ($y = $y0 + ($y1-$y0)/($x1-$x0)*($x-$x0));
      $found = 1;
      last;
    }
    if (!$found)
    {
      if ($x >= $$pxtab[$N-1]) { return $$pytab[$N-1]; }
      if ($x <= $$pxtab[0]) { return $$pytab[0]; }
    }
    else
    {
 return $y;
    }
}
```

Appendix E

Description of Computer Codes Used in the RWMC LLW Radiological Performance Assessment Analyses

Appendix E

Description of Computer Codes Used in the RWMC LLW Radiological Performance Assessment Analyses

This section provides a brief description of computer codes used for the analyses supporting the RWMC LLW radiological performance assessment.

E.1 MicroShield 5

MICROSHIELD Version 5.0 is the personal computer version of ISOSHLD, which is a computer code that performs gamma-ray shielding calculations for radioactive sources with a wide variety of source and shiel configurations. Attenuation calculations are performed by point kernel integrations (i.e., the dose at the exposure point is the contribution from a large number of point sources.) A numerical integration is carried out over the source volume to obtain the total dose. Build-up factors are used and are calculated by the code based on the number of mean free paths of material between the source and exposure point locations, the effective atomic number of a particular shield region, and the point isotropic NDA build-up data available as Taylor coefficients in the effective atomic number range of 4 to 82. For most problems, the user need only supply (a) the geometry and material composition of the source and of the shields and (b) the thicknesses and distances involved. Other data needed to complete the calculations are contained in data libraries used by the code.

The MICROSHIELD code was chosen for the external exposure analyses because it contains the source and shielding geometies appropriate for buried waste, it contains a transparent decay and ingrowth data base, and it meets appropriate quality assurance requirements. MICROSHIELD can also incorporate site-specific data, which enables more realistic dose assessments to be performed. MICROSHIELD is also used extensively at the INEEL for shielding calculations.

A comprehensive verification of MICROSHIELD has been conducted (Negin and Worku 1992) and a comparison of both American National Standards Institute (ANSI) and European Shielding Information Service (ESIS) benchmark shielding problems have been published (ANSI 1979; ESIS 1981). The MICROSHIELD computer code is maintained by Grove Engineering, Inc. (1996), which is responsible for configuration management.

E.2 RESRAD

RESRAD is a computer developed at Argonne National Laboratory for the U.S. Department of Energy to calculate site-specific RESidual RADioactive material guidelines as well as radiation dose and excess lifetime cancer risk to a chronically exposed on-site resident (Gilbert et al. 1989). This code system is designed to calculate site-specific residual radioactive material guidelines, and radiation dose and excess cancer risk to an on-site resident (maximally exposed individual). Nine environmental pathways are considered: direct exposure, inhalation of dust and radon, and ingestion of plant foods, meat, milk, aquatic foods, soil, and water.

RESRAD uses a pathway analysis method in which the relation between radionuclide concentrations in soil and the dose to a member of a critical population group is expressed as a pathway sum, which is the sum of products of "pathway factors". Pathway factors correspond to pathway segments connecting compartments in the environment between which radionuclides can be transported or radiation transmitted. Radiation doses, health risks, soil guidelines and media concentrations are calculated over user-specified time intervals. The source is adjusted over time to account for radioactive decay and ingrowth, leaching, erosion, and mixing. RESRAD uses a one-dimensional groundwater model that accounts for differential transport of parent and daughter radionuclides with different distribution coefficients.

RESRAD was selected for use in the PA because:

1. RESRAD is the only code designated by DOE in Order 5400.5 for the evaluation of radioactively contaminated sites;

2. the EPA Science Advisory Board reviewed the RESRAD model and used RESRAD in their rulemaking on radiation site cleanup regulations;

3. NRC has approved the use of RESRAD for dose evaluation by licensees involved in decommissioning;

4. RESRAD has been applied to over 300 sites in the U.S. and other countries;

5. the RESRAD code has been verified and has undergone several benchmarking analyses, and has beenincluded in the IAEA's VAMP and BIOMOVS II projects to compare environmental transport models.

E.3 TETRAD

The TETRAD code (Vinsome and Shook 1993) was used to simulate flow and transport for the Subsurface Disposal Area (Magnuson and Sondrup 1998). Documentation of the model selection process was explained in detail in Becker et al. (1996). In brief, the process consisted of developing a list of required and desired crieteria and then selecting a code that met those cirteria. In addition, verification and validation (Shook 1995; Magnuson 1996) were conducted to demonstrate the proficiency of the TETRAD simulator for use in modeling surface fate and transport at the SDA.

TETRAD has complete multi-phase, multi-component simulation capabilities. Movement of any number of components within aqueous, gaseous, and oleic phases were considered in the SDA simluation study. TETRAD uses a block-centered finite difference approach and has capabilities for local grid refinement, which were used extensively. The TETRAD simualtor also includes dual-porosity simulation capabiltieis. This feature was used to address gaseous-phase movement in both the fracture and matrix portions of the fractured basalts composing the majority of the subsurface beneath the SDA.

E.4 DUST-MS

Disposal Unit Soruce Term - Multiple Species was used to simulate the source release of contaminants into the subsurface. DUST-MS models container failure and three release mechanisms - diffusion, dissolution and surface washoff. Documentation of the model selection process was explained in detail in Becker et al. (1996). In brief, the release models were compared to closed form analytical solutions to verify the accuracy of the models.

DUST-MS was developed for the NRC for use in performance assessments of shallow land burial. DUST-MS is a 1D model so the output was put into the TETRAD subsurface model in locations representing the pits and trenches.

E.5 GWSCREEN

GWSCREEN is a groundwater assessment code that was developed for the assessment of the groundwater pathway from leaching of radioactive and nonradioactive substances from surface or buried sources. The code was designed for implementation in the Track I and Track II assessment of Comprehensive Environmental Response, Compensation, and Liability Act (CERCLA) sites identified as low probability hazard at the INEL (DOE-ID 1992a, 1992b). In addition, the code has been applied to numerous other sites and problems.

The code calculates the limiting soil concentration and inventory so that after leaching and transport of the contaminant to the aquifer, regulatory contaminant levels in groundwater are not exceeded. Groundwater concentrations and dose results are also output at user-specified times. The code uses a mass conservation approach to model three processes: (1) contaminant release from a source volume, (2) contaminant transport in the unsaturated zone, and (3) contaminant transport in the aquifer. The source model considers the sorptive properties and solubility of the contaminant. Transport in the unsaturated zone is described by a plug flow model. Transport in the aquifer is calculatd with a semianalytical solution to the advection dispersion equation in groundwater.

The GWSCREEN code, Version 2.5, includes transport, decay, and ingrowth of radioactive progeny. The simplifying but conservative assumption was made that progeny travel at the same rate as their parent.

GWSCREEN meets the requirements of Quality Level B documentation. Quality Level B documentation includes a software configuration management plan (Matthews 1992), verification and validation test plan (Rood 1993), and verification and validation report (Smith 1993).

E.6 ISCST3

The Industrial Source Complex – Short Term (ISCST3) model is used to predict pollutant concentrations from atmospheric transport of contaminants from continuous point, flare, area, line, volume and open pit sources. This versatile model is preferred by the EPA because of the man features that enable the user to estimate concentrations from nearly any type of source emitting non-reactive pollutants.

The ISCST3 code (EPA 1995) was used to model dispersion of airborne emissions from the RWMC because it is approved by the EPA and the State of Idaho to evaluate short-term concentrations from a variety of emission sources. In addition, INEEL-specific hourly meteorological data measured by the National Oceanographic and Atmospheric Administration (NOAA) can be used by the code.

E.7 References

American National Standards Institute (ANSI), 1979, *American National Standard for Claculation and Measurement of Direct and Scattered Gamma Radiation from LWR Nuclear Power Plants,* ANSI/ANS-6.6.1-1979, January.

Becker, B.H., T.A. Benson, C.S. Blackmore, D.E. Burns, B.N. Burton, N.L. Hampon, R.M. Huntley, R.W. Jones, D.K. Jorgensen, S. O. Magnuson, C. Shapiro, and R.L. VanHorn, 1996, *Work Plan for Operable Unit 7-13/14 Waste Area Group 7 Comprehensive Remedial Investigation/Feasibility Study,* INEL-95/0343, Lockheed Martin Technologies Company, May.

U.S. Environmental Protection Agency (EPA), 1995, *User's Guide for the Industrial Source Complex (ISC3) Dispersion Models,* EPA-450/B-95-003a.

European Shielding Information Service (ESIS), 1981, *Specification for Gamma Ray Shielding Benchmark Applicable to a Nuclear Radwaste Facility,* Newletter #37, ISPRA Establishment, Italy, April.

Gilbert, T. L. et al., 1989, *A Manual for Implementing Residual Radioactive Material Guidelines,* ANL/ES-160, DOE/CH/8901, June.

Grove Engineering, Inc., 1996, *MicroShield Version 5 User's Manual,* Grove Engineering, Rockville, Md, October.

Matthews, S.D., 1992, *Software Configuration Management Plan for Controlled Code Support System,* EGG-CATT-10196, April.

Rood, A.S., 1999, *GWSCREEN: A Semi-Analytical Model for Assessment of the Groundwater Pathway from Surface or Buried Contamination: Theory and User's Manual, Version 2.5,* INEEL/EXT-98-00750, Idaho National Engineering and Environmental Laboratory, Idaho Falls, ID.

Rood, A.S. 1993. *Software Verification and Validation Plan for the GWSCREEN Code,* EGG-GEO-10798, May.

Smith, C.S., 1993, *Independent Verification and Limited Benchmarking of the GWSCREEN Code,* EGG-GEO-10798, May.

Vinsome, P. K. W., and G. M. Shook, 1993, "Multi-Purpose Simulation," *Journal of Petroleum Science and Engineering,* Vol. 9, pp. 29-38.